POLYHEDRAL AND TROPICAL GEOMETRY IN NONLINEAR ALGEBRA

A Dissertation
Presented to
The Academic Faculty

By

Cvetelina Dimitrova Hill

In Partial Fulfillment
of the Requirements for the Degree
Doctor of Philosophy in the
School of Mathematics

Georgia Institute of Technology

August 2021

POLYHEDRAL AND TROPICAL GEOMETRY IN NONLINEAR ALGEBRA

Thesis committee:

Dr. Josephine Yu, Advisor
School of Mathematics
Georgia Institute of Technology

Dr. Matthew Baker
School of Mathematics
Georgia Institute of Technology

Dr. Grigoriy Blekherman
School of Mathematics
Georgia Institute of Technology

Dr. Elizabeth Gross
Department of Mathematics
University of Hawai'i at Mānoa

Dr. Anton Leykin
School of Mathematics
Georgia Institute of Technology

Date approved: 30 June, 2021

Yesterday I was clever, so I wanted to change the world. Today I am wise, so I am changing myself.

Rumi

For Maiche
Thank you for showing me how to be brave. I miss you.

“A single person is missing for you, and the whole world is empty.”
Joan Didion

ACKNOWLEDGMENTS

I am grateful for the support of all those around me throughout this expedition called graduate school. I would like to thank the following persons and organizations.

To my advisor Josephine Yu for believing in me and encouraging me to continue doing math even when I didn't think I could. I have learned so much from you, and not only mathematical content. I have learned a lot about doing, learning, reading, and teaching mathematics, and overall how to be a kind human in the world of academia. Thank you for your continuous support through all my struggles with the comprehensive exams, difficult research problems, overwhelming teaching assignments, and with my multitude of math insecurities. Thank you for giving me strength to stay and complete this program when I tried to leave so many times.

To Anton Leykin for serving on my oral exam and thesis committees. Thank you for giving me the opportunity to work on my first research project, which is the content of Chapter 4, and transition from learning to doing mathematics.

To Elizabeth Gross for serving on my thesis committee, and for mentoring and guiding me through the world of mathematical biology. Thank you for always being so supportive and caring. And thank you for giving me the opportunity to be creative with our project on chemical reaction networks, which is the content of Chapter 3 of this dissertation.

To Matt Baker and Greg Blekherman for serving on my oral exam and thesis committees. Thank you for your support, the helpful feedback, and fruitful conversations.

To many of the other faculty and staff members at Georgia Tech for teaching, mentoring, and supporting me, and for being kind to me: Luca Dieci, Mitchell Everett, Klara Grodzinsky, Christopher Heil, Jen Hom, Plamen Iliev, Sung Ha Kang, Michael Lacey, Dan Margalit, & Xingxing Yu.

To Mariana Montiel at Georgia State University: Thank you for sparking my interest in higher mathematics, and guiding my first independent study in algebra.

To Sara Lamboglia and Faye Simon for the great experience of working on tropical convexity. Thank you for many exhilarating and frustrating mathematical moments. The content of Chapter 2 is based on our joint work.

To all my other collaborators: Tim Duff, Elizabeth Gross, Anders Jensen, Kisun Lee, Anton Leykin, & Jeff Sommars.

To my Georgia Tech nonlinear algebra and combinatorics academic siblings: Skye Binegar, May Cai, Tim Duff, Marc Härkönen, & Kisun Lee.

To my nonlinear algebra friends Maggie Regan and Faye Simon for your unwavering support. To my Georgia Tech friends: Thibaud Alemany, Cathy & Forrest Keifer, Justin Lanier, and the Graduate student council.

To the Nonlinear Algebra group at the Institute for Computational and Experimental Research in Mathematics. To ICERM itself for providing the oportunity for a semester-long research visit and a week-long research experience through CollaborateICERM.

To T.O. and Merrie for your love and support. Thank you for the terrible puns and the delicious food.

To La for always being by my side. Thank you for helping me find the light in some of the darkest places and for reminding me to look up to the sun. Thank you for sharing my grief, sadness, joy, and happiness.

To Dr. Andreka Peat for teaching me how to be true to myself. Thank you for guiding me through the most difficult years of my life, and helping me emerge on the other side stronger and more whole.

To Dr. Farrah Fang for helping me stay on track with my plan to graduate. Thank you for helping me navigate graduate school without losing my mind.

To Dad & Elena, Mike & Holly, Lily, Vasil & Cori, and Ellery & Joe for being the best family I could have asked for. Thank you for being kind to me, supporting me, making me laugh, and for never asking me when and where I am going to use the stuff I am learning.

To Ester, Phoebe, and Maely for reminding me to be joyful and playful.

To my senior and junior canine assistants Typo & Calabi. I could not have written even half of this without your numerous interruptions for breaks: outside, treats, play, belly-rubs, or just because.

To Marlowe for putting up with me through getting yet another degree. Thank you for always believing in me, and for your unconditional love and support.

TABLE OF CONTENTS

LIST OF TABLES

LIST OF FIGURES

SUMMARY

This dissertation consists of four chapters on various topics in nonlinear algebra. Particularly, it focuses on solving algebraic problems and polynomial systems through the use of combinatorial tools. Chapter one gives a broad introduction and discusses connections to applied algebraic geometry, polyhedral, and tropical geometry.

Chapter two studies the interaction between tropical and classical convexity, with a focus on the tropical convex hull of convex sets and polyhedral complexes. We describe the tropical convex hull of a line segment and a ray. We show that tropical and ordinary convex hull commute in two dimensions, and we characterize tropically convex sets in any dimension. We show that the dimension of a tropically convex fan depends on the coordinates of its rays, and we give a combinatorial description for the dimension of the tropical convex hull of an ordinary affine space. Lastly, we prove a lower bound on the degree of a fan tropical curve using only tropical techniques.

Chapter three studies the steady-state degree and mixed volume of a chemical reaction network. The steady-state degree of a chemical reaction network is the number of complex steady-states, which is a measure of the algebraic complexity of solving the steady-state system. In general, the steady-state degree may be difficult to compute. Here, we give an upper bound to the steady-state degree of a reaction network by utilizing the underlying polyhedral geometry associated with the corresponding polynomial system. We focus on three case studies of infinite families of networks. For each family, we give a formula for the steady-state degree and the mixed volume of the corresponding polynomial system.

Chapter four presents methods for finding the solution set of a generic system in a family of polynomial systems with parametric coefficients. We present a framework for describing monodromy based solvers in terms of decorated graphs. The algorithm we develop is implemented as a package in Macaulay2 [42]. To demonstrate our method, we provide several examples, including an example arising from chemical reaction networks.

CHAPTER 1
INTRODUCTION

This dissertation consists of three stand-alone chapters following the introduction. The unifying connection between them is nonlinear algebra; particularly, solving algebraic problems and polynomial systems through the use of combinatorial tools. Here, we introduce the reader to the broad ideas throughout this work, and provide some examples. Relevant definitions, context, and background are addressed at the beginning of each chapter.

1.1 Nonlinear algebra & polynomial systems

The reader is likely familiar with linear algebra, which studies systems of linear equations. Broadly speaking, *nonlinear algebra* is the analogue of linear algebra where the objects of study are systems of polynomial equations, which need not be linear. Nonlinear algebra is closely related to applied algebraic geometry, as well as polyhedral and tropical geometry. The main focus of *applied algebraic geometry* is the study of *algebraic varieties*, i.e., the set of solutions to a system of polynomial equations. Given a variety, we would like to know some of its characteristics, such as the geometric and combinatorial structure it encodes. If the variety is a finite set, we may want to study the underlying polyhedral geometry and combinatorics, or find an upper bound for the number of solutions, or we may be interested in obtaining the numerical solutions. In the latter case, *numerical algebraic geometry* can be used to approximate the solutions to the system.

When the polynomial system is difficult to solve, we may instead want to find an upper bound for the number of solutions. Here, *polyhedral geometry* can be useful, as polynomial systems have a rich underlying polyhedral structure that can be used to obtain information about the system, such as the number of solutions, without solving it. One method for obtaining an upper bound for the number of solutions through polyhedral geometry is the computation of the *mixed volume* of the polynomial system. In 1975 Bernstein, Kushnirenko, and Khovanskii established that for a polynomial system, the number of isolated nonzero complex roots is bounded by the mixed volume of the *Newton polytopes* of the polynomials. Example 1.1.1 shows a polynomial system in two variables, the corresponding Newton polytopes, and the mixed volume of the system.

Example 1.1.1. Consider the polynomial system

$$
\begin{aligned}
x^3y^3 + x + y &= 0 \\
x^2y^2 + x^2 + y^2 - 1 &= 0
\end{aligned}
$$

in two variables over the complex numbers. The *Newton polytope* of a polynomial is the convex hull of the exponent vectors of each term in the polynomial. The Newton polytope P of the first polynomial is the convex hull of the points $(3, 3)$, $(0, 1)$, and $(1, 0)$; the Newton polytope Q of the second polynomial is the convex hull of $(2, 2)$, $(2, 0)$, $(0, 2)$, and $(0, 0)$. Both are shown in Figure 1.1.

Polynomial systems are not always easy to solve. In some cases, it is sufficient to have an upper bound on the number of solutions to the system. One such bound is the *mixed volume* of a polynomial system, which is the mixed volume of the Newton polytopes of the polynomials. In this two-dimensional example, the mixed volume is equal to the area of the *mixed cells* in the Minkowski sum of the Newton polytopes. The mixed cells here are the regions labeled C_1 and C_2 in Figure 1.1. The sum of the areas of C_1 and C_2 is 12, implying that there are at most 12 solutions to the polynomial system. Solving the system numerically using Macaulay2 [42], we see that there are exactly 12 solutions, two of which are real. $\triangle$

In some cases, we are primarily interested in the combinatorics of a given polynomial system. This is when we turn to *tropical geometry*, which lies at the intersection of algebraic geometry, polyhedral geometry, and combinatorics. It takes place over the trop-

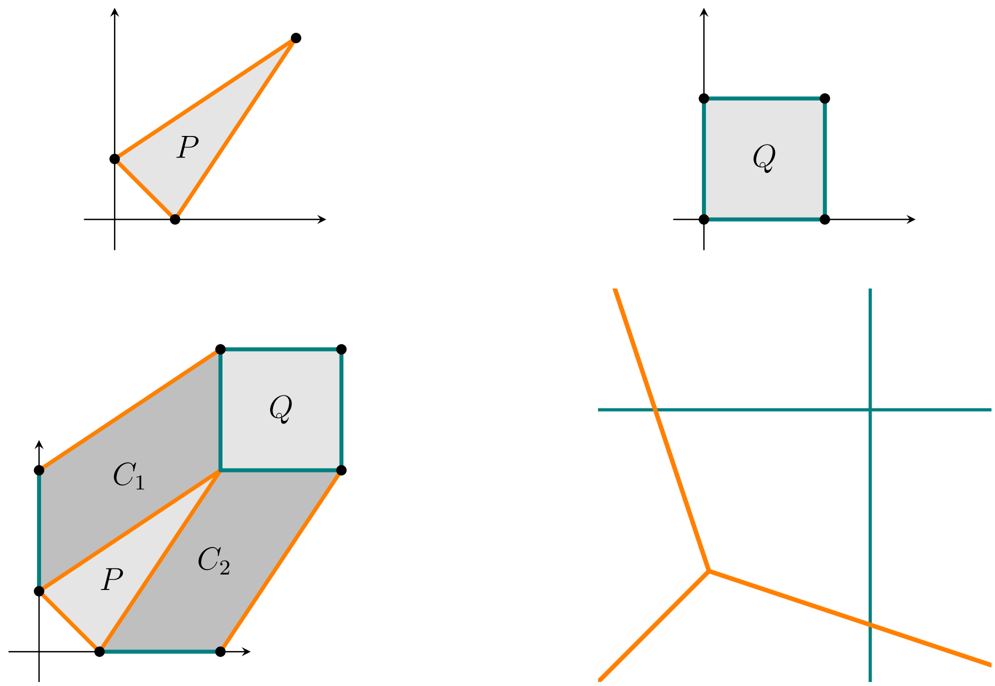

Figure 1.1: Top: Newton polytopes of the two polynomials from Example 1.1.1. Bottom left: The mixed volume of P and Q, which is the mixed volume of the polynomial system. The mixed cells in the Minkowski sum of P and Q are C_1 and C_2. Bottom right: The intersection of the tropical hypersurfaces defined by the two polynomials is the dual to the mixed subdivision.

ical semiring $\mathbb{R} \cup \{\infty\}$ where the usual operation of addition is replaced with taking the minimum, and the operation of multiplication is replaced with the usual addition. The techniques of tropical geometry transform a nonlinear polynomial equation into a piecewise linear function preserving some of the polynomial's key characteristics, including its combinatorial structure. Tropical geometry is sometimes referred to as the "combinatorial shadow" of algebraic geometry. Example 1.1.2 shows a tropical polynomial and the corresponding tropical curve it defines.

Example 1.1.2. Let $P(x, y)$ be a *tropical polynomial* in two variables defined by

$$\begin{aligned} P(x, y) &= 3 \odot x^2 \oplus x \odot y \oplus 3 \odot y^2 \oplus 1 \odot x \oplus 1 \odot y \oplus 0 \\ &= \min(3 + 2x, x + y, 3 + 2y, 1 + x, 1 + y, 0). \end{aligned}$$

The tropical curve in $\mathbb{R}^2$ defined by this polynomial is the dual to the subdivision it defines on its Newton polytope. The Newton polytope of $P(x, y)$ is the simplex with vertices

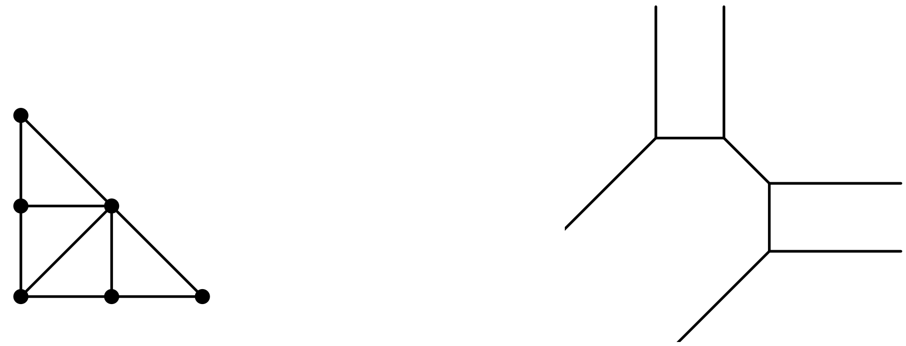

Figure 1.2: Induced subdivision of the Newton polytope of a tropical polynomial in two variables (left). The dual to this Newton polytope is the tropical curve with respect to the $\max$ convention, so we rotate the Newton polytope by 180 degrees. The tropical curve in $\mathbb{R}^2$ dual to the subdivision of the rotated simplex is shown on the right; this is the tropical curve defined by the tropical polynomial $P(x, y)$.

$(0, 0), (2, 0)$, and $(0, 2)$ with all lattice points marked. The tropical coefficients of each term of $P(x, y)$ determine the subdivision of the Newton polytope. Figure 1.2 shows the subdivision of the Newton polygon of $P(x, y)$ and the tropical curve defined by it. $\triangle$

1.2 Overview of the following chapters

1.2.1 Tropical convexity

The work presented in Chapter 2 is based on joint work with Sara Lamboglia and Faye Pasley Simon [51]. The project began in the fall of 2018 during the semester-long program on Nonlinear Algebra at the Institute for Computational and Experimental Research in Mathematics. In this chapter we discuss the interaction between tropical and classical convexity, with a focus on the tropical convex hull of convex sets and polyhedral complexes.

Tropical convexity is the analogue of classical convexity in the *tropical semiring* $\mathbb{R} \cup \infty$ with the operations of tropical addition $a \oplus b = \min(a, b)$ and tropical multiplication $a \odot b = a + b$. We say that a set $U \subset \mathbb{R}^{n+1}$ is *tropically convex* if it is closed under tropical addition and tropical scalar multiplication. That is, if for every $x, y \in U$ and $a, b \in \mathbb{R}$, the tropical linear combination $(a \odot x) \oplus (b \odot y)$ is in U. A tropically convex set satisfies $U = U + \mathbb{R}\mathbf{1}$, where $\mathbf{1} = (1, \ldots, 1)$; hence, it is customary to work in the tropical projective torus $\mathbb{R}^{n+1}/\mathbb{R}\mathbf{1}$. The quotient space $\mathbb{R}^{n+1}/\mathbb{R}\mathbf{1}$ and $\mathbb{R}^n$ as isomorphic as $\mathbb{R}$-vector spaces. We work with points in $\mathbb{R}^{n+1}/\mathbb{R}\mathbf{1}$ by choosing the coordinatization $x_0 = 0$. The *tropical convex hull* of a set $U \subset \mathbb{R}^{n+1}$ is defined as the smallest tropically convex subset of $\mathbb{R}^{n+1}$ containing U. This coincides with the set of all tropical linear combinations of points in U [21, Proposition 4].

The primary focus of tropical convexity is the study of *tropical polytopes*: the tropical convex hull of finite sets. One way to construct a tropical polytope in $\mathbb{R}^3/\mathbb{R}\mathbf{1}$ is to draw the tropical line segments between any two points. A tropical polytope, as in Figure 1.3(c), is not always classically convex, but does have an explicit description as the finite union of some ordinary polytopes [21]. Tropical polytopes are widely studied [21, 14, 13, 41, 78, 38, 2] and find applications in various areas of mathematics. Recently, techniques from tropical convexity have been applied to mechanism design [17], optimization [1], and maximum likelihood estimation [73]. Some specific applications are the resolution of monomial ideals [**D-Y**], and discrete event dynamic systems [3]. Moreover, computational tools exist to aid in further study of tropical polytopes [56, 2]. Tropical polytopes which are also ordinary polytopes are called *polytropes*, as discussed in [57]. Figure 1.3(d) shows a polytrope: an ordinary hexagon, which is also a tropical triangle. There also exist ordinary polytopes which are tropically convex, as in Figure 1.3(b), but they are not the tropical convex hull of a finite set of points. Example 1.2.1 shows some instances of tropically and classically convex sets.

Example 1.2.1. Consider the points $(0, 0, 0)$ and $(0, 4, 2)$ in the tropical projective torus $\mathbb{R}^3/\mathbb{R}\mathbf{1}$, which is isomorphic to $\mathbb{R}^2$, and the line segment between them. Figure 1.3(a) shows the tropical convex hull of this line segment, which is a tropically convex ordinary triangle. Let the points $(0, 0, 0), (0, 2, 3)$, and $(0, 3, 1)$ be the vertices of the triangle in Figure 1.3(b). This triangle is tropically convex, as it contains the tropical line segments

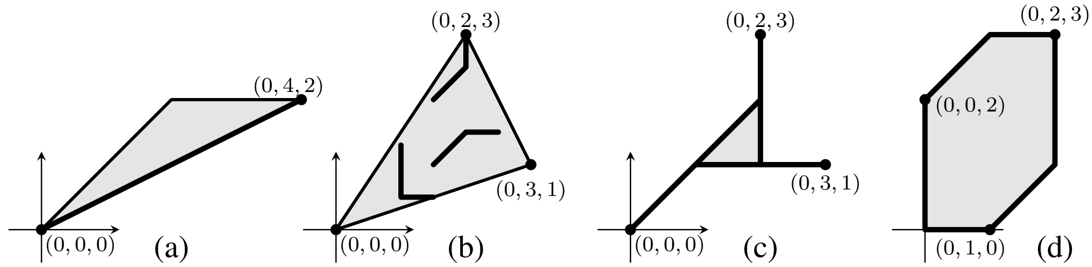

Figure 1.3: Left to right: The tropical convex hull of the line segment between $(0, 0, 0)$ and $(0, 4, 2)$ is a simplex; A tropically convex triangle contains the tropical line segments (bold) between any two points in the triangle; A tropical triangle, which is not classically convex. A polytrope: a tropical polytope, which is also an ordinary polytope. All images are in $\mathbb{R}^3/\mathbb{R}\mathbf{1} \cong \mathbb{R}^2$.

between any two points in the triangle. Figure 1.3(c) shows the tropical convex hull of the same three points, i.e., a tropical triangle. Note that it is not classically convex, since, for example, the line segment between $(0, 0, 0)$ and $(0, 2, 3)$ is not contained in the tropical triangle. The hexagon in Figure 1.3(d) is also a tropical triangle, as it is the tropical convex hull of the points $(0, 0, 2)$, $(0, 1, 0)$, and $(0, 2, 3)$; it is an example of a polytrope. $\triangle$

In Chapter 2 we further examine the relationship between classical and tropical convexity by studying the structure of the tropical convex hull of polyhedral and convex sets. The first result is the following:

Theorem (Theorems 2.2.10 and 2.2.21)**.** *If* $a, b \in \mathbb{R}^{n+1}/\mathbb{R}\mathbf{1}$ *and* $U \subset \mathbb{R}^3/\mathbb{R}\mathbf{1}$*, then*

(i) $\operatorname{tconv}\operatorname{conv}(a, b) = \operatorname{conv}\operatorname{tconv}(a, b)$*;*

(ii) $\operatorname{tconv}\operatorname{pos}(a) = \operatorname{pos}\operatorname{tconv}(0, a)$*;*

(iii) $\operatorname{tconv}\operatorname{conv} U = \operatorname{conv}\operatorname{tconv} U$*.*

In general, it is not true that ordinary and tropical convex hull commute as in part (i) above. Even small cases in $\mathbb{R}^4/\mathbb{R}\mathbf{1}$ can provide counterexamples; see Figure 2.3. However, the tropical convex hull of an ordinary polyhedron is itself an ordinary polyhedron. We characterize affine spaces, polyhedral sets, and convex cones that are tropically convex.

Theorem (Theorems 2.3.8 and 2.3.10)**.** *The following statements hold in* $\mathbb{R}^{n+1}/\mathbb{R}\mathbf{1}$*.*

(i) A full-dimensional ordinary polyhedron is tropically convex if and only if all of its defining halfspaces are tropically convex.

(ii) A convex cone is tropically convex if and only if its dual cone is generated by vectors with exactly one positive coordinate.

The tropical convex hull of an ordinary linear space L has been studied in [19] as the ∞th tropical secant variety of L. We give a combinatorial method for determining the dimension of the tropical convex hull of an ordinary affine space, and hence, an ordinary linear space.

Many properties and theorems valid in classical convexity are also valid in the tropical setting; for example, separation of convex sets [13, 41], Minkowski-Weyl Theorem [77, 37, 78], Carathéodory and Helly Theorems [21, 38], and Farkas Lemma [21]. Here we consider the classical result in algebraic geometry (see for example [28]) which bounds the degree of a projective variety X from below by

$$\dim \operatorname{span} X - \dim X + 1 \leq \deg X.$$

The description of the tropical convex hulls of line segments and rays provides information on their dimension. Using these results we study the tropical analogue of the above inequality in the case of tropical curves. A *tropical curve* $\Gamma \subset \mathbb{R}^{n+1}/\mathbb{R}\mathbf{1}$ is a one-dimensional balanced weighted polyhedral complex. See Section 2.4 for more details; see [64] for a comprehensive introduction to tropical curves. The tropical inequality we consider is

$$\dim \operatorname{tconv} \Gamma \leq \deg \Gamma,$$

where $\operatorname{span} X$ has been replaced by the tropical convex hull of Γ. In Section 2.4 we provide further details and a proof of the inequality relying entirely on tropical techniques.

I would like to acknowledge that the work in this chapter was partly supported by NSF-

DMS grant #1439786 while the authors were in residence at the Fall 2018 Nonlinear Algebra program at the Institute for Computational and Experimental Research in Mathematics in Providence, RI as well as during the Summer 2019 Collaborate@ICERM program. The author was also partially supported by the National Science Foundation under DMS grant #1600569. I am also particularly grateful to Josephine Yu for motivating this project, for helpful discussions, and a close reading.

1.2.2 Chemical reaction networks

Chapter 3 contains joint work with Elizabeth Gross [47]. We study the steady-state degree and mixed volume of a chemical reaction network.

A *chemical reaction network* $\mathcal{N} = (\mathcal{S}, \mathcal{C}, \mathcal{R})$ is a triple where $\mathcal{S} = \{A_1, A_2, \ldots, A_n\}$ is a set of n chemical *species*, $\mathcal{C} = \{y_1, y_2, \ldots, y_p\}$ is a set of p *complexes* (finite nonnegative-integer combinations of the species), and $\mathcal{R} = \{y_i \to y_j \mid y_i, y_j \in \mathcal{C}\}$ is a set of r *reactions*.

Each complex in $\mathcal{C}$ can be written in the form $y_{i1}A_1 + y_{i2}A_2 + \cdots + y_{in}A_n$ where $y_{ij} \in \mathbb{Z}_{\geq 0}$, and thus, we will view the elements of $\mathcal{C}$ as vectors in $\mathbb{Z}^n_{\geq 0}$, i.e. $y_i = (y_{i1}, y_{i2}, \ldots, y_{in})$. Additionally, to each complex of the chemical reaction network, we associate a monomial $x^{y_i} = x_{A_1}^{y_{i1}} x_{A_2}^{y_{i2}} \cdots x_{A_n}^{y_{in}}$ where $x_{A_i} = x_{A_i}(t)$ represents the concentration for species A_i with respect to time.

Let $y_i \to y_j$ be the reaction from the ith to the jth complex. To each reaction we associate a *reaction vector* $y_j - y_i$ that gives the net change in each species due to the reaction. Moreover, each reaction has an associated positive reaction rate constant k_{ij}. Given a chemical reaction network $(\mathcal{S}, \mathcal{C}, \mathcal{R})$ and a choice of $k_{ij} \in \mathbb{R}_{>0}$, the system of polynomial ordinary differential equations which describe the network dynamics under the assumption of mass-action kinetics is

$$\frac{dx}{dt} = \sum_{y_i \to y_j \in \mathcal{R}} k_{ij} x^{y_i} (y_j - y_i) =: f(x), \quad x \in \mathbb{R}^n.$$

Setting the left-hand side of the ODEs above equal to zero gives us a set of polynomial equations that we call the *steady-state equations*.

The stoichiometric subspace associated with the chemical reaction network $\mathcal{N} = (\mathcal{S}, \mathcal{C}, \mathcal{R})$ is a vector subspace of $\mathbb{R}^n$ spanned by the reaction vectors $y_j - y_i$, denoted by

$$S_{\mathcal{N}} := \mathbb{R}\{y_j - y_i \mid y_i \to y_j \in \mathcal{R}\}.$$

Given initial conditions $\mathbf{c} \in \mathbb{R}^n$, the stoichiometric compatibility class is the affine space $S_{\mathcal{N}} + \mathbf{c}$, and the *conservation equations* of $\mathcal{N}$ are the set of linear equations defining $S_{\mathcal{N}} + \mathbf{c}$.

Example 1.2.2. Consider the chemical reaction network $\{2A + B \to C, B \to 2B\}$ consisting of three species $\mathcal{S} = \{A, B, C\}$, four complexes $\mathcal{C} = \{2A + B, C, B, 2B\}$, and two reactions. Let k_1 and k_2 represent the positive reaction rate constants for each reaction, respectively. The exponent vectors for the first reaction are $(2, 1, 0)$ and $(0, 0, 1)$; for the second reaction they are $(0, 1, 0)$ and $(0, 2, 0)$. The monomials corresponding to the reactants are $x_A^2 x_B$ and x_B, and the reaction vectors are $(-2, -1, 1)$ and $(0, 1, 0)$. These give rise to the ordinary differential equations describing the network dynamics, as described above; the ODEs are the first three equations in the polynomial system (1.1).

Let c_A, c_B, and c_C be the initial concentrations for each respective species. The conservation equation defining the affine space $\mathcal{S}_{\mathcal{N}} + \mathbf{c}$ is the last equation in the polynomial system (1.1).

$$\begin{aligned} -2k_1 x_A^2 x_B &= 0 \\ -k_1 x_A^2 x_B + k_2 x_B &= 0 \\ k_1 x_A^2 x_B &= 0 \\ x_A + 2x_C - c_A - 2c_C &= 0. \end{aligned} \tag{1.1}$$

The number of complex solutions to this system for specific choices of k_1, k_2, c_A, and c_C is the *steady-state degree* of the network. $\triangle$

In Chapter 3, we are concerned with the parameterized system of equations formed by the steady-state and conservation equations, which we call the *steady-state system*. When the solution set of this polynomial system is zero-dimensional for generic rate constants $\mathbf{k}$ and initial conditions $\mathbf{c}$, we define the number of complex solutions to the system as the *steady-state degree* of the chemical reaction network $\mathcal{N}$. The steady-state degree is not only a bound on the number of real, positive steady-states, but also a measure of the algebraic complexity of solving the steady-state system for a given reaction network.

The steady-state system can be solved symbolically, using Gröbner bases, for example, or numerically, using homotopy-continuation-based solvers, such as Bertini [70], PHCpack [80], and HOM4PS2 [59]. In many cases, particularly when there are many variables, the steady-state degree of a family of networks can be difficult to establish. However, we can provide an upper bound by the Bézout bound, and in the absence of boundary solutions, the mixed volume of the polynomial system arising from the chemical reaction network. Here, we explore the mixed volumes of reaction networks further, giving formulas for three families of networks. In particular, we study the combinatorics of the Newton polytopes and their Minkowski sums that arise for these infinite families of networks.

The three infinite families of chemical reaction networks that we study are constructed by successively building on smaller networks to create larger ones. The base network for each family is: the cluster-stabilization subnetwork of the cell death model from [52], the Edelstein network [66], and the one-site phosphorylation cycle (see for example, motif (a) in [30]). For each network, we compute the mixed volume and steady-state degree of the networks using various techniques. As shown in Table 3.1, each of these examples illustrate a different relationship between the steady-state degree and the mixed volume of the steady-state system. The most significant of these three case studies is the exploration of the multi-site distributive phosphorylation system in Section 3.3.3. The n-site distributive phosphorylation system can be obtained by successively gluing together n copies of the

Table 1.1: Summary of results on the families of chemical reaction networks studied in this paper. See Theorems 3.3.8, 3.3.11, and 3.3.13; Propositions 3.3.2, 3.3.3, 3.3.4, 3.3.7, and 3.3.12; and Conjecture 3.3.18.

CRN family	**Bézout bound**	**Mixed volume**	**Steady-state degree**
Cluster-stabilization, CS_n	n	$n-2$	n (includes two boundary sols)
Edelstein, E_n	2^{n+1}	3	3
Multisite distributive phosphorylation, PC_n	2^{3n+1}	$\frac{(n+1)(n+4)}{2}-1$	Conjecture: $2n+1$

one-site phosphorylation cycle [46]. We give the mixed volume of the *randomized* steady-state system of n-site distributive phosphorylation. Determining the mixed volume requires computing the normalized volume of a $(3n+3)$-dimensional $(0,1)$-polytope with $5n+4$ vertices and $3n+7$ facets. We also show that this polytope of interest is the matching polytope of a graph.

I would like to acknowledge that this work was partially supported by NSF DMS-1600569, as well as by the National Science Foundation under Grant No. DMS-1439786 while the authors were in residence at the Institute for Computational and Experimental Research in Mathematics in Providence, RI, during the Fall 2018 semester.

1.2.3 Homotopy continuation

Chapter 4 contains joint work with Timothy Duff, Anders Jensen, Kisun Lee, Anton Leykin, and Jeff Sommars [26]. We study methods for finding the solution set of a generic system in a family of polynomial systems with parametric coefficients.

Homotopy continuation is a key technique of numerical algebraic geometry, the area which considers questions of complex algebraic geometry through algorithms that employ numerical approximate computations. The method of homotopy continuation is a standard technique used to compute approximations to solutions of polynomial systems. Families of polynomial systems with parametric coefficients play one of the central roles in this method. Most homotopy continuation techniques can be viewed as going from a generic system in the family to a particular one. Knowing the solutions of a generic system, we can find the solutions of a particular one.

The main problem we address in Chapter 4 is how to solve a generic system in a family of systems $F_p = \left(f_p^{(1)}, \ldots, f_p^{(N)}\right)$, where each polynomial $f_p^{(i)}$ has finitely many complex parameters p and variables $x_1, \ldots, x_n$. We are particularly interested in *linear parametric* families of systems. These are systems with affine linear parametric coefficients, such that for a generic choice of coefficients p, the set of solutions $x = (x_1, \ldots, x_n)$ to $F_p(x) = 0$ is nonempty. This implies that there are at least as many equations as variables; i.e., $N \geq n$. The number of parameters p is arbitrary, although we require that for a generic x there exists p, such that $F_p(x) = 0$.

Linear parametric systems form a large class which includes *sparse polynomial systems*. These are square systems, $n = N$, with a fixed monomial support for each equation, and a distinct parameter for the coefficient of each monomial. *Polyhedral homotopy* methods for solving sparse systems stem from the BKK (Bernstein, Khovanskii, Kouchnirenko) bound on the number of solutions [5]. The BKK bound is the number of solutions of a generic square system, which is the same as the mixed volume of the system. Polyhedral homotopies provide an optimal solution to sparse systems in the sense that they are designed to follow exactly as many paths as the number of solutions of a generic system given by the BKK bound.

The method we propose is not optimal in the above sense. The expected number of homotopy paths followed can be larger than the number of solutions, although not significantly larger. We use *linear segment homotopies*, which are significantly simpler, and less computationally expensive to follow in practice. Example 1.2.3 gives abrief overview of linear segment homotopies.

Example 1.2.3. Let $x \in \mathbb{C}^n$, and $F(x)$ and $G(x)$ be two polynomial systems. Suppose that we want to solve the *target* system $F(x)$, but its solutions are not easily obtained. However, the solutions of the *start* system $G(x)$ are easy to find. For example, $G(x)$ is the system on the left, and $F(x)$ is to the right:

$$x^2 - 1 = 0 \qquad\qquad x^2 + 2xy + 3y^2 - 1 = 0$$
$$y^2 - 1 = 0 \qquad\qquad xy + 2y^2 = 0.$$

We can use the linear segment homotopy between F and G defined by the family of systems

$$H(x,t) = (1-t)\gamma_1 G(x) + t\gamma_2 F(x),$$

where $t \in [0,1]$ and $\gamma_1, \gamma_2 \in \mathbb{C}$. At $t = 0$, $H(x,0) = 0$ agrees with $G(x) = 0$, hence it has the same solutions, and at $t = 1$, $H(x,1) = 0$ agrees with $F(x) = 0$. We can trace the solutions of $G(x) = 0$ to the solutions of $F(x) = 0$ as t goes from zero to one. We use the generic coefficients γ_1 and γ_2 to avoid singularities when tracing the solutions of G to those of F. $\triangle$

We consider the complex linear space of square systems F_p, where the monomial support of the polynomials $f_p^{(1)}, \ldots, f_p^{(n)}$ in the variables $x = (x_1, \ldots, x_n)$ is fixed, and the parameters $p \in \mathbb{C}^m$ vary. Our goal is to find all solutions to one generic system in the family by using the monodromy action on a set of known solutions in the family. Our main contribution is a new framework to describe algorithms for solving polynomial systems using monodromy; we call it the *Monodromy Solver* (MS) framework. To organize the discovery of new solutions in the MS framework, we represent the set of homotopies by a finite undirected graph. We provide several examples, including an example arising from chemical reaction networks.

Our current implementation in Macaulay2 [42] shows it is competitive with the state-of-the-art implementations of polyhedral homotopies in PHCpack [80] and HOM4PS2 [59] for solving sparse systems. In a setting more general than sparse, we demonstrate examples of linear parametric systems for which our implementation exceeds the capabilities of the existing sparse system solvers and blackbox solvers based on other ideas. Our method and its implementation not only provide a new general tool for solving polynomial systems, but also can solve some problems out of reach for other existing software.

I would like to acknowledge that this work was supported in part by the National Science Foundation under Grant No. DMS-1151297 and DMS-1719968.

CHAPTER 2

TROPICAL CONVEXITY

The work in this chapter, with modifications and additions, is based on joint work with Sara Lamboglia and Faye Pasley Simon [51].

2.1 Background and motivation

Tropical convexity is the analogue of classical convexity in the *tropical semiring* $(\mathbb{R}, \oplus, \odot)$. The tropical semiring is the set of real numbers together with the operations of *tropical addition*, equivalent to taking the minimum of two numbers, and *tropical multiplication*, equivalent to the sum of two numbers. For real numbers a and b, the operations are defined as follows:

$$a \oplus b = \min(a, b) \quad \text{and} \quad a \odot b = a + b.$$

If we consider two elements x and y in $\mathbb{R}^n$, a semimodule over the tropical semiring, and a scalar $c \in \mathbb{R}$, then we have the following tropical addition and tropical scalar multiplication:

$$(x_1, \ldots, x_n) \oplus (y_1, \ldots, y_n) = (x_1 \oplus y_1, \ldots, x_n \oplus y_n) \quad \text{and}$$
$$c \odot (x_1 \ldots, x_n) = (c \odot x_1, \ldots, c \odot x_n).$$

A comprehensive introduction to tropical geometry in general, and tropical convexity in particular can be found in [64, 21]. The following is an explicit example of the tropical operations described above.

Example 2.1.1. Using real numbers and points in $\mathbb{R}^3$, the tropical operations are:

Tropical addition:	$2 \oplus 5 = 2,$	$0 \oplus 3 = 0,$	$-1 \oplus 1 = -1$
Tropical multiplication:	$2 \odot 5 = 7,$	$0 \odot 3 = 3,$	$-1 \odot 1 = 0$
Tropical addition:	$(0, 1, -2) \oplus (3, -1, 2) = (0, -1, -2)$		
Tropical scalar multiplication:	$3 \odot (1, -4, 0) = (4, -1, 3).$		△

A set $U \subset \mathbb{R}^{n+1}$ is *tropically convex* if for every $x, y \in U$ and $a, b \in \mathbb{R}$ the tropical linear combination $(a \odot x) \oplus (b \odot y)$ is in U. It is customary to work with tropically convex sets in the tropical projective torus $\mathbb{R}^{n+1}/\mathbb{R}\mathbf{1}$, since any tropically convex set U satisfies $U = U + \mathbb{R}\mathbf{1}$, where $\mathbf{1} = (1, \ldots, 1)$. Moreover, the quotient space $\mathbb{R}^{n+1}/\mathbb{R}\mathbf{1}$ and $\mathbb{R}^n$ are isomorphic as $\mathbb{R}$-vector spaces via the map

$$\begin{aligned} \phi : \ \mathbb{R}^{n+1}/\mathbb{R}\mathbf{1} &\to \mathbb{R}^n \\ (x_0, \ldots, x_n) &\mapsto (x_1 - x_0, \ldots, x_n - x_0). \end{aligned} \tag{2.1}$$

The *tropical convex hull* of a set $U \subset \mathbb{R}^{n+1}$ is defined as the smallest tropically convex subset of $\mathbb{R}^{n+1}$ containing U. Develin and Sturmfels [21, Proposition 4] show that the tropical convex hull of a set $U \subset \mathbb{R}^{n+1}$ coincides with the set of all tropical linear combinations of points in U, that is

$$(a_1 \odot u_1) \oplus (a_2 \odot u_2) \oplus \cdots \oplus (a_k \odot u_k), \quad \text{for } u_1, \ldots, u_k \in U, \text{ and } a_1, \ldots, a_k \in \mathbb{R}. \tag{2.2}$$

Throughout this chapter we show images of tropically convex sets in the tropical projective torus $\mathbb{R}^3/\mathbb{R}\mathbf{1}$ and $\mathbb{R}^4/\mathbb{R}\mathbf{1}$. We represent these by choosing the coordinatization $x_0 = 0$ and projecting to $\mathbb{R}^2$ and $\mathbb{R}^3$, respectively, by deleting the first coordinate. For example, a point $(x_0, x_1, x_2) \in \mathbb{R}^3/\mathbb{R}\mathbf{1}$ is translated to $(0, x_1 - x_0, x_2 - x_0)$ and represented as $(x_1 - x_0, x_2 - x_0)$ in $\mathbb{R}^2$.

Example 2.1.2. Let $x = (1, -1, 0)$ and $y = (-2, 1, -1)$ be two points in $\mathbb{R}^3/\mathbb{R}\mathbf{1}$. We can identify x with $-1 \odot x = (0, -2, -1)$ and y with $2 \odot y = (0, 3, 1)$. These two points can be represented in the plane $\mathbb{R}^2$ as the projection onto the last two coordinates, as shown in Figure 2.1. The tropical convex hull of x and y is the tropical line segment between them.

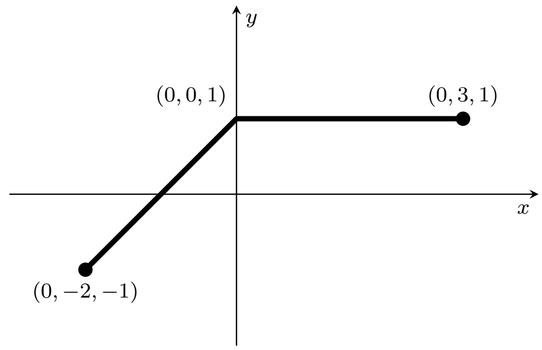

Figure 2.1: The tropical line segment connecting the points $(0, -2, -1)$ and $(0, 3, 1)$ with *pseudovertex* $(0, 0, 1)$.

For example, we have that $(2 \odot x) \oplus y = (2, 0, 1) \oplus (0, 3, 1) = (0, 0, 1)$, which is the *pseudovertex* of the tropical line segment. $\triangle$

The goal of this chapter is to explore the interplay between tropical convexity and its classical counterpart. We aim to describe the tropical convex hull of polyhedra, polyhedral complexes, and in particular, tropical curves.

The primary focus of tropical convexity is the study of *tropical polytopes*: the tropical convex hull of finite sets. These are widely studied [21, 14, 13, 41, 78, 38, 2] and find applications in various areas of mathematics. Recently, techniques from tropical convexity have been applied to mechanism design [17], optimization [1], and maximum likelihood estimation [73]. Some specific applications are the resolution of monomial ideals [22], and discrete event dynamic systems [3]. Moreover, computational tools exist to aid in further study of tropical polytopes [56, 2].

A tropical polytope is not always classically convex, as can be seen in Figure 2.2 (left). However, it does have an explicit description as the finite union of some ordinary polytopes [21]. Tropical polytopes, which are also ordinary polytopes, are called *polytropes* as discussed in [57]. An example of a polytrope is shown in Figure 2.2 (middle). On the other hand, there exist ordinary polytopes which are tropically convex, but are not finitely generated in the tropical sense. That is, they are not the tropical convex hull of a finite set of points. An ordinary polytope, which is also tropically convex can be seen in Figure 2.2 (right).

Example 2.1.3. Figure 2.2 below depicts a tropical polytope which is not classically convex (left), a polytrope (middle), and a classical polytope which is tropically convex but is not a tropical polytope (right). The tropical polytope is the tropical convex hull of the

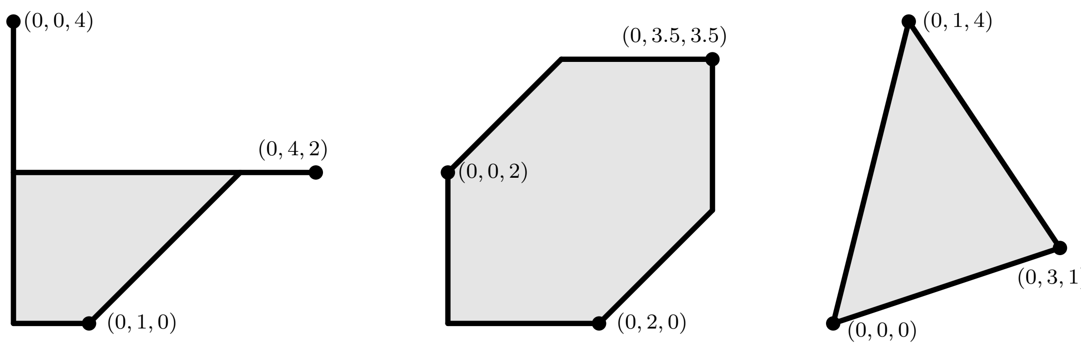

Figure 2.2: From left to right: a tropical polytope, a polytrope, a tropically convex classical polytope.

points $(0, 1, 0)$, $(0, 0, 4)$, and $(0, 4, 2)$. The polytrope is the tropical convex hull of the points $(0, 2, 0)$, $(0, 0, 2)$ and $(0, 3.5, 3.5)$. It is a polytope in both the classical and tropical sense. The classical polytope, which is also tropically convex, is the convex hull of the points $(0, 0, 0)$, $(0, 3, 1)$, and $(0, 1, 4)$. $\triangle$

In this chapter, we further examine the relationship between classical and tropical convexity by studying the structure of the tropical convex hull of polyhedral sets. Tropical convex hulls of polyhedra already appear in the literature, but only in special cases. For example, the tropical convex hull of a linear space is a union of secondary cones [19]. Another result shows that the tropical convex hull of a line segment in special position is homeomorphic to a simplex [48]. In Theorem 2.2.10 we show that the classical and tropical convex hull commute for two points in any dimension. Furthermore, the two operations commute for any set in $\mathbb{R}^3/\mathbb{R}\mathbf{1}$, as Theorem 2.2.21 shows.

In general, it is not true that ordinary and tropical convex hull commute. Even small cases in $\mathbb{R}^4/\mathbb{R}\mathbf{1}$ can provide counterexamples, as shown in Figure 2.3. Nonetheless, the tropical convex hull of an ordinary polyhedron is itself an ordinary polyhedron. In Section 2.3 we characterize tropically convex ordinary halfspaces (Proposition 2.3.6), polyhedral sets (Theorem 2.3.8), and convex cones (Theorem 2.3.10). Furthermore, we give a combinatorial description of the dimension of the tropical convex hull of an ordinary affine space.

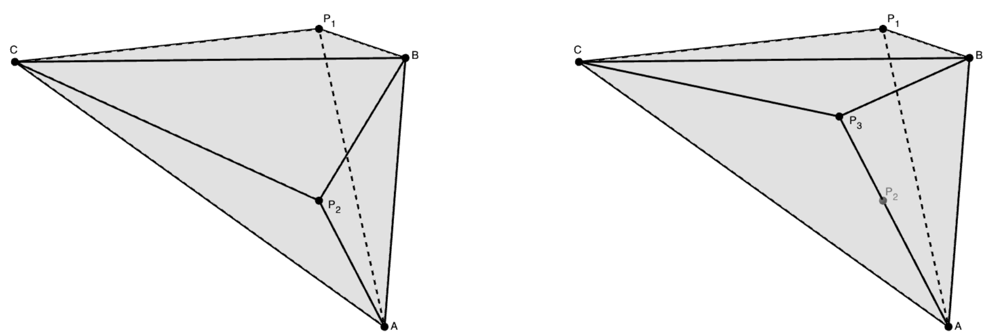

Figure 2.3: Let $A = (0,0,0), B = (1,2,2)$, and $C = (3,1,2)$. The polytope on the left is the convex hull of $\operatorname{tconv}(A,B,C)$; the polytope on the right is the tropical convex hull of the triangle $\operatorname{conv}(A,B,C)$. Observe that although $\operatorname{conv}\operatorname{tconv}(A,B,C) \neq \operatorname{tconv}\operatorname{conv}(A,B,C)$, we have the containment $\operatorname{conv}\operatorname{tconv}(A,B,C) \subset \operatorname{tconv}\operatorname{conv}(A,B,C)$.

Many properties and theorems valid in classical convexity are also valid in the tropical setting; for example, separation of convex sets [13, 41], Minkowski-Weyl Theorem [77, 37, 78], Carathéodory and Helly Theorems [21, 38], and Farkas Lemma [21]. Here we consider the classical result in algebraic geometry (see for example [28]) which bounds the degree of a projective variety X from below by

$$\dim \operatorname{span} X - \dim X + 1 \leq \deg X. \tag{2.3}$$

Our description of the tropical convex hulls of line segments and rays provides information on their dimensions. Using this result we study a tropical analogue of (2.3) in the case of tropical curves. A tropical curve $\Gamma \subset \mathbb{R}^{n+1}/\mathbb{R}\mathbf{1}$ is a balanced weighted polyhedral complex.

We define this in more detail is Section 2.4; see [64] for a more comprehensive introduction to tropical curves.

In the inequality (2.3), we can substitute $\operatorname{span} X$ either with the tropical convex hull of a tropical curve Γ or with a tropical linear space of smallest dimension containing Γ. The latter may not be unique and it is not easy to determine. Thus, we choose to replace $\operatorname{span} X$ with the tropical convex hull $\operatorname{tconv} \Gamma$. The tropical analogue of (2.3) we consider is

$$\dim \operatorname{tconv} \Gamma \leq \deg \Gamma. \tag{2.4}$$

The following is an example of the tropical convex hull of a tropical curve.

Example 2.1.4. Let $\Gamma \subset \mathbb{R}^3/\mathbb{R}\mathbf{1}$ be the tropical curve of degree two depicted in Figure 2.4. Note that Γ is a one-dimensional polyhedral complex. It has two rays in each of the

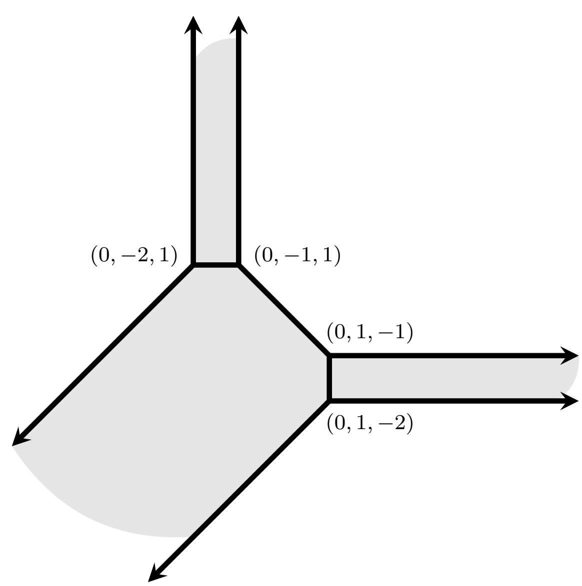

Figure 2.4: Tropical curve $\Gamma \subset \mathbb{R}^3/\mathbb{R}\mathbf{1}$ of degree two (bold) and its tropical convex hull (shaded region).

directions $(0,1,0)$, $(0,0,1)$, and $(0,-1,-1)$, and three bounded cells as the ordinary line segments between $(0,-2,1)$ and $(0,-1,1)$, $(0,-1,1)$ and $(0,1,-1)$, and $(0,1,-1)$ and $(0,1,-2)$. The tropical convex hull of Γ is the two-dimensional shaded region shown in Figure 2.4. $\triangle$

If Γ is *realizable*, i.e., Γ can be realized as the tropicalization of an algebraic curve, then (2.4) follows immediately from the classical inequality (2.3). The tropical curve Γ in Example 2.1.4 is realizable. For example, the polynomial $p(x,y) = 3t^3x^2 + 5xy - 7t^3y^2 + 8tx - ty + 1$ over the field of Puiseux series $\mathbb{C}\{\{t\}\}$ tropicalizes to $P(x,y)$, the tropical polynomial of Example 1.1.2. In Section 2.4 we give a proof of (2.4) for fan tropical curves, balanced weighted polyhedral fans, that relies entirely on tropical techniques.

The structure of this chapter is as follows. In Section 2.2 we recall basic definitions of tropical convexity. In Section 2.2.1 we describe the tropical convex hull of a line segment and a ray as ordinary polyhedra. Using these results, we show the dimensions are easily calculable using coordinates of the respective endpoints. Results stating that that ordinary and tropical convex hull commute in two dimensions are in Section 2.2.2. In Section 2.3 we prove that convexity and polyhedrality are preserved after taking the tropical convex hull. The characterization of tropically convex ordinary halfspaces and convex sets can be found in Section 2.3.1, affine spaces and their tropical convex hull are the subject of Section 2.3.2. Finally, in Section 2.4, we use our results to prove inequality (2.4) in the case of fan tropical curves.

2.2 Line segments, rays, and sets in $\mathbb{R}^3/\mathbb{R}\mathbf{1}$

Key definitions from tropical convexity are presented in the first part of this section. A description of the tropical convex hull of any arbitrary set is given in Proposition 2.2.5. In Theorem 2.2.10 we show that ordinary and tropical convex hull commute in any dimension in the case of two points. Corollary 2.2.16 uses this result to provide a way to find the dimension of the tropical convex hull of a line segment or a ray using the coordinates of its endpoints. In Theorem 2.2.21, we prove that ordinary and tropical convex hull always commute in the two-dimensional tropical projective torus.

A set $U \subset \mathbb{R}^{n+1}/\mathbb{R}\mathbf{1}$ is *tropically convex* if $(a \odot x) \oplus (b \odot y)$ is in U for any $x, y \in U$ and $a, b \in \mathbb{R}$. Recall from Section 2.1 that we work in the tropical projective torus $\mathbb{R}^{n+1}/\mathbb{R}\mathbf{1}$, since a tropically convex set U is closed under tropical scalar multiplication, i.e., $U = U + \mathbb{R}\mathbf{1}$. This implies that $\operatorname{tconv} U = \operatorname{tconv} U'$ where $U' = \{(0, u_1 - u_0, \ldots, u_n - u_0) \mid (u_0, u_1, \ldots, u_n) \in U\}$. Hence, given a set $V \subset \mathbb{R}^{n+1}/\mathbb{R}\mathbf{1}$, we consider its tropical convex hull to be the image in $\mathbb{R}^{n+1}/\mathbb{R}\mathbf{1}$ of the tropical convex hull of $\{(0, v_1, \ldots, v_n) \in \mathbb{R}^{n+1} \mid v + \mathbb{R}\mathbf{1} \subset V\}$. Additionally, for $\operatorname{conv}\operatorname{tconv} V$, we first identify $\operatorname{tconv} V$ with its image under the projection ϕ from (2.1) and then work with its convex hull in $\mathbb{R}^n$. This is equivalent to taking the convex hull in $\mathbb{R}^{n+1}$ and then taking the quotient with $\mathbf{1} \in \mathbb{R}^{n+1}$.

The *tropical convex hull* of $U \subset \mathbb{R}^{n+1}$ is the smallest tropically convex set that contains U. This is defined equivalently in [77] as

$$\operatorname{tconv} U = \bigcup_{V \subset U : |V| < \infty} \operatorname{tconv} V. \tag{2.5}$$

If $V = \{v_1, \ldots, v_k\}$ is a finite set, then by [77, Definition 2.1] its tropical convex hull is given by

$$\operatorname{tconv} V = \{a_1 \odot v_1 \oplus \cdots \oplus a_k \odot v_k \mid v_i \in V, a_i \in \mathbb{R}\}.$$

Furthermore, points in $\operatorname{tconv} V$ can be characterized by types as defined in [21]. Let $[n] = \{1, \ldots, n\}$ and $[n]_0 = \{0, 1, \ldots, n\}$. Given a point $x \in \mathbb{R}^{n+1}/\mathbb{R}\mathbf{1}$, the *type of x relative to V*, or *covector* in [33, 63], is the $(n+1)$-tuple $T_x = (T_0, T_1, \ldots, T_n)$ such that $T_j \subseteq [k]$ for all $j \in [n]_0$, and $i \in T_j$ if the minimum for $v_i - x$ is obtained in the jth coordinate. This is equivalent to saying that $i \in T_j$ if $x \in v_i + \mathcal{S}_j$, where $\mathcal{S}_j$ is a *sector* of $\mathbb{R}^n$ spanned by $\{-e_i : i \in [n]_0, i \neq j\}$ for $j \in [n]_0$. Here, $e_0, e_1 \ldots, e_n$ represent the standard unit vectors in $\mathbb{R}^{n+1}$ with $e_{ij} = 1$ if $i = j$ and $e_{ij} = 0$ otherwise. The cone $\mathcal{S}_j$ is the closure of one of the $n+1$ connected components of $\mathbb{R}^n \setminus L_{n-1}$. By L_{n-1} we mean the max-standard tropical hyperplane. This is the tropicalization of $V(x_1 + \ldots + x_n + 1)$ with the max convention, i.e., the tropical linear form $x_1 \oplus \cdots \oplus x_n \oplus 0$, where $a \oplus b = \max(a, b)$. Figure 2.5 visualizes the $\min$- and $\max$-standard tropical hyperplanes in $\mathbb{R}^3/\mathbb{R}\mathbf{1}$ and the $\min$-standard tropical hyperplane in $\mathbb{R}^4/\mathbb{R}\mathbf{1}$. An example of the cell decomposition of $\mathbb{R}^3/\mathbb{R}\mathbf{1}$ and the computation of some types relative to a finite set of points V can be found in Example 2.2.3.

Remark 2.2.1. Given a finite set of points $V = \{v_1, \ldots, v_k\} \subset \mathbb{R}^{n+1}/\mathbb{R}\mathbf{1}$, we want to classify all types for $x \in \mathbb{R}^{n+1}/\mathbb{R}\mathbf{1}$ relative to V. Hence, for each $j \in [n]_0$ and each $i \in [k]$, we want to determine all points x for which T_j contains i. That is, all points x for which v_i is located in the jth min sector $x + \mathcal{S}_j^{\min}$. Equivalently, we may instead consider all points x which are located in the jth max sector $v_i + \mathcal{S}_j^{\max}$. The latter provides a quick way for drawing the tropical convex hull in two and three dimensions. For a finite set $V \subset \mathbb{R}^{n+1}/\mathbb{R}\mathbf{1}$, we draw a max-standard tropical hypeplane with apex at each of the vertices $v_i \in V, i \in [k]$. The union of the bounded cells in the resulting cell decomposition of $\mathbb{R}^{n+1}/\mathbb{R}\mathbf{1}$ is the tropical convex hull $\operatorname{tconv} V$. The reader may wish to consult [21, Section 3] for further details. $\triangle$

Example 2.2.2. The min-standard tropical hyperplane, $L_1^{\min}$ in $\mathbb{R}^3/\mathbb{R}\mathbf{1}$, is a one-dimensional polyhedral fan centered at the origin with rays $e_0 = (0, -1, -1), e_1 = (0, 1, 0)$, and $e_2 = (0, 0, 1)$. The three closed sectors are the connected components of $(\mathbb{R}^3/\mathbb{R}\mathbf{1}) \setminus L_1^{\min}$; namely, $\mathcal{S}_0 = \operatorname{pos}(e_1, e_2), \mathcal{S}_1 = \operatorname{pos}(e_0, e_2)$, and $\mathcal{S}_2 = \operatorname{pos}(e_0, e_1)$. Similarly, the max-standard tropical hyperplane $L_1^{\max} \subset \mathbb{R}^3/\mathbb{R}\mathbf{1}$ is a one-dimensional polyhedral fan centered at the origin with rays $-e_0, -e_1$, and $-e_2$. Both tropical hyperplanes are depicted in the first two pictures of Figure 2.5. The third picture in Figure 2.5 shows the min-standard tropical

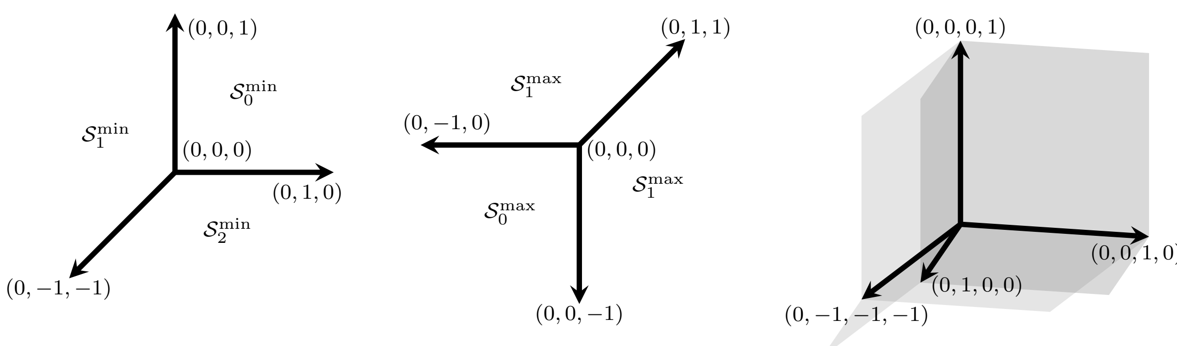

Figure 2.5: Left to right: Min-standard tropical hyperplane in $\mathbb{R}^3/\mathbb{R}\mathbf{1}$ (left); Max-standard tropical hyperplane in $\mathbb{R}^3/\mathbb{R}\mathbf{1}$ (middle); Min-standard tropical hyperplane in $\mathbb{R}^4/\mathbb{R}\mathbf{1}$ (right).

hyperplane in $\mathbb{R}^4/\mathbb{R}\mathbf{1}$. It is a two-dimensional fan centered at the origin with six maximal cones. The four closed sectors are $\mathcal{S}_0 = \operatorname{pos}(e_1, e_2, e_3)$, $\mathcal{S}_1 = (e_0, e_2, e_3)$, $\mathcal{S}_2 = (e_0, e_1, e_3)$, and $\mathcal{S}_3 = (e_0, e_1, e_2)$. $\triangle$

Example 2.2.3. Let $v_1 = (0, 1, 0), v_2 = (0, 4, 2)$, and $v_3 = (0, 0, 4)$. Figure 2.6 shows the polyhedral decomposition of $\mathbb{R}^3/\mathbb{R}\mathbf{1}$ relative to $V = \{v_1, v_2, v_3\}$. The solid lines and shaded region represent the tropical triangle $\operatorname{tconv}(v_1, v_2, v_3)$. The tropical polytope is the union of all the bounded cells in the polyhedral decomposition of $\mathbb{R}^3/\mathbb{R}\mathbf{1}$ relative to V. The

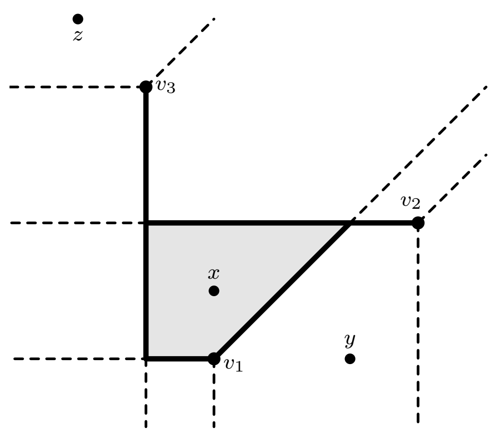

Figure 2.6: The polyhedral decomposition of $\mathbb{R}^3/\mathbb{R}\mathbf{1}$ from Example 2.2.3 and the tropical triangle $\operatorname{tconv}(v_1, v_2, v_3)$ in bold and shaded.

type of $x = (0, 1, 1)$ is $T_x = (\{2\}, \{3\}, \{1\})$ since $\min(v_1 - x)$ is obtained in the third coordinate, $\min(v_2 - x)$ is obtained in the first coordinate, and $\min(v_3 - x)$ is obtained in the second coordinate. Similarly, the type of $y = (0, 3, 0)$ is $T_y = (\{2\}, \{1, 3\}, \emptyset)$, since the minimum is never achieved in the third coordinate for any $v_i - x$. The the type of $z = (0, -1, 5)$ is $T_z = (\emptyset, \emptyset, \{1, 2, 3\})$ since the minimum is always achieved in the third coordinate. $\triangle$

The tropical analogue of the classical Farkas Lemma is the following proposition.

Proposition 2.2.4. *[21, Proposition 9] For all $x \in \mathbb{R}^{n+1}/\mathbb{R}\mathbf{1}$, exactly one of the following is true.*

(i) The point x is in the tropical polytope $P = \operatorname{tconv} V$.

(ii) There exists a tropical hyperplane which separates x from P.

The proof of Proposition 2.2.4 [21] states that $x \in \operatorname{tconv} V$ if and only if the jth entry of T_x is nonempty for all j, meaning there exists at least one v_i such that $x \in v_i + \mathcal{S}_j$ [58, Lemma 28]. As a consequence, we have the following proposition which also holds true in the case of $U \subset (\mathbb{R} \cup \{\infty\})^n$ [63, Proposition 7.3]. We include a proof for completeness. Figure 2.7 gives an example of (2.6) in $\mathbb{R}^3/\mathbb{R}\mathbf{1}$.

Proposition 2.2.5. *If $U \subset \mathbb{R}^{n+1}/\mathbb{R}\mathbf{1}$, then the tropical convex hull of U is equal to the intersection of the Minkowski sums of U with each of the sectors. That is*

$$\operatorname{tconv} U = \bigcap_{j=0}^{n} (U + \mathcal{S}_j). \tag{2.6}$$

Proof. If $x \in \operatorname{tconv} U$, then (2.5) implies that $x \in \operatorname{tconv} V$ for some finite set $V \subset U$. By the Tropical Farkas Lemma [21] we obtain $x \in \bigcap_{j=0}^{n}(V+\mathcal{S}_j)$, hence $x \in \bigcap_{j=0}^{n}(U+\mathcal{S}_j)$. On the other hand, if $x \in \bigcap_{j=0}^{n}(U+\mathcal{S}_j)$, then there exist $u_1, \ldots, u_n \in U$ such that $x \in u_j + \mathcal{S}_j$ for every j. For $V = \{u_1, \ldots, u_n\}$ it follows that $x \in \bigcap_{j=0}^{n}(V + \mathcal{S}_j) = \operatorname{tconv} V \subset \operatorname{tconv} U$. $\square$

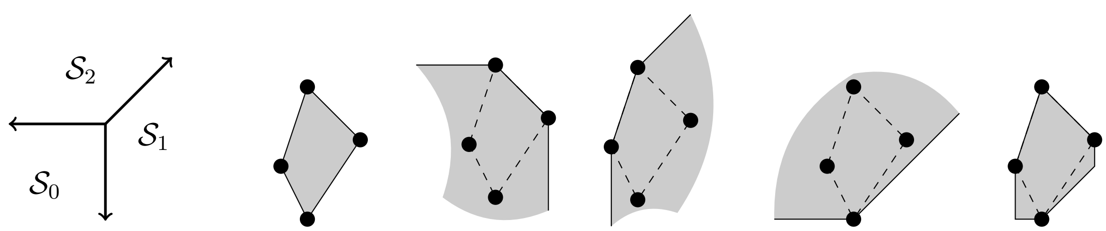

Figure 2.7: Illustration of Proposition 2.2.5 in $\mathbb{R}^3/\mathbb{R}\mathbf{1}$. From left to right: The three sectors, a polytope P, the Minkowski sums $P + \mathcal{S}_0$, $P + \mathcal{S}_1$, $P + \mathcal{S}_2$, and $\operatorname{tconv} P$.

As a direct consequence of Proposition 2.2.5 we obtain Corollary 2.2.6 stating that the convexity of a set is preserved under taking tropical convex hull. Note that it can also be proven directly by using the definition of tropical convex hull. Lemma 2.2.7 shows that repeatedly taking the convex hull and tropical convex hull of a set stabilizes after one step. That is, even though for an arbitrary set U, $\operatorname{tconv}\operatorname{conv} U$ and $\operatorname{conv}\operatorname{tconv} U$ are not necessarily the same, it is the case that $\operatorname{tconv}\operatorname{conv} U = \operatorname{tconv}(\operatorname{conv}\operatorname{tconv} U)$.

Corollary 2.2.6. *If* $P \subset \mathbb{R}^{n+1}/\mathbb{R}\mathbf{1}$ *is convex, then* $\operatorname{tconv} P$ *is convex.*

Proof. Let $P \subset \mathbb{R}^{n+1}/\mathbb{R}\mathbf{1}$ be a convex set. By Proposition 2.2.5 the tropical convex hull of P is $\operatorname{tconv} P = \bigcap_{j=0}^{n}(P + \mathcal{S}_j)$. Each of the sets $P + \mathcal{S}_j$ are convex, since they are each the Minkowski sum of convex sets. Moreover, the intersection of convex sets is convex. Hence, $\operatorname{tconv} P$ is convex. $\square$

Corollary 2.2.7. *If* $U \subset \mathbb{R}^{n+1}/\mathbb{R}\mathbf{1}$, *then* $\operatorname{tconv}\operatorname{conv} U = \operatorname{tconv}(\operatorname{conv}\operatorname{tconv} U)$.

Proof. We have that $U \subseteq \operatorname{tconv} U$ for any $U \subset \mathbb{R}^{n+1}/\mathbb{R}\mathbf{1}$, and hence, $\operatorname{conv} U \subseteq \operatorname{conv}\operatorname{tconv} U$. Taking the tropical convex hull of both sides we obtain the containment $\operatorname{tconv}\operatorname{conv} U \subseteq \operatorname{tconv}(\operatorname{conv}\operatorname{tconv} U)$.

Similarly, since $U \subseteq \operatorname{conv} U$, it follows that $\operatorname{tconv} U \subseteq \operatorname{tconv}\operatorname{conv} U$. Corollary 2.2.6 implies that $\operatorname{tconv}\operatorname{conv} U$ is convex. Combining these two facts we have that $\operatorname{conv}\operatorname{tconv} U \subseteq \operatorname{tconv}\operatorname{conv} U$. Since $\operatorname{tconv}\operatorname{conv} U$ is also tropically convex, as it is the tropical convex hull of a set, it also follows that $\operatorname{tconv}(\operatorname{conv}\operatorname{tconv} U) \subseteq \operatorname{tconv}\operatorname{conv} U$. $\square$

Example 2.2.8. Let $V = \{v_1, v_2, v_3\} \subset \mathbb{R}^4/\mathbb{R}\mathbf{1}$ where $v_1 = (0,0,0,0)$, $v_2 = (0,1,2,0)$, $v_3 = (0,2,1,3)$, and $v_4 = (0,0,3,4)$. The vertices of $\operatorname{tconv}\operatorname{conv} V$ are the columns of matrix A, and the vertices of $\operatorname{conv}\operatorname{tconv} V$ are the columns of matrix B.

$$A = \begin{pmatrix} 0 & 0 & 0 & 0 & 0 & 0 & 0 & 0 & 0 & 0 \\ 0 & 1 & 0 & 1 & 2 & 0 & 0 & 2 & 0 & 0 \\ 0 & 1 & 2 & 2 & 1 & 3 & 1 & 1 & 2 & 3 \\ 0 & 0 & 0 & 0 & 1 & 1 & 3 & 3 & 4 & 4 \end{pmatrix}, \quad B = \begin{pmatrix} 0 & 0 & 0 & 0 & 0 & 0 & 0 & 0 & 0 & 0 \\ 0 & 1 & 0 & 1 & 2 & 0 & 0 & 2 & 0 & 0 \\ 0 & \frac{1}{2} & 2 & 2 & 1 & 3 & 1 & 1 & 2 & 3 \\ 0 & 0 & 0 & 0 & 1 & 1 & 3 & 3 & 4 & 4 \end{pmatrix}$$

The polytope $\operatorname{conv}\operatorname{tconv} V$ is contained in the polytope $\operatorname{tconv}\operatorname{conv} V$, although it is not tropically convex. The vertices of $\operatorname{conv}\operatorname{tconv} V$ are vertices and pseudovertices of $\operatorname{tconv} V$,

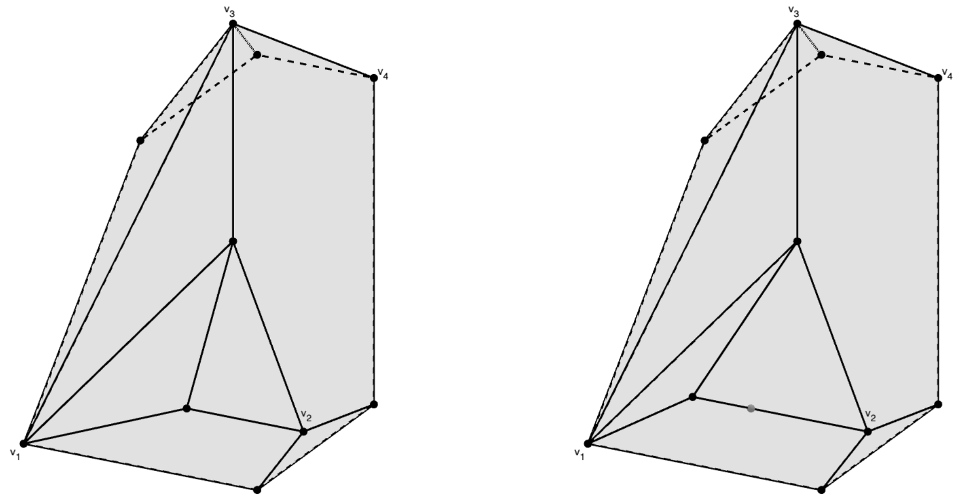

Figure 2.8: The the convex hull of a tropical polytope $\operatorname{tconv} V$ (left) is contained in the tropical convex hull of the polytope $\operatorname{conv} V$ (right).

which includes the set V. Figure 2.8 shows $\operatorname{conv} \operatorname{tconv} V$ on the left and $\operatorname{tconv} \operatorname{conv} V$ on the right. The tropical convex hull of V is a three-dimensional tropical polytope, and the convex hull of V is a tetrahedron. $\triangle$

2.2.1 Line segments & rays

Let a and b be points in $\mathbb{R}^{n+1}/\mathbb{R}\mathbf{1}$. For the remainder of this section we assume that

$$a = (0, \ldots, 0) \text{ and } 0 = b_0 < b_1 < \cdots < b_n. \tag{2.7}$$

In this case, using [21, Proposition 3], the tropical line segment $\operatorname{tconv}(a, b)$ is a concatenation of line segments with $n+1$ *pseudovertices* in $\mathbb{R}^{n+1}/\mathbb{R}\mathbf{1}$ given by $p_0 = a$ and

$$p_j = (0, b_1, \ldots, b_{j-1}, b_j, \ldots, b_j) \text{ for } j \in [n]. \tag{2.8}$$

If a and b do not satisfy (2.7), we can apply first a linear transformation which translates a to the origin and then another that relabels the coordinates so that $0 = b_0 \leq b_1 \leq \ldots \leq b_n$. If $b_i = b_j$ for some $i \neq j$, or $b_j = 0$ for some j, then the pseudovertices of $\operatorname{tconv}(a, b)$

lie in the tropically convex hyperplane $x_i - x_j = 0$ or $x_j = 0$, and the same holds for $\operatorname{conv}\operatorname{tconv}(a, b)$ [21, Theorem 2]. Thus $\operatorname{tconv}\operatorname{conv}(a, b)$ and $\operatorname{conv}\operatorname{tconv}(a, b)$ lie in the hyperplane $x_i - x_j = 0$ or $x_j = 0$. Each of these hyperplanes is isomorphic to $\mathbb{R}^{n-1}$. We can repeat this process until the appropriate projection of b has distinct positive coordinates.

Example 2.2.9. Let $a = (0, 0, 0)$ and $b = (0, 2, 5)$ be two points in $\mathbb{R}^3/\mathbb{R}\mathbf{1}$. The tropical convex hull of a and b is a concatenation of two classical line segments. Since the coordinates of b are ordered, using (2.8) we have the pseudovertex $p_1 = (0, 2, 2)$.

Let $c = (0, 0, 0, 0)$ and $d = (0, 2, 3, 5)$ be two points in $\mathbb{R}^4/\mathbb{R}\mathbf{1}$. By (2.8), or using the algorithm in the proof of [21, Proposition 3], we find that $q_1 = (0, 2, 2, 2)$ and $q_2 = (0, 2, 3, 3)$.

The following theorem shows that the tropical convex hull and convex hull commute for two points in $\mathbb{R}^{n+1}/\mathbb{R}\mathbf{1}$ for all n.

Theorem 2.2.10. *If a, b are points in $\mathbb{R}^{n+1}/\mathbb{R}\mathbf{1}$, then*

(i) $\operatorname{tconv}\operatorname{conv}(a, b) = \operatorname{conv}\operatorname{tconv}(a, b)$;

(ii) $\operatorname{tconv}\operatorname{pos}(a) = \operatorname{pos}\operatorname{tconv}(0, a)$.

Example 2.2.11. Before proving Theorem 2.2.10, we consider the convex hull of the two tropical line segments from Example 2.2.9. The convex hull of $\operatorname{tconv}(a, b)$ results in a triangle with vertices a, p_1, and b, and the convex hull of $\operatorname{tconv}(c, d)$ is a tetrahedron with vertices c, q_1, q_2, and d. Note that the triangle and tetrahedron contain the line segments $\operatorname{conv}(a, b)$ and $\operatorname{conv}(c, d)$, respectively, as edges. Both polytopes are shown in Figure 2.9. Applying Proposition 2.2.5 to compute the tropical convex hull of each of the line segments, we obtain the same triangle and tetrahedron, respectively. $\triangle$

Corollary 2.2.6 implies the forward containment of Theorem 2.2.10(i). For the converse, we use an explicit description of $\operatorname{conv}\operatorname{tconv}(a, b)$ given in the following lemma.

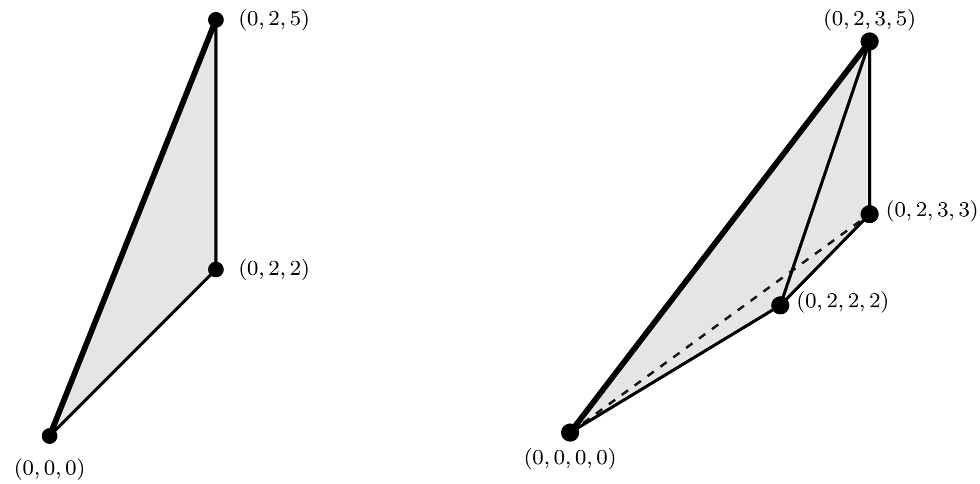

Figure 2.9: The tropical convex hull of a line segment (bold) coincides with the convex hull of a tropical line segment in $\mathbb{R}^3/\mathbb{R}\mathbf{1}$ (left) and $\mathbb{R}^4/\mathbb{R}\mathbf{1}$ (right).

Lemma 2.2.12. *If* $a, b \in \mathbb{R}^{n+1}/\mathbb{R}\mathbf{1}$ *satisfy* $a = (0, \ldots, 0)$ *and* $0 = b_0 < b_1 < \cdots < b_n$, *then* $\operatorname{conv}\operatorname{tconv}(a, b)$ *is a full-dimensional simplex whose* $\mathcal{H}-$*representation is given by*

$$\begin{aligned} b_1 - x_1 &\geq 0 \\ -(b_{j+1} - b_j)x_{j-1} + (b_{j+1} - b_{j-1})x_j - (b_j - b_{j-1})x_{j+1} &\geq 0 \quad \text{for } j \in [n-1]. \\ -x_{n-1} + x_n &\geq 0. \end{aligned} \tag{2.9}$$

Proof. Observe that the vertices of $\operatorname{conv}\operatorname{tconv}(a, b)$ are the pseudovertices $p_0, \ldots, p_n$ of $\operatorname{tconv}(a, b)$ as described in (2.8). These are $n+1$ affinely independent points of $\mathbb{R}^{n+1}/\mathbb{R}\mathbf{1} \cong \mathbb{R}^n$ since the vectors $p_1 - a = p_1, \ldots, p_{n-1} - a = p_{n-1}, b - a = b$ are linearly independent. This implies $\operatorname{conv}\operatorname{tconv}(a, b)$ is a simplex. Hence, each of its $n+1$ facets is the convex hull of n vertices. To show that (2.9) is the $\mathcal{H}-$representation of $\operatorname{conv}\operatorname{tconv}(a, b)$ we will show that the corresponding equation of each one of the $n+1$ inequalities is one of the facet-defining hyperplanes of $\operatorname{conv}\operatorname{tconv}(a, b)$.

Let $x = (0, x_1, \ldots, x_n)$ be a point in $\operatorname{conv}\operatorname{tconv}(a, b) = \operatorname{conv}(a, p_1, \ldots, p_{n-1}, b)$. The

jth coordinate of x is given by

$$x_j = \lambda_1 b_1 + \ldots + \lambda_{j-1} b_{j-1} + (\lambda_j + \lambda_{j+1} + \ldots + \lambda_n)\, b_j,$$

where $\lambda_1 + \ldots + \lambda_n \leq 1$ and $\lambda_i \geq 0$ for every i. Substituting the coordinates of x into the first linear form of (2.9) we obtain $(1 - \lambda_1 - \cdots - \lambda_n)b_1$. Since $\lambda_1 + \ldots + \lambda_n \leq 1$ and $b_1 \geq 0$ it follows that $b_1 - x_1 \geq 0$. Note that equality occurs if and only if x is in the facet $\operatorname{conv}(p_1, \ldots, p_{n-1}, b)$. Thus, $b_1 - x_1 = 0$ defines this facet of $\operatorname{conv} \operatorname{tconv}(a, b)$, that is $\{b_1 - x_1 = 0\} \cap \operatorname{conv} \operatorname{tconv}(a, b) = \operatorname{conv}(p_1, \ldots, p_{n-1}, b)$.

After substituting into the second linear form of (2.9) we have that

$$-(b_{j+1} - b_j)x_{j-1} + (b_{j+1} - b_{j-1})x_j - (b_j - b_{j-1})x_{j+1} = \lambda_j(b_{j-1} - b_j)(b_j - b_{j+1}).$$

Since $\lambda_j \geq 0$ and $b_j \geq b_{j-1}$ for each j, we know x satisfies the second inequality. Here equality occurs if and only if x is in the facet $\operatorname{conv}(a, p_1, \ldots, p_{j-1}, p_{j+1}, \ldots, p_{n-1}, b)$, so

$$-(b_{j+1} - b_j)x_{j-1} + (b_{j+1} - b_{j-1})x_j - (b_j - b_{j-1})x_{j+1} = 0$$

defines this facet of $\operatorname{conv} \operatorname{tconv}(a, b)$ for each $j \in [n-1]$.

Lastly, we have that $-x_{n-1} + x_n = \lambda_n(b_n - b_{n-1}) \geq 0$. Equality holds if and only if x is in the facet $\operatorname{conv}(a, p_1, \ldots, p_{n-1})$, and hence this facet is defined by $-x_{n-1} + x_n = 0$. $\square$

Example 2.2.13. The facet-defining hyperplanes of the tetrahedron in Example 2.2.11 are

$$\begin{aligned} 2 + x_0 - x_1 &\geq 0 \\ -x_0 + 3x_1 - 2x_3 &\geq 0 \\ -2x_1 - x_2 + 3x_3 &\geq 0 \\ x_2 - x_3 &\geq 0. \end{aligned}$$

Lemma 2.2.14. *If* $a, b \in \mathbb{R}^{n+1}/\mathbb{R}\mathbf{1}$ *and* V *is a finite subset of* $\operatorname{conv}(a,b)$*, then*

$$\operatorname{tconv}(V) \subset \operatorname{conv}\operatorname{tconv}(a,b).$$

Proof. Without loss of generality, assume $a = (0,\dots,0)$ and $0 = b_0 < b_1 < \dots < b_n$. Let $V = \{\lambda_1 b, \lambda_2 b, \dots, \lambda_r b\} \subset \operatorname{conv}(a,b)$ for some parameters $\lambda_i \in [0,1]$. Assume the parameters are ordered $0 \leq \lambda_1 \leq \lambda_2 \leq \dots \leq \lambda_r \leq 1$. Take $x \in \operatorname{tconv} V$ and let T_x be the type of x relative to V. By [21, Lemma 10], the point x satisfies

$$x_k - x_j \leq \lambda_i(b_k - b_j) \text{ for } j,k \in [n]_0 \text{ with } i \in T_j. \tag{2.10}$$

We will show that x satisfies the $\mathcal{H}$-representation of $\operatorname{conv}\operatorname{tconv}(a,b)$ given in Lemma 2.2.12. Since the union of all coordinates T_j of T_x covers $[r]$, (2.10) implies that

$$0 \leq \frac{x_{j+1} - x_j}{b_{j+1} - b_j} \leq \frac{x_j - x_{j-1}}{b_j - b_{j-1}} \leq 1 \quad \text{ for all } j \in [n-1].$$

For $j = 1$, this implies $\dfrac{x_1}{b_1} \leq 1$, so $b_1 - x_1 \geq 0$. For $j \in [n-1]$, rewriting the inequality $\dfrac{x_{j+1} - x_j}{b_{j+1} - b_j} \leq \dfrac{x_j - x_{j-1}}{b_j - b_{j-1}}$ shows that $-(b_{j+1} - b_j)x_{j-1} + (b_{j+1} - b_{j-1})x_j - (b_j - b_{j-1})x_{j+1} \geq 0$. Lastly, if $j = n-1$, then $0 \leq \dfrac{x_n - x_{n-1}}{b_n - b_{n-1}}$, so $-x_{n-1} + x_n \geq 0$. $\square$

Proof of Theorem 2.2.10. For part (i), assume without loss of generality that $a = (0,\dots,0)$ and $0 = b_0 < b_1 < \cdots < b_n$. Corollary 2.2.6 and the containment $\operatorname{tconv}(a,b) \subset \operatorname{tconv}\operatorname{conv}(a,b)$ imply that $\operatorname{conv}\operatorname{tconv}(a,b) \subseteq \operatorname{tconv}\operatorname{conv}(a,b)$. Now take $x \in \operatorname{tconv}\operatorname{conv}(a,b)$. Since the tropical convex hull of a set is the union of the tropical convex hulls of all of its finite subsets, it follows that there is a finite set $V \subset \operatorname{conv}(a,b)$ such that $x \in \operatorname{tconv}(V)$. Lemma 2.2.14 implies $\operatorname{tconv}(V) \subset \operatorname{conv}\operatorname{tconv}(a,b)$, so $x \in \operatorname{conv}\operatorname{tconv}(a,b)$.

To show part (ii), take $x \in \operatorname{tconv}\operatorname{pos}(a)$. There exist scalars $\lambda_0, \dots, \lambda_n \geq 0$ such that $\lambda_j a \in \operatorname{pos}(a)$ for each $j \in [n]_0$ and $x \in \operatorname{tconv}(0, \lambda_0 a, \dots, \lambda_n a)$. Assume the scalars are ordered $\lambda_0 \leq \lambda_1 \leq \lambda_2 \leq \dots \leq \lambda_n$ so $x \in \operatorname{tconv}\operatorname{conv}(0, \lambda_n a)$. By Theorem 2.2.10$(i)$ it follows that $x \in \operatorname{conv}\operatorname{tconv}(0, \lambda_n a)$. Furthermore, this means $x \in \operatorname{pos}\operatorname{tconv}(0, \lambda_n a)$. The pseudovertices of $\operatorname{tconv}(0, \lambda_n a)$ and $\operatorname{tconv}(0, a)$ are scalar multiples of one another meaning $x \in \operatorname{pos}\operatorname{tconv}(0, a)$. The other inclusion $\operatorname{pos}\operatorname{tconv}(0, a) \subset \operatorname{tconv}\operatorname{pos}(0, a)$ follows from Corollary 2.2.6. □

Example 2.2.15. Returning to the tetrahedron of Example 2.2.11, the dimension of the tropical convex hull of the line segment $\operatorname{conv}(a, b)$ is three. Moreover, note that the difference $b - a$ has three distinct nonzero entries. Consider the tropical convex hull of the line segment between the origin ant the point $c = (0, 2, 5, 5)$. This is a two-dimensional simplex in $\mathbb{R}^4/\mathbb{R}\mathbf{1}$ with vertices $(0, 0, 0, 0)$, $(0, 2, 2, 2)$, and $(0, 2, 5, 5)$. Here, the difference between the point c and the origin contains two distinct nonzero entries. △

In fact, we can determine the dimension of the tropical convex hull of a line segment, or a ray, by the number of distinct nonzero coordinates. The corollary below formalizes this.

Corollary 2.2.16. *If a and b are points in $\mathbb{R}^{n+1}/\mathbb{R}\mathbf{1}$, then*

(i) $\dim\operatorname{tconv}\operatorname{conv}(a, b)$ *is the number of distinct nonzero coordinates of $a - b$;*

(ii) $\dim\operatorname{tconv}\operatorname{pos}(a)$ *is the number of distinct nonzero coordinates of a.*

Proof. Part (i) follows from the proof of Lemma 2.2.12 since $\operatorname{tconv}\operatorname{conv}(a, b)$ is a full-dimensional simplex in $\mathbb{R}^d$ where d is the number of nonzero distinct coordinates in $a - b$. For part (ii) observe that the generators of $\operatorname{pos}\operatorname{tconv}(0, a)$ are the pseudovertices of $\operatorname{tconv}(0, a)$ which are vertices of $\operatorname{tconv}\operatorname{conv}(0, a)$. □

As a consequence of Corollary 2.2.16 we have the following result for tropically convex fans. One direction of Lemma 2.2.17 also appears in [49, Lemma 3.6]. An application of this lemma appears in Section 2.4.

Lemma 2.2.17. *If F is a tropically convex fan in $\mathbb{R}^{n+1}/\mathbb{R}\mathbf{1}$, then $\dim F$ is equal to the maximum number of distinct nonzero coordinates of a point in F.*

Proof. Let d be the maximum number of nonzero distinct coordinates of any point in F, and let x be one such point in F. If F is a tropically convex fan it contains $\operatorname{tconv}\operatorname{pos}(x)$. Corollary 2.2.16 implies that $\dim \operatorname{tconv}\operatorname{pos}(x) = d$, hence $\dim\ F \geq d$.

Suppose that $\dim F > d$. If F is a tropically convex fan, let C be a cone contained in F such that $\dim C = \dim F$. By hypothesis, each point in C has at most d nonzero distinct coordinates. This implies that C is contained in the union of finitely many linear spaces in $\mathbb{R}^{n+1}/\mathbb{R}\mathbf{1}$ of dimension at most d. This contradicts the assumption that $\dim C = \dim F > d$. Hence, $\dim F = d$. $\square$

A similar result holds for convex sets that are also tropically convex and contain the origin. The proof of Lemma 2.2.18 is omitted as it employs the same techniques as the proof of Lemma 2.2.17.

Lemma 2.2.18. *If P is a convex set in $\mathbb{R}^{n+1}/\mathbb{R}\mathbf{1}$ containing the origin and P is tropically convex, then $\dim P$ is equal to the maximum number of distinct nonzero coordinates of a point in P.*

2.2.2 Sets in $\mathbb{R}^3/\mathbb{R}\mathbf{1}$

In this section we consider arbitrary sets in $\mathbb{R}^3/\mathbb{R}\mathbf{1}$ and give a generalization of Theorem 2.2.10.

Lemma 2.2.19. *If $V \subset \mathbb{R}^3/\mathbb{R}\mathbf{1}$ is finite, then $\operatorname{tconv}\operatorname{conv} V = \operatorname{conv}\operatorname{tconv} V$.*

Proof. We prove the lemma by showing that each vertex of $\operatorname{tconv}\operatorname{conv} V$ is either a point in V or a pseudovertex of $\operatorname{tconv} V$.

By Proposition 2.2.5 we know $\operatorname{tconv}\operatorname{conv} V = \bigcap_{j=0}^{2}(\mathcal{S}_j + \operatorname{conv} V)$. A face of a Minkowski sum of polyhedra is a Minkowski sum of a face from each summand. Since $\mathcal{S}_j$ has only one vertex, namely the origin, it follows that the vertices of $\mathcal{S}_j + \operatorname{conv} V$ are vertices of $\operatorname{conv} V$. The facets of $\mathcal{S}_j + \operatorname{conv} V$ arise as either the sum of the vertex of $\mathcal{S}_j$ and an edge of $\operatorname{conv} V$, or as the sum of a vertex of $\operatorname{conv} V$ and a ray of $\mathcal{S}_j$. In the former case, these are simply the edges of $\operatorname{conv} V$. In the latter case, these are the unbounded edges parallel to a ray of $\mathcal{S}_j$ and the vertex of each of them is a vertex $v \in V$.

From this description of the facets and vertices of $\mathcal{S}_j + \operatorname{conv} V$ we deduce that a vertex of $\operatorname{tconv} \operatorname{conv} V$ is either a vertex of $\operatorname{conv} V$ or it is the intersection of a facet of $\mathcal{S}_i + \operatorname{conv} V$ and a facet of $\mathcal{S}_j + \operatorname{conv} V$ for some $i, j \in [2]_0$. Note that if both of these facets were edges of $\operatorname{conv} V$, then their intersection is a vertex of $\operatorname{conv} V$. If neither of the facets is an edge of $\operatorname{conv} V$, then the intersection point is a pseudovertex of $\operatorname{tconv}(v, w)$ and is contained in $\operatorname{conv} \operatorname{tconv} V$. Suppose that only one of the facets is an edge of $\operatorname{conv} V$. This intersection point must be a vertex of $\operatorname{conv} V$. Otherwise it is in the interior of the edge of $\operatorname{conv} V$, which implies that the ray intersecting the edge also intersects the interior of $\operatorname{conv} V$ and hence is not a facet. $\square$

Example 2.2.20. Let $V = \{v_1, \ldots, v_5\} \subset \mathbb{R}^3/\mathbb{R}\mathbf{1}$ for $v_1 = (0,3,1), v_2 = (0,1,4), v_3 = (0,3,7), v_4 = (0,8,5)$, and $v_5 = (0,7,3)$. The convex hull of V is an ordinary polytope that is not tropically convex, since, for example, it does not contain $v_1 \oplus v_2 = (0,1,1)$. The tropical convex hull of V is a tropical polytope that is not convex. Combining the two

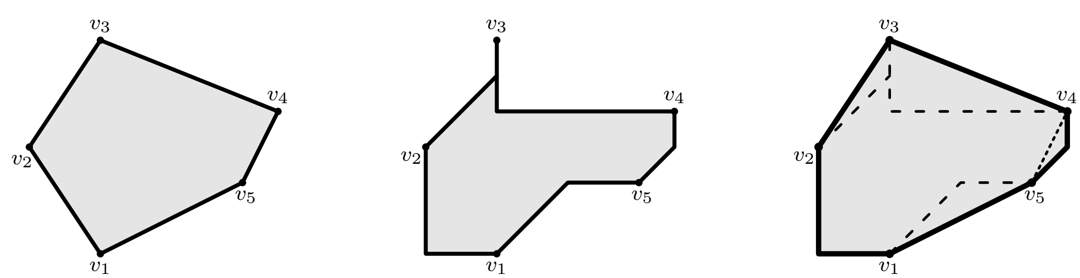

Figure 2.10: For the set $V \subset \mathbb{R}^3/\mathbb{R}\mathbf{1}$ from Example 2.2.20: the polytope $\operatorname{conv} V$ (left), the tropical polytope $\operatorname{tconv} V$ (middle), and the tropically convex polytope $\operatorname{tconv} \operatorname{conv} V = \operatorname{conv} \operatorname{tconv} V$.

operations we get a tropically convex ordinary polytope shown in Figure 2.10 (right). Note that $\operatorname{tconv} \operatorname{conv} V$ is not a tropical polytope as it is not the tropical convex hull of a finite set of points. $\triangle$

A natural question to ask is whether the two operations commute for any set in $\mathbb{R}^3/\mathbb{R}\mathbf{1}$. Figure 2.11 shows the two operations applied to the set U containing a point and a circle

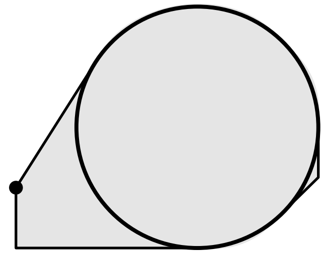

Figure 2.11: Convex hull and tropical convex hull applied to a set in $\mathbb{R}^3/\mathbb{R}\mathbf{1}$ containing a point and a circle. The result is a convex set that is also tropically convex.

in $\mathbb{R}^3/\mathbb{R}\mathbf{1}$. In this example it is also the case that $\operatorname{tconv}\operatorname{conv} U = \operatorname{conv}\operatorname{tconv} U$. The following theorem formalizes these observations.

Theorem 2.2.21. *If* $U \subset \mathbb{R}^3/\mathbb{R}\mathbf{1}$, *then* $\operatorname{tconv}\operatorname{conv} U = \operatorname{conv}\operatorname{tconv} U$.

Proof. The forward containment is implied by the fact that $\operatorname{tconv}\operatorname{conv} U$ is convex by Corollary 2.2.6.

For backward containment, suppose that $x \in \operatorname{tconv}\operatorname{conv} U$. Then by (2.5) it follows that there exists a finite set $V \subset \operatorname{conv} U$, such that $x \in \operatorname{tconv} V$. The classical Carathéodory Theorem implies that each point $v_i \in V$ can be written as a convex combination of finitely many points in U. Call this set $A_i \subset U$. Since V is finite, it follows that $A = \bigcup_i A_i$ is a finite subset of U and $V \subset \operatorname{conv} A$. Now we have $x \in \operatorname{tconv} V \subset \operatorname{tconv}\operatorname{conv} A$. It follows $x \in \operatorname{conv}\operatorname{tconv} A$ by Lemma 2.2.19. Since $A \subset U$, this implies $x \in \operatorname{conv}\operatorname{tconv} U$. $\square$

As already mentioned, Theorem 2.2.21 does not hold in general when $n \geq 3$. See Figure 2.3 and Example 2.2.8 for examples.

2.3 Polyhedral sets

In this section we examine the tropical convex hull of polyhedral sets, halfspaces, affine and linear spaces, and arbitrary convex sets. The main result of this section is Theorem 2.3.8 which characterizes all ordinary convex sets in $\mathbb{R}^{n+1}/\mathbb{R}\mathbf{1}$ that are tropically convex.

Remark 2.3.1. In the statement of the following lemma, when we say that the tropical convex hull of a polyhedral complex (fan) is a polyhedral complex (fan), we mean that it is the underlying set of a polyhedral complex (fan) and there exists a polyhedral (fan) structure on that set. $\triangle$

Lemma 2.3.2. *If* $P \subset \mathbb{R}^{n+1}/\mathbb{R}\mathbf{1}$ *is a polyhedron (resp. cone, polyhedral complex, fan, polytope), then* $\operatorname{tconv} P$ *is a polyhedron (resp. cone, polyhedral complex, fan, polytope).*

Proof. If P is a polyhedron then $\operatorname{tconv} P$ is a polyhedron since it is the intersection of the finitely many polyhedra $P + \mathcal{S}_j$. If P is a cone then $P + \mathcal{S}_j$ is a cone for every j and (2.6) implies that $\operatorname{tconv} P$ is also a cone.

Now let P be a polyhedral complex, so $P = \cup_{i=1}^{N} P_i$ where each P_i is a polyhedron. By (2.6) it follows that

$$\operatorname{tconv} P = \operatorname{tconv}\left(\bigcup_{i=1}^{N} P_i\right) = \bigcap_{j=0}^{n}\bigcup_{i=1}^{N}(P_i + \mathcal{S}_j).$$

Observe that by distributing the intersection over the union of Minkowski sums we obtain the union of N^{n+1} sets. Each set in the union is an intersection of $n+1$ Minkowski sums of the form $(P_{i_0} + \mathcal{S}_0) \cap \ldots \cap (P_{i_n} + \mathcal{S}_n)$, where $(i_0, \ldots, i_n) \in \{N\}^{n+1}$, so

$$\operatorname{tconv} P = \bigcup_{(i_0,\ldots,i_n)\in\{N\}^{n+1}} ((P_{i_0} + \mathcal{S}_0) \cap \cdots \cap (P_{i_n} + \mathcal{S}_n)).$$

It follows that $\operatorname{tconv} P$ is the underlying set of a polyhedral complex since the finite intersection of polyhedra is a polyhedron. If P is a fan, the results on polyhedral complexes and cones imply $\operatorname{tconv} P$ is the underlying set of a fan.

Lastly, let P be a polytope. To show $\operatorname{tconv} P$ is a polytope it suffices to show it is bounded. Suppose $\operatorname{tconv} P$ is not bounded. Hence it contains a ray $w + \operatorname{pos}(v)$. Since P is bounded, again (2.6) implies that $\operatorname{pos}(v)$ is contained in each sector $\mathcal{S}_j$. This is not possible since the intersection of all sectors is the origin. $\square$

2.3.1 Halfspaces

The goal of this subsection is to characterize tropically convex ordinary halfspaces. We begin by considering the Minkowski sum of a halfspace with each of the closed sectors $\mathcal{S}_j, j \in [n]_0$. Consequently, in Proposition 2.3.4, we aim to describe the tropical convex hull of an ordinary halfspace.

Lemma 2.3.3. *Let $\mathcal{H}$ be a halfspace in $\mathbb{R}^{n+1}/\mathbb{R}\mathbf{1}$. If $\mathcal{S}_j$ is one of the standard closed sectors in $\mathbb{R}^{n+1}/\mathbb{R}\mathbf{1}$ for $j \in [n]_0$, then either $\mathcal{H} + \mathcal{S}_j = \mathcal{H}$ or $\mathcal{H} + \mathcal{S}_j = \mathbb{R}^{n+1}/\mathbb{R}\mathbf{1}$.*

Proof. Let $\mathcal{H}$ be defined by $\{(x_0, x_1, \ldots, x_n) \in \mathbb{R}^{n+1}/\mathbb{R}\mathbf{1} \mid \sum_{k=0}^{n} a_k x_k \geq 0\}$ and let $\mathcal{S}_j$ be one of the standard sectors in $\mathbb{R}^{n+1}/\mathbb{R}\mathbf{1}$ for $j \in [n]_0$. If $\mathcal{S}_j \subset \mathcal{H}$, then it follows immediately that $\mathcal{H} + \mathcal{S}_j = \mathcal{H}$.

Suppose that $\mathcal{S}_j \not\subset \mathcal{H}$ for some $j \in [n]_0$. This means that at least one of the rays $\operatorname{pos}(-e_i), i \neq j$, generating $\mathcal{S}_j$ is contained in $\mathcal{H}^c$; equivalently $-\sum_{k=0}^{n} a_k e_{ik} < 0$. Let y be a point in $\mathcal{H}^c$. Then we have that $-\sum_{k=0}^{n} a_k e_{ik} = -a_i < 0$ and $\sum_{k=0}^{n} a_k y_k < 0$. Let $\lambda \in \mathbb{R}$ be such that

$$\lambda \geq -\frac{\sum_{k=0}^{n} a_k y_k}{a_i} > 0.$$

Hence, $\lambda \sum_{k=0}^{n} a_k e_{ik} + \sum_{k=0}^{n} a_k y_k \geq 0$ and $\sum_{k=0}^{n} a_k (y_k + \lambda e_{ik}) \geq 0$. It follows that $y + \lambda e_i \in \mathcal{H}$. This shows that if $\mathcal{S}_j \not\subset \mathcal{H}$, then any point in $\mathcal{H}^c$ can be written as $(y + \lambda e_i) - \lambda e_i, i \neq j$, for $y + \lambda e_i \in \mathcal{H}$ and $-\lambda e_i \in \mathcal{S}_j$. Thus, $\mathcal{H} + \mathcal{S}_j = \mathbb{R}^{n+1}/\mathbb{R}\mathbf{1}$. □

Proposition 2.3.4. *If $\mathcal{H}$ is a halfspace in $\mathbb{R}^{n+1}/\mathbb{R}\mathbf{1}$, then either $\operatorname{tconv} \mathcal{H} = \mathcal{H}$ or $\operatorname{tconv} \mathcal{H} = \mathbb{R}^{n+1}/\mathbb{R}\mathbf{1}$.*

Proof. By Proposition 2.2.5 we know $\operatorname{tconv} \mathcal{H} = \bigcap_{j=0}^{n} (\mathcal{S}_j + \mathcal{H})$. Using Lemma 2.3.3, if there exists $j \in [n]_0$ such that $\mathcal{S}_j \subset \mathcal{H}$, then $\operatorname{tconv} \mathcal{H} = \mathcal{H}$. Otherwise $\operatorname{tconv} \mathcal{H} = \mathbb{R}^{n+1}/\mathbb{R}\mathbf{1}$. □

Example 2.3.5. Let $\mathcal{H}_1 = \{(x_0, x_1, x_2) \in \mathbb{R}^3/\mathbb{R}\mathbf{1} \mid 2x_0 - x_1 - x_2 \geq 0\}$ and $\mathcal{H}_2 = \{(x_0, x_1, x_2) \in \mathbb{R}^3/\mathbb{R}\mathbf{1} \mid 2x_0 + x_1 - 3x_2 \geq 0\}$ be two halfspaces in $\mathbb{R}^3/\mathbb{R}\mathbf{1}$, as shown in

Figure 2.12. To compute the tropical convex hull of $\mathcal{H}_1$ we note that $\mathcal{H}_1 + \mathcal{S}_0 = \mathcal{H}_1$ and

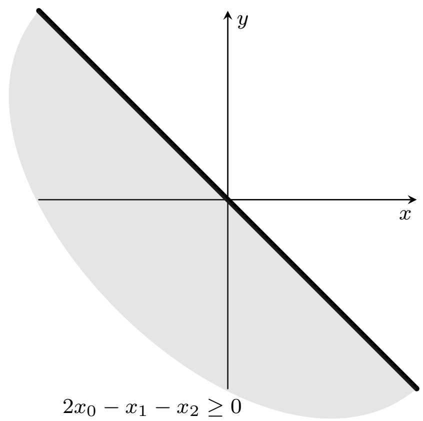

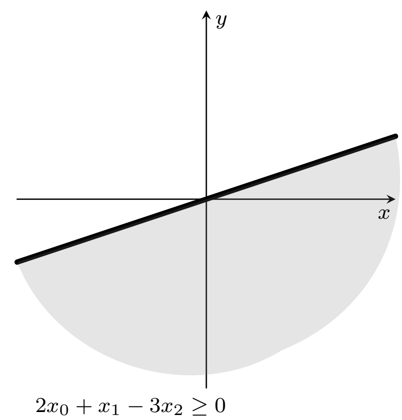

Figure 2.12: The halfspace on the left is tropically convex, while the halfspace on the right is not.

$\mathcal{H}_1 + \mathcal{S}_1 = \mathcal{H}_1 + \mathcal{S}_2 = \mathbb{R}^3/\mathbb{R}\mathbf{1}$. Hence, by Proposition 2.2.5, $\operatorname{tconv} \mathcal{H}_1 = \bigcap_{j=0}^{n}(\mathcal{H}_1 + \mathcal{S}_j) = \mathcal{H}_1$. Thus, the halfspace $\mathcal{H}_1$ is tropically convex. The Minkowski sum of $\mathcal{H}_2$ with each of the sectors $\mathcal{S}_j, j \in [2]_0$ is the entire space $\mathbb{R}^{n+1}/\mathbb{R}\mathbf{1}$. Hence, $\operatorname{tconv} \mathcal{H}_2 = \mathbb{R}^{n+1}/\mathbb{R}\mathbf{1}$ and the halfspace $\mathcal{H}_2$ is not tropically convex. Indeed, for any two points on the boundary of $\mathcal{H}_2$ the tropical line segment between them lies in $\mathcal{H}_2^c$. △

Determining whether a halfspace is tropically convex can be done based only on its inner normal vector without any additional computations. In particular, a halfspace is tropically convex if and only if its inner normal vector has exactly one positive entry and the sum of all entries is zero, as the following proposition states.

Proposition 2.3.6. *A halfspace $\mathcal{H} = \{(x_0, x_1, \ldots, x_n) \in \mathbb{R}^{n+1}/\mathbb{R}\mathbf{1} \mid \sum_{k=0}^{n} a_k x_k \geq b, b \in \mathbb{R}\}$ is tropically convex if and only if there exists a $j \in [n]_0$ such that $S_j \subset \mathcal{H}$. This happens if and only if $\sum_{k=0}^{n} a_k = 0$ and there is exactly one $j \in [n]_0$ such that $a_j > 0$.*

Proof. First we consider the case of $b = 0$ and $\mathcal{H} = \{(x_0, x_1, \ldots, x_n) \in \mathbb{R}^{n+1}/\mathbb{R}\mathbf{1} \mid \sum_{k=0}^{n} a_k x_k \geq 0\}$. By Proposition 2.3.4, $\operatorname{tconv} \mathcal{H} = \mathcal{H}$ if and only if $\mathcal{H}$ contains one of the sectors $\mathcal{S}_j, j \in [n]_0$. For a fixed $j, \mathcal{S}_j$ is generated by $-e_i, i \neq j$. So, $\mathcal{S}_j$ is contained in $\mathcal{H}$ if and only if the generating rays satisfy the inequality $\sum_{k=0}^{n} a_k e_{ik} \geq 0$. Since $\sum_{k=0}^{n} a_k = 0$, the inequality is satisfied if and only if $a_j > 0$. Tropical convexity is preserved under translations, hence, the translated halfspace $\mathcal{H} = \{(x_0, x_1, \ldots, x_n) \in \mathbb{R}^{n+1}/\mathbb{R}\mathbf{1} \mid \sum_{k=0}^{n} a_k x_k \geq b, b \in \mathbb{R}\}$ will remain tropically convex for any $b \in \mathbb{R}$. $\square$

Develin and Sturmfels showed that ordinary hyperplanes of the form $\{x \in \mathbb{R}^{n+1}/\mathbb{R}\mathbf{1} \mid x_i - x_j = b, b \in \mathbb{R}\}$ are tropically convex [21, Theorem 2]. Using this result, the following Lemma characterizes tropically convex affine spaces.

Lemma 2.3.7. *An affine space is tropically convex if and only if it is an intersection of hyperplanes of the form* $\{x \in \mathbb{R}^{n+1}/\mathbb{R}\mathbf{1} \mid x_i - x_j = b, b \in \mathbb{R}, i \neq j\}$ *or* $\{x \in \mathbb{R}^{n+1}/\mathbb{R}\mathbf{1} \mid x_i = b, b \in \mathbb{R}\}$.

Proof. After a translation, we may assume that the affine space contains the origin. Hence, we may assume that we are working with a linear space, and the hyperplanes we consider are $\{x \in \mathbb{R}^{n+1}/\mathbb{R}\mathbf{1} \mid x_i - x_j = 0, i \neq j\}$ and $\{x \in \mathbb{R}^{n+1}/\mathbb{R}\mathbf{1} \mid x_i = 0\}$. By [21, Theorem 2] hyperplanes of the form $\{x_i - x_j = 0\}$ and $\{x_i = 0\}$ are tropically convex. Hence, the intersection of any hyperplanes of this form is also tropically convex.

Conversely, let $L \subset \mathbb{R}^n$ be a linear space and suppose L is tropically convex. Consider $\operatorname{conv}(0, x)$ for some $x \in L$. By Corollary 2.2.16, the dimension of the tropical convex hull of $\operatorname{conv}(0, x)$ is equal to the number of distinct nonzero coordinates of x. Since L is tropically convex, x has at most $\dim L$ distinct nonzero coordinates by Lemma 2.2.17. This implies L is contained in the union of the intersections of some hyperplanes $\{x_i - x_j = 0\}$ and $\{x_i = 0\}$. Since L is convex, it follows that L is just an intersection of $\{x_i - x_j = 0\}$ and $\{x_i = 0\}$ for some $i \neq j$ and k. $\square$

In the following theorems we characterize polyhedral sets and convex cones that are tropically convex.

Theorem 2.3.8. *A full-dimensional ordinary polyhedron is tropically convex if and only if all of its facet-defining halfspaces are tropically convex.*

Proof. Let $P \subset \mathbb{R}^{n+1}/\mathbb{R}\mathbf{1}$ be a full-dimensional, ordinary polyhedron. Since P is full-dimensional, it has a unique, irredundant hyperplane representation. If all facet-defining halfspaces of P are tropically convex, then P is tropically convex, as it is the intersection of tropically convex sets.

Suppose that P is tropically convex and there exists a facet-defining halfspace $\mathcal{H}$ of P that is not tropically convex. Let H be the hyperplane at the boundary of $\mathcal{H}$. Since $\mathcal{H}$ is not tropically convex, it follows that H is not tropically convex. Otherwise, by Lemma 2.3.7 H is parallel to one of the facets of the standard tropical hyperplane, so both $\mathcal{H}$ and $-\mathcal{H}$ are tropically convex. Let $x', y' \in \mathcal{H}$ such that $\operatorname{tconv}(x', y') \not\subset \mathcal{H}$. This implies that there exist $x, y \in \operatorname{tconv}(x', y') \cap H$ such that $(\operatorname{tconv}(x, y) \setminus \{x, y\}) \subset \mathcal{H}^c$. Recall that a tropical line segment is a concatenation of ordinary line segments whose slopes are linearly independent $(0, 1)$-vectors. Hence, at least one of the $(0, 1)$-vectors defining the line segments in $\operatorname{tconv}(x, y)$ is in $\mathcal{H}^c$. Up to translation, we may assume that at least one of the points x or y is in P. If both points are in P, it follows that $\operatorname{tconv}(x, y) \not\subset P$, since $\operatorname{tconv}(x, y) \subset \mathcal{H}^c$. This contradicts the assumption that P is tropically convex. Without loss of generality, we may assume that $x \in P$ and $y \notin P$. Consider the line segment $\operatorname{conv}(x, y) \subset H$, which must intersect the boundary of P at a point $z \in H$. The slopes of the ordinary line segments in $\operatorname{tconv}(x, z)$ are the same as those of $\operatorname{tconv}(x, y)$. Hence, at least one of the line segments in $\operatorname{tconv}(x, z)$ will be in $\mathcal{H}^c$. This is a contradiction, since P is tropically convex.

Note that this result may also be obtained directly as a consequence of Proposition 2.3.6 by using the explicit representation of a pseudovertex of $\operatorname{tconv}(x, z)$ as described in [21, Proposition 3]. □

Corollary 2.3.9. *If $P \subset \mathbb{R}^{n+1}/\mathbb{R}\mathbf{1}$ is a polyhedron of dimension $d < n$, then P is tropically convex if and only if its affine span is tropically convex and there exists a $\mathcal{H}$-representation of P given by tropically convex halfspaces and hyperplanes.*

Proof. After translation, we may assume that P contains the origin. Hence, the affine span of P, $\operatorname{aff} P$ is a d-dimensional linear subspace L.

If L is not tropically convex, then using an argument similar to that in the proof of Theorem 2.3.8, it follows that there exist two points $x, z \in P$, such that $\operatorname{tconv}(x, z) \notin P$. Hence, P is not tropically convex.

If L is tropically convex, then by Lemma 2.3.7 P is contained in the intersection of finitely many hyperplanes of the form $\{x_k = 0\}$ for $k \in [n]$, and $\{x_i - x_j = 0 \mid i \neq j\}$ for $i, j \in [n]$. Now we can work in L by deleting the x_k and x_i coordinates. Note that the restriction of this projection map to P is a linear bijection. We now consider P in the d-dimensional linear subspace L. Equivalently, we can work in $\mathbb{R}^{d+1}/\mathbb{R}\mathbf{1}$ where P is full-dimensional and has a unique, irredundant halfspace representation. By Theorem 2.3.8 it follows that P is tropically convex in L if and only if the halfspaces defining P in L are tropically convex. Hence, the inner normal vectors of the defining halfspaces satisfy Proposition 2.3.6. The lift of each halfspace to $\mathbb{R}^{n+1}/\mathbb{R}\mathbf{1}$ will have the same equation, hence it would still satisfy the conditions of Proposition 2.3.6. We can take the additional hyperplanes representing P in $\mathbb{R}^{n+1}/\mathbb{R}\mathbf{1}$ to be of the form $\{x_k = 0\}$ for $k \in [n]$, and $\{x_i - x_j = 0 \mid i \neq j\}$ for $i, j \in [n]$. In particular, these are the hyperplanes defining L. Hence, P is tropically convex since it is the intersection of tropically convex sets. □

Theorem 2.3.10. *A convex cone $P \subset \mathbb{R}^{n+1}/\mathbb{R}\mathbf{1}$ is tropically convex if and only if its dual cone P^* is generated by vectors with exactly one positive coordinate.*

Proof. Suppose P is tropically convex, and hence, $P = \operatorname{tconv} P$. Let P^* be the dual cone of P defined as follows:

$$P^* = \left\{ y \in \mathbb{R}^{n+1} \mid y^T x \geq 0, \text{ for all } x \in P \right\}.$$

The dual cone P^* is a closed convex cone, which is the conical hull of its generators. In this proof we use the property that the dual of the Miknowski sum of convex cones is the intersection of the duals of the cones. That is, if C_1 and C_2 are convex cones, then

$(C_1 + C_2)^* = C_1^* \cap C_2^*$. Lastly, observe that the dual of the sector $\mathcal{S}_j$ is

$$\mathcal{S}_j^* = \operatorname{pos}(\{e_j - e_i \mid i \neq j\}). \tag{2.11}$$

We now use Proposition 2.2.5 to write $P = \operatorname{tconv} P = \bigcap_{j=0}^{n}(P + \mathcal{S}_j)$. Next, we compute the dual P^* as follows:

$$\begin{aligned} P^* &= \left[\bigcap_{j=0}^{n}(P + \mathcal{S}_j)\right]^* = \sum_{j=0}^{n}(P + \mathcal{S}_j)^* \\ &= \sum_{j=0}^{n}(P^* \cap \mathcal{S}_j^*) \\ &= \operatorname{pos}(P^* \cap \mathcal{S}_0^*, \ldots, P^* \cap \mathcal{S}_n^*). \end{aligned}$$

This implies that the vectors generating P^* are also generators of the components $P^* \cap \mathcal{S}_j^*$. Note that vectors in $P^* \cap \mathcal{S}_j^*$, $j \in [n]_0$, have exactly one positive entry, as shown in (2.11). Thus, the vectors generating P^* must have exactly one positive entry.

Suppose that P^* is generated by vectors with exactly one positive coordinate entry. Then by Proposition 2.3.6 each halfspace corresponding to a supporting hyperplane of P is tropically convex. Hence, P is tropically convex, as it is the intersection of tropically convex sets. $\square$

Example 2.3.11. Let $P \subset \mathbb{R}^3/\mathbb{R}\mathbf{1}$ be the polytope shown in Figure 2.13 with the facet-defining halfspaces

$$\begin{aligned} -4x_0 + 5x_1 - x_2 &\geq 0 \\ -x_0 + 2x_1 - x_2 &\geq -2 \\ 6x_0 - x_1 - 5x_2 &\geq -30 \\ 7x_0 - 5x_1 - 2x_2 &\geq -35 \\ -5x_0 - x_1 + 6x_2 &\geq 0. \end{aligned}$$

The inner normal vector of each halfspace has exactly one positive entry and the sum of all

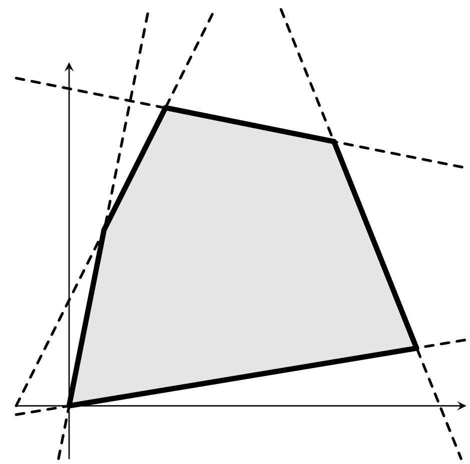

Figure 2.13: A tropically convex polytope is defined by tropically convex halfspaces.

the entries is zero. Hence, the hypothesis of Theorem 2.3.8 is satisfied and P is a tropically convex polytope.

We would like to remind the reader that tropically convex polytopes are not necessarily tropical polytopes. For example, P cannot be generated as the tropical convex hull of a finite set of points in $\mathbb{R}^3/\mathbb{R}\mathbf{1}$. △

Remark 2.3.12. The authors of [32] characterize distributive polyhedra. Any such polyhedron P has the property that for any $x, y \in P$, the componentwise maximum and minimum, $\min(x, y)$ and $\max(x, y)$, are contained in P. Tropically convex polyhedra are not necessarily distributive polyhedra, as they may not contain the componentwise maximum of any two elements. For example, consider the triangle $P \subset \mathbb{R}^3/\mathbb{R}\mathbf{1}$ in Figure 2.14 with vertices the origin, $(0, 3, 1)$, and $(0, 1, 3)$. This is a tropically convex polytope by Theorem 2.2.21, but not a distributive polytope. In particular, it is not max-closed since $\max((0, 3, 1), (0, 1, 3)) = (0, 3, 3) \notin P$. In order for a polyhedron to be distributive, it must be closed with respect to both componentwise $\min$ and $\max$. One example of distributive polytopes are polytropes. △

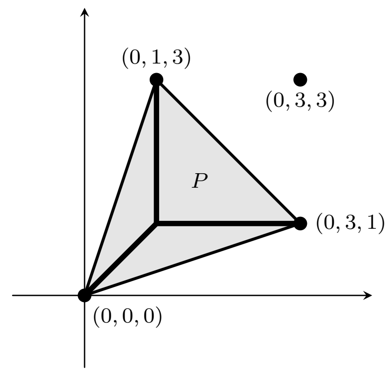

Figure 2.14: A tropically convex triangle P that is not distributive since it does not contain the point $\max((0,3,1),(0,1,3)) = (0,3,3)$. The tropical convex hull of the vertices is shown in bold.

2.3.2 Affine and linear spaces

We now turn our attention to the tropical convex hull of affine and linear spaces. In [19], Develin studies tropical secant varieties of ordinary linear spaces. Here, the ∞th tropical secant variety of a linear space L is the tropical convex hull of L. [19, Theorem 2.1, Corollary 2.3]. In the Proposition 2.3.13 we give a combinatorial method for determining the dimension of the tropical convex hull of an ordinary affine space, and hence, an ordinary linear space.

Proposition 2.3.13. *Let $L \subset \mathbb{R}^{n+1}/\mathbb{R}\mathbf{1}$ be an affine space, and let M_L be the matrix whose rows are the generators of the linear space parallel to L. The dimension of the tropical convex hull of L is equal to one less than the number of distinct columns of M_L.*

Proof. After translation, we may assume that L is a linear space, and hence, L is a fan. By Lemma 2.2.17 the dimension of the tropical convex hull of L is equal to the maximum number of distinct nonzero coordinates of a point in $\operatorname{tconv} L$. Let k be the dimension of L and d be the dimension of its tropical convex hull with $k \le d \le n$. Hence, there exists a point in $\operatorname{tconv} L$ with $d+1$ distinct coordinates.

Suppose that two columns of M_L, v_i and v_j for $i \neq j$, are identical, and let y be a point in L. Then y is a linear combination of the k generators of L, which are the rows of M_L. Hence, for some scalars $a_\ell, \ell \in [k]$, we have that $y_i = \sum_{\ell=1}^k a_\ell v_{\ell i} = \sum_{\ell=1}^k a_\ell v_{\ell j} = y_j$. This implies that if two columns are the same, then the corresponding coordinates of any point in L, and hence in $\operatorname{tconv} L$, would also be the same.

Conversely, suppose that two columns of M_L, v_i and v_j for $i \neq j$, are distinct. That is, $v_{\ell i} \neq v_{\ell j}$ for at least one $\ell \in [k]$. Let $y = \sum_{\ell=1}^{k} a_\ell v_\ell$ for $a = (a_1, \ldots, a_k) \in \mathbb{R}^k$. If $y_i = y_j$, then $\sum_{\ell=1}^{k} a_\ell (v_{\ell i} - v_{\ell j}) = 0$. Note that the equation $\sum_{\ell=1}^{k} a_\ell (v_{\ell i} - v_{\ell j}) = 0$ is a hyperplane in $\mathbb{R}^k$, and hence, it is of dimension $k-1$. It follows that the set of $a \in \mathbb{R}^k$ for which $y_i \neq y_j$ is a Zariski open set, implying that for a generic choice of $a \in \mathbb{R}^k$, the ith and jth coordinates of y would be distinct. Hence, there exists a choice of scalars $a \in \mathbb{R}^k$ for which distinct columns of M_L give rise to distinct coordinates of $y \in L$. Note that a point in $\operatorname{tconv} L$ cannot have more distinct coordinates than a point in L. Thus, the maximal number of distinct coordinates of a point in $\operatorname{tconv} L$ is equal to the number of distinct columns of M_L, implying that $\dim \operatorname{tconv} L$ is one less than the number of distinct columns of M_L. $\square$

Example 2.3.14. Let L_1, L_2, and L_3 be the ordinary linear spaces generated by the rows of the matrices M_{L_1}, M_{L_2}, and M_{L_3}, respectively.

$$M_{L_1} = \begin{pmatrix} 0 & 1 & 1 & 2 \\ 0 & 0 & 2 & 1 \end{pmatrix}, \quad M_{L_2} = \begin{pmatrix} 0 & 1 & 1 & 2 \\ 0 & 2 & 2 & 1 \end{pmatrix}, \quad M_{L_3} = \begin{pmatrix} 0 & 3 & 1 & 2 & 2 \\ 0 & 0 & 3 & 1 & 1 \end{pmatrix}.$$

There are four distinct columns in M_{L_1}, hence, $\dim \operatorname{tconv} L_1$ must be three. Indeed, note that L_1 is the hyperplane $2x_0 - 3x_1 - x_2 + 2x_3 = 0$ in $\mathbb{R}^4/\mathbb{R}\mathbf{1}$. By Lemma 2.3.7, L_1 is not tropically convex, and hence $\dim \operatorname{tconv} L_1 = 3$. Proposition 2.3.13 tells us that the dimension of $\operatorname{tconv} L_2$ must be two. We can verify this by determining that L_2 is the hyperplane $x_1 - x_2 = 0$, which is tropically convex. Lastly, we see that the tropical convex hull of the two-dimensional linear space $L_3 \subset \mathbb{R}^5/\mathbb{R}\mathbf{1}$ has dimension three, as there are four distinct columns in M_{L_3}.

Corollary 2.3.15. *If $P \subset \mathbb{R}^{n+1}/\mathbb{R}\mathbf{1}$ is a convex set and L is the affine hull of P, then*

$\dim \operatorname{tconv} P = \dim \operatorname{tconv} L$.

Proof. After translation, we may assume that P contains the origin in its relative interior and that L is a linear space. Since $L = \operatorname{aff} P$, it follows that $\operatorname{tconv} P \subset \operatorname{tconv} L$, and hence $\dim \operatorname{tconv} P \leq \dim \operatorname{tconv} L$. Moreover, $L \subset \operatorname{aff} \operatorname{tconv} P$, and since $\operatorname{tconv} P$ is convex by Corollary 2.2.6, it follows that $\dim \operatorname{aff} \operatorname{tconv} P = \dim \operatorname{tconv} P$. We claim that $\operatorname{aff} \operatorname{tconv} P$ is a tropically convex linear space. Hence, $\operatorname{tconv} L \subset \operatorname{aff} \operatorname{tconv} P$, and $\dim \operatorname{tconv} L \leq \dim \operatorname{aff} \operatorname{tconv} P$, implying that $\dim \operatorname{tconv} L \leq \dim \operatorname{tconv} P$.

Note that $\operatorname{aff} \operatorname{tconv} P$ is the unique linear space of dimension $\dim \operatorname{tconv} P$ containing the convex set $\operatorname{tconv} P$. Suppose that $\operatorname{aff} \operatorname{tconv} P$ is not tropically convex. Then there exist points $x, y \in \operatorname{aff} \operatorname{tconv} P$ such that $\operatorname{tconv}(x, y) \not\subset \operatorname{aff} \operatorname{tconv} P$. Up to translation, we may assume that at least one of the points x or y is in $\operatorname{tconv} P$. If both are in $\operatorname{tconv} P$, then we are done. Without loss of generality, assume that $x \in \operatorname{tconv} P$ and $y \notin \operatorname{tconv} P$. Consider the line segment $\operatorname{conv}(x, y) \subset \operatorname{aff} \operatorname{tconv} P$, which must intersect the boundary of $\operatorname{tconv} P$ at a point z. Recall that a tropical line segment is a concatenation of ordinary line segments whose slopes are linearly independent $(0, 1)$-vectors. The slopes of the ordinary line segments in $\operatorname{tconv}(x, z)$ are the same as those of $\operatorname{tconv}(x, y)$. Since $\operatorname{tconv}(x, y) \not\subset \operatorname{aff} \operatorname{tconv} P$, it follows that at least one of the $(0, 1)$-vectors defining the line segments in $\operatorname{tconv}(x, y)$ is not in $\operatorname{aff} \operatorname{tconv} P$. Since the line segments of $\operatorname{tconv}(x, z)$ have the same slopes, at least one of them will be outside of $\operatorname{aff} \operatorname{tconv} P$, and hence $\operatorname{tconv}(x, z) \not\subset \operatorname{tconv} P$. This is a contradiction since $\operatorname{tconv} P$ is tropically convex. Thus, $\dim \operatorname{tconv} P = \dim \operatorname{tconv} L$. $\square$

The following proposition characterizes convex sets whose tropical convex hull is full-dimensional.

Proposition 2.3.16. *If $P \subset \mathbb{R}^{n+1}/\mathbb{R}\mathbf{1}$ is a convex set, then $\operatorname{tconv} P$ is full-dimensional if and only if P is not contained in a tropically convex hyperplane.*

Proof. If $\operatorname{tconv} P$ is full-dimensional, then P cannot be contained in a tropically convex hyperplane. Otherwise, its tropical convex hull would be of lower dimension.

Conversely, suppose that P is not contained in a tropically convex hyperplane. Translate P so that it contains the origin. By Lemma 2.3.7, the only tropically convex hyperplanes containing the origin are of the form $\{x_i = x_j\}$ and $\{x_i = 0\}$. Then there exists a point $y \in P$ with n distinct nonzero coordinates. Note that $y \in \operatorname{tconv} P$, and recall that by Corollary 2.2.6, $\operatorname{tconv} P$ is convex. Then, Lemma 2.2.18 implies that $\dim \operatorname{tconv} P = n$. $\square$

We conjecture that this statement can be generalized for any set U, not necessarily convex.

Conjecture 2.3.17. *If $U \subset \mathbb{R}^{n+1}/\mathbb{R}\mathbf{1}$, then $\operatorname{tconv} U$ is full-dimensional if and only if U is not contained in a tropical hyperplane.*

2.4 Lower bound on the degree of a tropical curve

Let Γ be a *tropical curve* in $\mathbb{R}^{n+1}/\mathbb{R}\mathbf{1}$. This is a *weighted balanced rational polyhedral complex* of dimension one. We say that a polyhedral complex Γ is *pure* if every maximal polyhedron is of the same dimension. A *weighted* polyhedral complex is a pure polyhedral complex Γ with an associated weight $w_\sigma \in \mathbb{N}$ for each maximal-dimensional cone $\sigma \in \Gamma$. Given a weighted rational polyhedral complex Γ, we say that Γ is *balanced* if the following conditions hold [64, Sections 3.3, 4]:

(i) If Γ is a one-dimensional rational fan, let $v_1, \dots, v_k$ be the primitive integer vectors corresponding to the rays of Γ. By primitive we mean that $\gcd(v_1, \dots, v_k) = 1$. Let w_i be the weight of the cone containing the lattice point v_i. Then we say that Γ is balanced if

$$\sum_{i=1}^{k} w_i v_i = 0.$$

(ii) Let Γ be an arbitrary d-dimensional weighted rational polyhedral complex in $\mathbb{R}^{n+1}/\mathbb{R}\mathbf{1}$. Fix a $(d-1)$-dimensional cone τ of Γ. Let $L = \operatorname{span}(x - y | x, y \in \tau)$ be the affine span of τ. Let $star_\Gamma(\tau)$ be the rational polyhedral fan whose support is

$\{w \in \mathbb{R}^n |$ there exists$\epsilon > 0$ for which $w' + \epsilon w \in \Gamma$ for all $w' \in \tau\} + L$. This has one cone for each polyhedron $\sigma \in \Gamma$ that contains τ, and has lineality space L. The quotient $star_\Gamma(\tau)/L$ is a one-dimensional fan with weights inherited from Γ. We say that Γ is balanced at τ if the one-dimensional fan $star_\Gamma(\tau)/L$ is balanced. The polyhedral complex Γ is balanced if Γ is balanced at all $(d-1)$-dimensional cones.

Example 2.4.1. Let Γ be the polyhedral fan shown in Figure 2.15. This is a one-dimensional

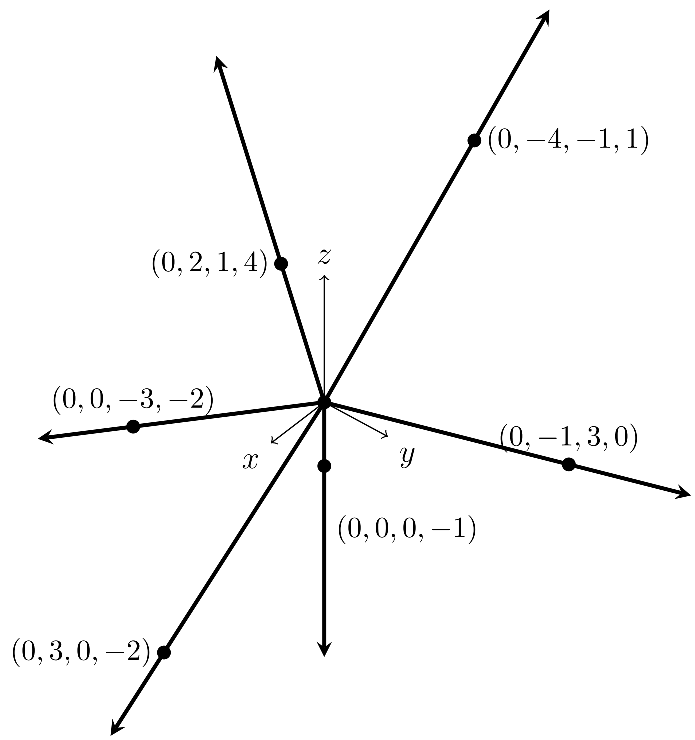

Figure 2.15: A one-dimensional weighted balanced rational polyhedral fan in $\mathbb{R}^4/\mathbb{R}\mathbf{1}$.

weighted balanced rational polyhedral fan in $\mathbb{R}^4/\mathbb{R}\mathbf{1}$. Note that Γ has one node at the origin, and six rays given as the primitive integer vectors generating them. The weight assigned to each ray of Γ is one. We compute the sum

$$\sum_{i=1}^{6} v_i = \begin{pmatrix} 0 \\ 2 \\ 1 \\ 4 \end{pmatrix} + \begin{pmatrix} 0 \\ -4 \\ -1 \\ 1 \end{pmatrix} + \begin{pmatrix} 0 \\ -1 \\ 3 \\ 0 \end{pmatrix} + \begin{pmatrix} 0 \\ 0 \\ 0 \\ -1 \end{pmatrix} + \begin{pmatrix} 0 \\ 3 \\ 0 \\ -2 \end{pmatrix} + \begin{pmatrix} 0 \\ 0 \\ -3 \\ -2 \end{pmatrix} = \begin{pmatrix} 0 \\ 0 \\ 0 \\ 0 \end{pmatrix},$$

which is zero, verifying that Γ is balanced.

Let $r_1, \ldots, r_k$ be the rays of a tropical curve Γ where $r_i = w + \operatorname{pos}(v_i)$ for some $w \in \mathbb{R}^{n+1}/\mathbb{R}\mathbf{1}$. Since $\Gamma \subset \mathbb{R}^{n+1}/\mathbb{R}\mathbf{1}$ we can choose each $v_i \in \mathbb{R}^{n+1}/\mathbb{R}\mathbf{1}$ to be the minimal nonnegative integer vector representative that generates r_i. If the multiplicity of the ray r_i in Γ is m_i, then by [7, Lemma 2.9] the *degree* of Γ, $\deg \Gamma$, is defined by

$$(\deg \Gamma)\mathbf{1} = \sum_{i=1}^{k} m_i v_i. \tag{2.12}$$

Remark 2.4.2. In the remainder of this section we use the above definition (2.12) of degree for a tropical curve Γ. Although we will not be using the following terminology, we provide the references if the reader is interested in further details on the degree of a tropical curve. An equivalent definition describes the degree of $\Gamma \subset \mathbb{R}^{n+1}/\mathbb{R}\mathbf{1}$ to be the multiplicity at the origin of the stable intersection between Γ and the standard tropical hyperplane [64, Definition 3.6.5]. For realizable curves, this is equal to the degree of any classical curve which tropicalizes to Γ [64, Corollary 3.6.16]. $\triangle$

Example 2.4.3. Consider the weighted balanced rational polyhedral fan Γ from Example 2.4.1, which is a tropical curve. We can choose a minimal nonnegative integer vector generating each ray. Recalling that the multiplicity of each ray is one, we can compute the degree of Γ using equation (2.12):

$$\sum_{i=1}^{6} v_i = \begin{pmatrix} 0 \\ 2 \\ 1 \\ 4 \end{pmatrix} + \begin{pmatrix} 4 \\ 0 \\ 3 \\ 5 \end{pmatrix} + \begin{pmatrix} 1 \\ 0 \\ 4 \\ 1 \end{pmatrix} + \begin{pmatrix} 1 \\ 1 \\ 1 \\ 0 \end{pmatrix} + \begin{pmatrix} 2 \\ 5 \\ 2 \\ 0 \end{pmatrix} + \begin{pmatrix} 3 \\ 3 \\ 0 \\ 1 \end{pmatrix} = 11 \begin{pmatrix} 1 \\ 1 \\ 1 \\ 1 \end{pmatrix}.$$

Hence, the degree of Γ is 11. $\triangle$

A *fan tropical curve* is a tropical curve which is a weighted balanced polyhedral fan of dimension one. The main result of this section is Theorem 2.4.9, which states that a fan tropical curve Γ satisfies the inequality

$$\dim \operatorname{tconv} \Gamma \leq \deg \Gamma. \tag{2.4}$$

The proof relies entirely on tropical and combinatorial techniques, and uses results from Sections 2.2 and 2.3.

Given an $n \times n$ matrix M, the *tropical rank* of M is the largest integer r such that M has a tropically nonsingular $r \times r$ submatrix. We say that an $r \times r$ real matrix $M = (m_{ij})$ is *tropically singular* if the minimum in the evaluation of the *tropical determinant*

$$\bigoplus_{\sigma \in S_r} m_{1,\sigma_1 2,\sigma_2} \odot \cdots_{r,\sigma_r} = \min\left(m_{1,\sigma_1} + m_{2,\sigma_2} + \cdots + m_{r,\sigma_r} | \sigma \in S_r\right)$$

is achieved at least twice. Here S_r denotes the symmetric group on $[r]$.

For completeness, we state the following two results which are referenced throughout the subsequent proofs. Following each result, we provide an example illustrating the statements.

Theorem 2.4.4. *[20, Theorem 4.2] The tropical rank of a $k \times n$ matrix M is equal to one plus the dimension of the tropical convex hull of the columns of M in $\mathbb{R}^k/\mathbb{R}\mathbf{1}$.*

Example 2.4.5. Let M be the 3×4 matrix given by

$$M = \begin{pmatrix} 0 & 3 & 0 & 2 \\ 0 & 0 & 2 & 1 \\ 4 & 3 & 1 & 0 \end{pmatrix}.$$

To compute the tropical rank of M we compute the tropical determinant of each 3×3

submatrix of M. We have that

$$M_1 = \text{tropDet}\begin{pmatrix} 3 & 0 & 2 \\ 0 & 2 & 1 \\ 3 & 1 & 0 \end{pmatrix} = \min(5,5,0,3,7,4) = 0.$$

Similarly we compute $M_2 = \min(2,2,0,3,8,5) = 0$, $M_3 = \min(0,4,3,5,6,8) = 0$, and

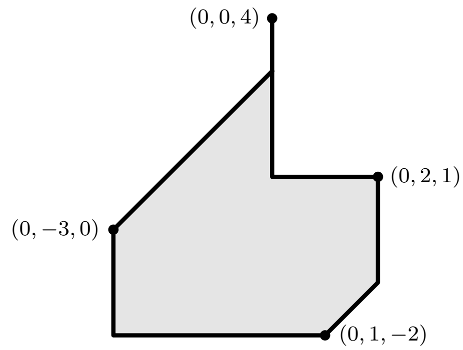

Figure 2.16: The tropical convex hull of the columns of M in Example 2.4.5 is two-dimensional. Hence the tropical rank of M is three.

$M_4 = \min(1,5,4,3,4,9) = 1$. The minimum is unique for each tropical minor, hence, all 3×3 submatrices are non-singular. Therefore, the tropical rank of M is three. Figure 2.16 shows the tropical convex hull of the columns of M, which is two-dimensional. This confirms that the tropical rank of M is three by Theorem 2.4.4. △

Lemma 2.4.6. *[72, Lemma 5.1] An $n \times n$ matrix M is tropically singular if and only if its rows lie on a tropical hyperplane in $\mathbb{R}^n/\mathbb{R}\mathbf{1}$.*

Example 2.4.7. Let Γ be a tropical curve of degree two in $\mathbb{R}^4/\mathbb{R}\mathbf{1}$ whose rays are generated by the columns of the matrix

$$M_\Gamma = \begin{pmatrix} 0 & 0 & 2 & 0 \\ 1 & 0 & 0 & 1 \\ 0 & 1 & 1 & 0 \\ 0 & 1 & 0 & 1 \end{pmatrix}.$$

Note that since $\deg \Gamma = 2$, then there are at least two zeros in each row of M_Γ. Hence, the rows of M_Γ are contained in the standard tropical hyperplane and M_Γ is tropically singular. Indeed, $\operatorname{tropDet} M_\Gamma = 0$ and this minimum is achieved three times. Observe that Γ contains a ray that is not tropically convex: $\operatorname{pos}(2,0,1,0)$. By Corollary 2.2.16 $\dim \operatorname{tconv} \operatorname{pos}(2,0,1,0) = 2$ and hence $\dim \operatorname{tconv} \Gamma \geq 2$. As Theorem 2.4.9 states, the dimension of the tropical convex hull of Γ cannot exceed its degree, and thus $\dim \operatorname{tconv} \Gamma = 2$. Moreover, the columns of M_Γ, and hence Γ itself, are also contained in the standard tropical hyperplane. This means that the dimension of the smallest tropical linear space containing Γ is two. That is the *Kapranov rank* of the matrix M_Γ is two. See [20] for detailed discussion on the different notions of rank of a tropical matrix. $\triangle$

As a first step towards proving (2.4), we prove the following lemma.

Lemma 2.4.8. *If $\Gamma \subset \mathbb{R}^{n+1}/\mathbb{R}\mathbf{1}$ is a fan tropical curve and $W \subset \Gamma$ is finite, then*

$$\dim \operatorname{tconv} W \leq \deg \Gamma.$$

Proof. Let $\deg \Gamma = d$ and Γ be given by rays $r_1 = \operatorname{pos}(v_1), \ldots, r_k = \operatorname{pos}(v_k)$ with primitive nonnegative integer vectors $v_1, \ldots, v_k$. Let $W \subset \Gamma$ be a finite set of points and $\operatorname{Supp} W$ denote the set of primitive nonnegative integer vectors of rays which contain a point of W. That is,

$$\operatorname{Supp} W = \{v_i \mid w \in \operatorname{pos}(v_i) \text{ for some } w \in W\}.$$

First suppose $|\operatorname{Supp} W| = 1$, so $W \subset r_i$ for some $i \in [k]$ and $\dim \operatorname{tconv} W \leq \dim \operatorname{tconv} r_i$. Each ray of Γ has at most d nonzero distinct entries since $\deg \Gamma = d$. By Lemma 2.2.17 this means $\dim \operatorname{tconv} r_i \leq d$ for all $i \in [k]$ and $\dim \operatorname{tconv} W \leq d$.

Let M be the $(n+1) \times k$ matrix whose columns are $v_1, \ldots, v_k$. We also assume $n+1$, $k \geq d+2$. Otherwise, the result is trivially true. We will show that the tropical rank of M is at most $d+1$, implying that $\operatorname{tconv}(v_1, \ldots, v_k) \leq d$. Let D be any $(d+2) \times (d+2)$ submatrix of M. Each row of D has all nonnegative entries and must have at least two zeros because $\deg \Gamma = d$. Hence, the rows of D lie in the tropicalization of the ordinary hyperplane $V(x_0 + \ldots + x_{d+1})$ in $\mathbb{R}^{d+2}/\mathbb{R}\mathbf{1}$. By Lemma 2.4.6 this implies D is tropically singular, so the tropical rank of M is at most $d+1$. Using Theorem 2.4.4 we deduce that the dimension of the tropical convex hull of the columns of M is at most d.

Now suppose $|\operatorname{Supp} W| = |W|$, so each point of W is on a distinct ray of Γ. More specifically, each point of W is a classical scalar multiple of some distinct v_i. The tropical convex hull of any $d+2$ columns of M has dimension at most d and the same holds if each column is scaled since the location of the zero entries is not affected.

Next suppose $1 < |\operatorname{Supp} W| < |W|$ and let $W = \{w_1, \ldots, w_s\}$. Let M' be the $(n+1) \times s$ matrix whose columns are $w_1, \ldots, w_s$. In particular, its columns are classical scalar multiples of some v_is in $\operatorname{Supp} W$. We know from the previous case that M is tropically singular and the tropical rank is at most $d+1$. By Lemma 2.4.6 we have that the columns of any $(d+2) \times (d+2)$ submatrix of M are contained in some hyperplane in $\mathbb{PT}^{d+1}$. If a point is contained in a tropical hyperplane, so is any classical scalar multiple of that point since any tropical hyperplane is a fan. For this reason, the columns of any $(d+2) \times (d+2)$ submatrix of M' must also be contained in at least one of these hyperplanes of $\mathbb{PT}^{d+1}$ from before. Therefore, M' has tropical rank at most $d+1$ and $\dim \operatorname{tconv} W \leq d$. □

Theorem 2.4.9. *If* $\Gamma \subset \mathbb{R}^{n+1}/\mathbb{R}\mathbf{1}$ *is a fan tropical curve, then* $\dim \operatorname{tconv} \Gamma \leq \deg \Gamma$.

Proof. Let $\deg \Gamma = d$ and suppose $\dim \operatorname{tconv} \Gamma = d+1$. Since $\operatorname{tconv} \Gamma$ is a fan, there exists a point p with $d+2$ distinct coordinates by Lemma 2.2.17. Moreover, Γ contains the ray $\operatorname{pos}(p)$. Note that we can choose p to be the minimal nonnegative integer vector that generates this ray. Since p has $d+2$ distinct coordinates, we may assume that $0 = p_0 < p_1 < \cdots < p_{d+1}$. Let $\lambda_i p$ be $d+2$ distinct points on the ray $\operatorname{pos}(p)$ and assume $\lambda_1 < \lambda_2 < \cdots < \lambda_{d+2}$. Let M_p be the $(n+1) \times (d+2)$ matrix whose columns are $\lambda_i p$ for

$i \in [d+2]$. Then, up to permutation of rows, M_p contains the $(d+2) \times (d+2)$ submatrix

$$D = \begin{pmatrix} 0 & 0 & \dots & 0 \\ \lambda_1 p_1 & \lambda_2 p_1 & \dots & \lambda_{d+2} p_1 \\ \vdots & \vdots & \ddots & \vdots \\ \lambda_1 p_d & \lambda_2 p_d & \dots & \lambda_{d+2} p_d \\ \lambda_1 p_{d+1} & \lambda_2 p_{d+1} & \dots & \lambda_{d+2} p_{d+1} \end{pmatrix}.$$

We will show that D has tropical rank $d+2$ by showing that the tropical determinant of D has a unique minimum attained on its antidiagonal. Using Laplace expansion along the first row, we write the tropical determinant of D as

$$\operatorname{tropDet}(D) = \min_{i \in [d+2]} 0 + \operatorname{tropDet}(D_i)$$

where D_i is the $(d+1) \times (d+1)$ submatrix of D obtained by deleting its first row and ith column. We first claim that $\operatorname{tropDet}(D_i) = m_i$ for any $i \in [d+2]$ where

$$m_i = \lambda_1 p_{d+1} + \lambda_2 p_d + \lambda_3 p_{d-1} + \cdots + \lambda_{i-1} p_{d-i+3} + \lambda_{i+1} p_{d-i+2} + \cdots + \lambda_{d+1} p_2 + \lambda_{d+2} p_1.$$

Recall that for a $(d+1) \times (d+1)$ matrix X, its tropical determinant can be written

$$\operatorname{tropDet}(X) = \bigoplus_{\sigma \in S_{d+1}} x_{1\sigma(1)} \odot x_{2\sigma(2)} \odot \cdots \odot x_{d+1,\sigma(d+1)}.$$

Let

$$\begin{aligned} \sigma(m_i) = \lambda_1 p_{\sigma(d+1)} + \lambda_2 p_{\sigma(d)} + \lambda_3 p_{\sigma(d-1)} + \cdots + \lambda_{i-1} p_{\sigma(d-i+3)} \\ + \lambda_{i+1} p_{\sigma(d-i+2)} + \cdots + \lambda_{d+1} p_{\sigma(2)} + \lambda_{d+2} p_{\sigma(1)}. \end{aligned}$$

Any permutation σ can be decomposed into adjacent transpositions of the form $\tau = (j, j+$

1). It suffices to show that $m_i < \tau(m_i)$ to conclude $m_i < \sigma(m_i)$ for any permutation $\sigma \in S_{d+1}$. Let $\tau(m_i)$ represent the expression m_i where p_j and p_{j+1} have been exchanged. First, suppose that $j > d - i + 2$, which implies that

$$m_i - \tau(m_i) = (\lambda_{d-j+2} - \lambda_{d-j+1})(p_j - p_{j+1}) < 0.$$

Similarly, if $j < d - i + 2$, then

$$m_i - \tau(m_i) = (\lambda_{d-j+3} - \lambda_{d-j+2})(p_j - p_{j+1}) < 0.$$

If $j = d - i + 2$, then

$$m_i - \tau(m_i) = (\lambda_{i+1} - \lambda_{i-1})(p_{d-i+2} - p_{d-i+3}) < 0.$$

It follows that $m_i < \tau(m_i)$ for any transposition $\tau = (j, j+1)$.

Finally, we have $\operatorname{tropDet}(D) = \min_{i \in [d+2]} m_i$. For any $i \in [d+1]$

$$m_{i+1} - m_i = (a_i - a_{i+1}) p_{d-i+2} < 0.$$

meaning $m_{i+1} < m_i$. Hence the unique minimum is obtained for $i = d+2$. This implies D has tropical rank at least $d+2$, so by Theorem 2.4.4 the dimension of the tropical convex hull of the columns of D is at least $d+1$ which contradicts Lemma 2.4.8. □

The following proposition shows that (2.4) holds for some special types of tropical curves which are not fans.

Proposition 2.4.10. *Let* Γ *be a tropical curve in* $\mathbb{R}^{n+1}/\mathbb{R}\mathbf{1}$ *with rays* $r_1, \ldots, r_k$. *If* $\dim \operatorname{tconv} \Gamma = \max_{i \in [k]} \{\dim \operatorname{tconv} r_i\}$, *then* $\dim \operatorname{tconv} \Gamma \leq \deg \Gamma$.

Proof. Let $\dim \operatorname{tconv} \Gamma = \max_{i \in [k]} \{\dim \operatorname{tconv} r_i\} = d$ and $v_1, \ldots, v_k \in \mathbb{R}^{n+1}/\mathbb{R}\mathbf{1}$ be the minimal nonnegative integer vectors such that $r_i = w_i + \operatorname{pos}(v_i) \subset \mathbb{R}^{n+1}/\mathbb{R}\mathbf{1}$ for $i \in [k]$.

Then there exists some $j \in [k]$ such that $\dim \operatorname{tconv}\ r_j = d$. By Corollary 2.2.16 v_j has $d+1$ distinct nonnegative entries, and hence, the maximum component of v_j is at most d. By (2.12) we have that $\dim \operatorname{tconv} \Gamma = d \leq \deg \Gamma$. $\square$

However, the hypothesis of Proposition 2.4.10 does not hold for all tropical curves.

Example 2.4.11. Let Γ be the fan tropical curve in $\mathbb{R}^3/\mathbb{R}\mathbf{1}$ with rays spanned by $(0,1,0)$, $(0,0,1)$, $(0,0,-1)$, and $(0,-1,0)$ emanating from the origin. Each ray $r \subset \Gamma$ is tropically convex so $\max_{r\in\Gamma}\{\dim \operatorname{tconv} r\} = 1$. However, $\dim \operatorname{tconv} \Gamma = 2$. In fact, $\operatorname{tconv} \Gamma$ con-

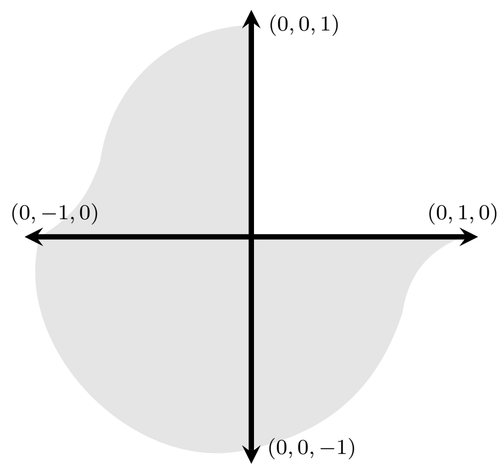

Figure 2.17: Fan tropical curve $\Gamma \subset \mathbb{R}^3/\mathbb{R}\mathbf{1}$ with rays $e_1, -e_1, e_2, -e_2$. The tropical convex hull of Γ is the two-dimensional shaded region.

tains the three cones spanned by the pairs of vectors $(0,0,1)$ and $(0,-1,0)$, $(0,-1,0)$ and $(0,0,-1)$, and $(0,0,-1)$ and $(0,1,0)$, as shown in Figure 2.17. $\triangle$

Finally, we give an example of a tropical curve where the smallest dimension of a linear space containing it is larger than the dimension of the tropical convex hull of the curve.

Example 2.4.12. Consider the tropical curve Γ_F over the field of Puiseux series $\mathbb{C}\{\{t\}\}$

given by the fan whose rays are the columns of M_F :

$$M_F = \begin{pmatrix} 1 & 1 & 1 & 0 & 0 & 0 & 0 \\ 1 & 0 & 0 & 1 & 1 & 0 & 0 \\ 1 & 0 & 0 & 0 & 0 & 1 & 1 \\ 0 & 1 & 0 & 1 & 0 & 1 & 0 \\ 0 & 0 & 1 & 0 & 1 & 1 & 0 \\ 0 & 0 & 1 & 1 & 0 & 0 & 1 \\ 0 & 1 & 0 & 0 & 1 & 0 & 1 \end{pmatrix}.$$

Note that the matrix M_F is the cocircuit matrix of the *Fano matroid*. The curve Γ_F has degree three and there is no two dimensional tropical linear space containing it [64, Section 5.3]. We now prove that $\dim \operatorname{tconv} \Gamma_F = 2$. The proof strategy is similar to the proof of Theorem 2.4.9. However, Γ_F has the special property that all its rays are tropically convex, which is a key component of the proof.

Let $v_1, v_2, \ldots, v_7 \in \mathbb{R}^7/\mathbb{R}\mathbf{1}$ denote the columns of M_F. Using Macaulay2 [42] we compute that the tropical rank of M_F is 3. By Theorem 2.4.4 $\dim \operatorname{tconv}(v_1, \ldots, v_7) = 2$ hence $\dim \operatorname{tconv} \Gamma_F \geq 2$. We will show that $\dim \operatorname{tconv} V \leq 2$ for any finite $V \subset \Gamma_F$. Note that this is not implied by Lemma 2.4.8.

For a finite set $V \subset \Gamma_F$ we can consider $\operatorname{Supp} V$ as in the proof of Lemma 2.4.8. Suppose that $|\operatorname{Supp} V| = 7$, implying that each point of $V \subset \Gamma_F$ is on a distinct ray. The tropical rank of M_F is 3 and is invariant under positive scaling of the columns of M_F, which implies $\dim \operatorname{tconv}(\lambda_1 v_1, \ldots, \lambda_7 v_7) \leq 2$ for any $\lambda_i > 0$. If all seven points are on the same ray we have that $\dim \operatorname{tconv} \operatorname{pos}(v_i) = 1$ for each $i \in [7]$, since each ray is tropically convex. Hence, $\dim \operatorname{tconv} V = 1$. For the last case, suppose $V \subset \Gamma_F$ is such that $|\operatorname{Supp} V| < 7$. For each $i \in [7]$ let $V_i = \{\lambda_{i1} v_i, \ldots, \lambda_{ik_i} v_i\} \subset V$ and $\lambda_{\max_i} = \max\{\lambda_{i1}, \ldots, \lambda_{ik_i}\}$. Since each V_i lies on a tropically convex ray, it follows that $V_i \subseteq \operatorname{tconv}(0, \lambda_{\max_i} v_i) \subset \operatorname{tconv}(\lambda_{\max_1} v_1, \ldots, \lambda_{\max_7} v_7)$. Hence, $\operatorname{tconv} V \subset \operatorname{tconv}(\lambda_{\max_1} v_1, \ldots, \lambda_{\max_7} v_7)$. The dimension of the tropical convex hull of any choice of the columns of M_F is at most 2, hence $\dim \operatorname{tconv} V \leq 2$.

In order to prove that $\dim \operatorname{tconv} \Gamma_F \leq 2$ we use a similar argument to the one in the proof of Theorem 2.4.9. Suppose that $\dim \operatorname{tconv} \Gamma_F = 3$. By Corollary 2.2.16, $\operatorname{tconv} \Gamma_F$ contains a point p with four distinct coordinates. Since Γ_F is a fan, Corollary 2.3.2 implies that $\operatorname{tconv} \Gamma_F$ contains the ray $\operatorname{pos}(p)$, and we can choose p to be the minimal nonnegative integer vector generating the ray. We may assume that $0 = p_0 < p_1 < p_2 < p_3$. Let a_1p, a_2p, a_3p, and a_4p be four distinct points on $\operatorname{pos}(p)$ with $0 < a_1 < a_2 < a_3 < a_4$. Let M_p be the matrix with columns a_ip for $i \in [4]$. Up to permutation of the rows, M_p contains the 4×4 submatrix

$$D = \begin{pmatrix} 0 & 0 & 0 & 0 \\ a_1p_1 & a_2p_1 & a_3p_1 & a_4p_1 \\ a_1p_2 & a_2p_2 & a_3p_2 & a_4p_2 \\ a_1p_3 & a_2p_3 & a_3p_3 & a_4p_3 \end{pmatrix}.$$

The tropical determinant of D is $a_1p_3+a_2p_2+a_3p_1$, and D is tropically nonsingular. Hence, the tropical rank of M_p is at least 4 and $\dim \operatorname{tconv}(a_1p, \ldots, a_4p) \geq 3$. Each $a_ip \in \operatorname{tconv} \Gamma_F$ can be written as a tropical linear combination of a finite number of points on Γ_F. Hence, $\operatorname{tconv}(a_1p, \ldots, a_4p) \subset \operatorname{tconv} W$ for a finite $W \subset \Gamma_F$. This is a contradiction because $\dim \operatorname{tconv} W \leq 2$ for all finite $W \subset \Gamma_F$. Thus $\dim \operatorname{tconv} \Gamma_F = 2$. $\triangle$

CHAPTER 3
THE STEADY-STATE DEGREE AND MIXED VOLUME OF A CHEMICAL REACTION NETWORK

The work in this chapter, with some modifications, is taken from the author's paper in collaboration with Elizabeth Gross [47]. The paper has been accepted for publication in Advances in Applied Mathematics.

3.1 Overview

Chemical reaction networks (CRNs), under the assumption of mass-action kinetics, are polynomial systems commonly used in systems biology to model mechanisms such as inter- and intracellular signaling. In this paper, we study the Newton polytopes of the steady-state systems of several reaction networks. The geometry of these polytopes can inform us about the steady-state degree of the network, and consequently, the algebraic complexity of exploring regions of multistationarity.

One way to evaluate whether a given reaction network is an appropriate model for a biological process is to consider its capacity for multiple positive real steady-states. If a reaction network has this capacity, we call the network *multistationary*. Multistationarity for reaction networks with mass-action kinetics has been extensively studied (see [55]) with algebraic methods playing a key role [23].

Once multistationarity is established, then bounds on the number of real positive steady-states [6, 31, 68, 71] and the regions of multistationarity can be explored [15, 16, 40, 45]. One method to explore regions of multistationarity, which is used in [45, 16, 69], is to sample parameters in a systematic way and repeatedly solve the *steady-state system*. The steady-state system of a reaction network is the parameterized polynomial system formed by the steady-state equations and the conservation equations. Solving steady-state systems can be done symbolically, using Gröbner bases, resultants, or other structured matrix methods, or numerically, using solvers based on polynomial homotopy continuation such as *Bertini* [70], *PHCpack* [80], and *HOM-4-PS2* [59]. Such methods and solvers will return all complex solutions, and so a final step requires filtering for real, positive solutions. We call the number of complex steady-states for generic rate constants and initial conditions the *steady-state degree* of a chemical reaction network. The steady-state degree is not only a bound on the number of real, positive steady-states, but is also a measure of the algebraic complexity of solving the steady-state system for a given reaction network, for example, the complexity of symbolic elimination methods is related to the steady-state degree. The steady-state degree is similar to the maximum likelihood degree studied in algebraic statistics [10] and the Euclidean distance degree studied in optimization [24]; the former is a measure of the algebraic complexity of maximum likelihood estimation and the latter is a measure of the algebraic complexity of minimizing the distance between a point and a variety. From the viewpoint of using numerical algebraic geometry to explore regions of multistationarity, the steady-state degree is the number of paths that need to be tracked when using a parameter-homotopy to solve the steady-state system and can serve as a stopping criterion for monodromy-based solvers, such as the one described in Chapter 4.

Using the steady-state degree as motivation, in this chapter we study the polyhedral geometry associated to the steady-state and conservation equations. In many cases, particularly when there are many variables involved, the steady-state degree of a family of networks can be difficult to establish. However, we can provide an upper bound by the Bézout bound and, in the absence of boundary solutions, the mixed volume of the polynomial system arising from the chemical reaction network. As an example, the mixed volume was used to bound the steady-state degree of a model of ERK regulation in [71]. In this paper, we explore the mixed volumes of reaction networks further, giving formulas for three families of networks. In particular, we study the combinatorics of the Newton polytopes and their Minkowski sums that arise for three infinite families of networks.

The three infinite families of chemical reaction networks that we study are constructed by successively building on smaller networks to create larger ones. The base network for each family is: the cluster-stabilization subnetwork of the cell death model from [52], the Edelstein network [66], and the one-site phosphorylation cycle (see for example, motif (a) in [30]). For each network, we compute the mixed volume and steady-state degree of the networks using various techniques such as explicit computation, reducing to semi-mixed and unmixed volume computation [12], and in the case of a randomized system, constructing a unimodular triangulation.

Table 3.1: Summary of results on the families of chemical reaction networks studied in this paper. See Theorems 3.3.8, 3.3.11, and 3.3.13; Propositions 3.3.2, 3.3.3, 3.3.4, 3.3.7, and 3.3.12; and Conjecture 3.3.18.

CRN family	**Bézout bound**	**Mixed volume**	**Steady-state degree**
Cluster-stabilization, CS_n	n	$n-2$	n (includes two boundary sols)
Edelstein, E_n	2^{n+1}	3	3
Multisite distributive phosphorylation, PC_n	2^{3n+1}	$\frac{(n+1)(n+4)}{2} - 1$	Conjecture: $2n+1$

As shown in Table 3.1, each of these examples illustrate a different relationship between the steady-state degree and the mixed volume of the the steady-state system. For the first family, based on a cluster model for cell death, we see that that the steady-state degree is actually slightly larger than the mixed volume, due to the presence of boundary steady-states. In the second family, based on the Edelstein model, the mixed volume and steady-state degree agree. In the third family, multisite distributive phosphorylation, we see that the mixed volume is quadratic in the number of sites, while the steady-state degree is conjecturally linear in the number of sites. We chose these three families for this case study due to the fact that they illustrate three different relationships between the steady-state degree and the mixed volume, and the techniques needed for analysis progressively increase in difficulty.

The most significant of these three case studies is the exploration of the multisite distributive phosphorylation system in Section 3.3.3. The n-site distributive phosphorylation system can be obtained by successively gluing together n copies of the one-site phosphorylation cycle [46]. The regions of multistationarity of this network have been recently investigated (e.g. see [6, 16, 53]) in the field of chemical reaction network theory. In addition, the number of real positive solutions has been well-studied. For example, the authors of [82] show that the number of real positive solutions is bounded above by $2n - 1$ and below by $n + 1$ when n is even and n when n is odd. Furthermore, the authors of [34] show that the $2n - 1$ bound can be achieved when $n = 3$ and $n = 4$, while the authors of [39] describe parameter regions where the steady-state system has $n + 1$ real positive solutions when n is even and n when n is odd. In Section 3.3.3, we give the mixed volume of the *randomized* steady-state system of n-site distributive phosphorylation. The randomized system is a square system obtained from the overdetermined steady-state system by taking random combinations of the polynomials. Determining the mixed volume requires computing the normalized volume of a $(3n + 3)$-dimensional $0 - 1$ polytope with $5n + 4$ vertices and $3n+7$ facets. At the end of Section 3.3.3 we show that this polytope of interest is the matching polytope of a graph.

The chapter is organized as follows. In Section 3.2, we give the necessary background, definitions, and motivation. In Section 3.3, we systematically explore each of the three families of networks.

3.2 Background & motivation

A *chemical reaction network* $\mathcal{N} = (\mathcal{S}, \mathcal{C}, \mathcal{R})$ is a triple where $\mathcal{S} = \{A_1, A_2, \ldots, A_n\}$ is a set of n chemical *species*, $\mathcal{C} = \{y_1, y_2, \ldots, y_p\}$ is a set of p *complexes* (finite nonnegative-integer combinations of the species), and $\mathcal{R} = \{y_i \to y_j \mid y_i, y_j \in \mathcal{C}\}$ is a set of r *reactions*.

Each complex in $\mathcal{C}$ can be written in the form $y_{i1}A_1 + y_{i2}A_2 + \cdots + y_{in}A_n$ where $y_{ij} \in \mathbb{Z}_{\geq 0}$, and thus, we will view the elements of $\mathcal{C}$ as vectors in $\mathbb{Z}^n_{\geq 0}$, i.e. $y_i = (y_{i1}, y_{i2}, \ldots, y_{in})$.

Additionally, to each complex of the chemical reaction network, we associate a monomial $x^{y_i} = x_{A_1}^{y_{i1}} x_{A_2}^{y_{i2}} \cdots x_{A_n}^{y_{in}}$ where $x_{A_i} = x_{A_i}(t)$ represents the concentration for species A_i with respect to time. For example, for the reaction $A + B \to 4B + C$, the monomial corresponding to the reactant $A + B$ is $x_A x_B$. The exponent vectors for this reaction are $y_1 = (1, 1, 0)$ and $y_2 = (0, 4, 1)$.

Let $y_i \to y_j$ be the reaction from the i-th to the j-th complex. To each reaction we associate a *reaction vector* $y_j - y_i$ that gives the net change in each species due to the reaction. Moreover, each reaction has an associated positive reaction rate constant k_{ij}. Given a chemical reaction network $(\mathcal{S}, \mathcal{C}, \mathcal{R})$ and a choice of $k_{ij} \in \mathbb{R}_{>0}$, the system of polynomial ordinary differential equations which describe the network dynamics under the assumption of mass-action kinetics is

$$\frac{dx}{dt} = \sum_{y_i \to y_j \in \mathcal{R}} k_{ij} x^{y_i} (y_j - y_i) =: f(x), \quad x \in \mathbb{R}^n. \tag{3.1}$$

Setting the left-hand side of the ODEs above equal to zero gives us a set of polynomial equations that we call the *steady-state equations*.

The stoichiometric subspace associated with the chemical reaction network $\mathcal{N} = (\mathcal{S}, \mathcal{C}, \mathcal{R})$ is a vector subspace of $\mathbb{R}^n$ spanned by the reaction vectors $y_j - y_i$, denoted by

$$S_{\mathcal{N}} := \mathbb{R}\{y_j - y_i \mid y_i \to y_j \in \mathcal{R}\}. \tag{3.2}$$

Given initial conditions $\mathbf{c} \in \mathbb{R}^n$, the stoichiometric compatibility class is the affine space $S_{\mathcal{N}} + \mathbf{c}$, and the *conservation equations* of $\mathcal{N}$ are the set of linear equations defining $S_{\mathcal{N}} + \mathbf{c}$.

Example 3.2.1. Consider the chemical reaction network with species $\mathcal{S} = \{A, B, C\}$ and

$$A + B \underset{k_{10}}{\overset{k_{01}}{\rightleftarrows}} 4B + C$$

$$2A \underset{k_{32}}{\overset{k_{23}}{\rightleftarrows}} C$$

complexes $\mathcal{C} = \{A + B, 4B + C, 2A, C\}$. The exponent vectors for the reactions are $y_0 = (1, 1, 0), y_1 = (0, 4, 1), y_2 = (2, 0, 0)$, and $y_3 = (0, 0, 1)$. The system of polynomial ordinary differential equations is

$$\begin{aligned} k_{10}x_B^4x_C - k_{01}x_Ax_B - 2k_{23}x_A^2 + 2k_{32}x_C &= 0 \\ -3k_{10}x_B^4x_C + 3k_{01}x_Ax_B &= 0 \\ -k_{10}x_B^4x_C + k_{01}x_Ax_B + k_{23}x_A^2 - k_{32}x_C &= 0. \end{aligned}$$

The stoichiometric subspace is the span of the reaction vectors $(1, -3, -1)$, $(-1, 3, 1)$, $(2, 0, -1)$, and $(-2, 0, 1)$. The conservation equation defining the stoichiometric compatability class is

$$3x_A - x_B + 6x_C - 3c_A + c_B - 6c_C = 0. \quad \triangle$$

In this chapter, we are concerned with the parameterized system of equations formed by the steady-state and conservation equations, which we call the *steady-state system*, we view the polynomials of the steady-state system as polynomials in the ring $\mathbb{Q}(\mathbf{k}, \mathbf{c})[x_1, \ldots x_n]$. When the solution set of this polynomial system is zero-dimensional for generic parameters $\mathbf{k}$ and $\mathbf{c}$, we define the number of complex solutions to the system for generic parameters as the *steady-state degree* of $\mathcal{N}$, where we distinguish *boundary* steady-states as complex solutions $x \in \mathbb{C}^n$ such that $x_i = 0$, for one or more $i = 1, \ldots, n$.. Notice, that while our definitions related to reaction networks are over the positive reals, since this is the region of interest in applications, the definition of steady-state degree is in terms of *complex* solutions. Moving from $\mathbb{R}$ to $\mathbb{C}$ is quite common in applied algebraic geometry as there are some gains that can be made working over an algebraically closed set; this will be the setting here.

The steady-state degree can be computed symbolically (using Gröbner bases) or numerically (using polynomial homotopy continuation), however, both these methods become computationally expensive when a large number of species are involved. In such cases we would like to know an upper bound on the degree. Two such bounds are the Bézout bound and the Bernstein-Kushnirenko-Khovanskii (BKK) bound. Given a zero-dimensional polynomial system $P = (f_1, \ldots, f_m)$ with $f_i \in \mathbb{Q}[x_1, \ldots, x_n]$, the Bézout bound on the number of solutions in $\mathbb{C}^n$ is the product of the degrees of all the polynomials in the system. The BKK bound on the number of solutions in $(\mathbb{C}^*)^n$ is the mixed volume of P, which requires P to be a square system, i.e., a system of n equations in n variables, in this case, $m = n$. The mixed volume of P is the mixed volume of the *Newton polytopes* of $f_1, \ldots, f_n$, i.e., it is the coefficient of the term $\lambda_1 \cdots \lambda_n$ in the expansion of $\mathrm{vol}(\lambda_1 \operatorname{Newt}(f_1) + \cdots + \lambda_n \operatorname{Newt}(f_n))$. Chen provides sufficient conditions under which the mixed volume of the Newton polytopes is the normalized volume of the convex hull of their union. We state these results below and reference them later in this note.

Theorem 3.2.2. *[12, Theorem 1.2] For finite sets $S_1, \ldots, S_n \subset \mathbb{Q}^n$, let $\widetilde{S} = S_1 \cup \cdots \cup S_n$. If for every proper positive dimensional face F of $\mathrm{conv}(\widetilde{S})$ we have $F \cap S_i \neq \emptyset$ for each $i = 1, \ldots, n$ then $\mathrm{MV}(\mathrm{conv}\, S_1, \ldots, \mathrm{conv}\, S_n) = n! \,\mathrm{vol}_n(\mathrm{conv}(\widetilde{S}))$.*

Example 3.2.3. Let P and Q be the two-dimensional polytopes shown in Figure 3.1, with $P = \mathrm{conv}((0,0), (0,4), (1,4), (6,1), (6,0))$ and $Q = \mathrm{conv}((0,2), (5,4), (6,4), (6,3), (4,0))$. Let $U = \mathrm{conv}(P \cup Q)$ be the union of the two polytopes. As can be seen in Figure 3.1, the intersection of every proper positive dimensional face of U with P and Q is nonempty. Here

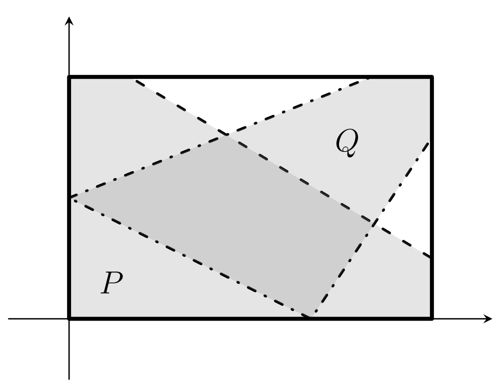

Figure 3.1: Polytopes P and Q from Example 3.2.3 and U: the convex hull of their union; this is the rectangle shown in bold. The mixed volume of P and Q is the normalized volume of U.

the only proper positive-dimensional faces are the edges of U. Hence, we can apply Theorem 3.2.2 to compute the mixed volume of P and Q by computing the normalized volume of U. That is, $\mathrm{MV}(P,Q) = 2!\,\mathrm{vol}_2(U)$. The volume of U is 24, hence $\mathrm{MV}(P,Q) = 48$. We can also see this from Figure 3.2, as the mixed volume is the area of the mixed cells C_1

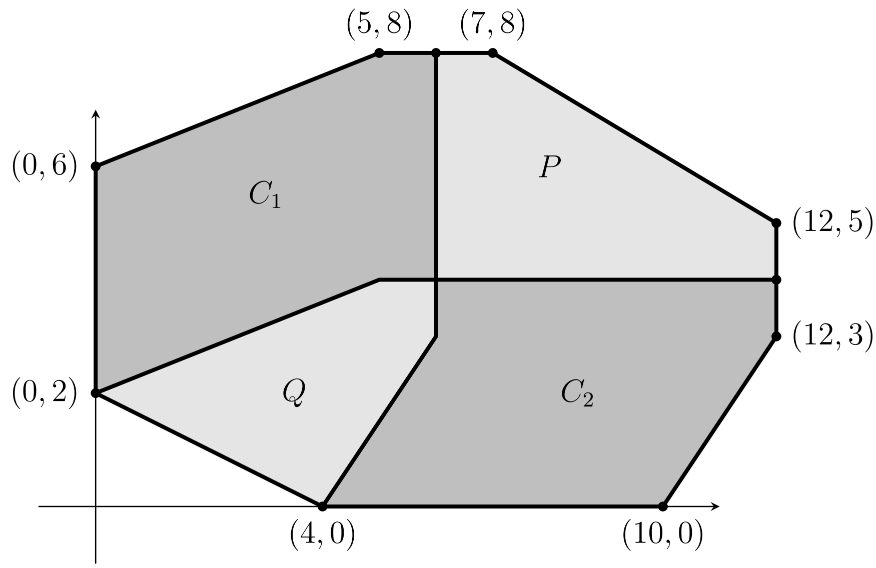

Figure 3.2: The mixed cells of the Minkowski sum of P and Q are C_1 and C_2, each with area 24.

and C_2. The area of each cell is 24. $\triangle$

Theorem 3.2.4. *[12, Theorem 1.3] Given n nonempty finite sets $S_1, \ldots, S_n \subset \mathbb{Q}^n$, let $\widetilde{S} = S_1 \cup \cdots \cup S_n$. If every positive dimensional face F of $\mathrm{conv}(\widetilde{S})$ satisfies one of the following conditions:*

(i) $F \cap S_i \neq \emptyset$ for all $i \in \{1, \ldots, n\}$;

(ii) $F \cap S_i$ is a singleton for some $i \in \{1, \ldots, n\}$;

(iii) For each $i \in I := \{i \mid F \cap S_i \neq \emptyset\}$, $F \cap S_i$ is contained in a common coordinate subspace of dimension $|I|$, and the projection of F to this subspace is of dimension less than $|I|$;

then $\mathrm{MV}(\mathrm{conv}\, S_1, \ldots, \mathrm{conv}\, S_n) = n!\,\mathrm{vol}_n(\mathrm{conv}(\widetilde{S}))$.

Corollary 3.2.5. *[12, Corollary 5.1] Given nonempty finite sets $S_{i,j} \subset \mathbb{Q}^n$ for $i = 1, \ldots, m$ and $j = 1, \ldots, k_i$ with $k_i \in \mathbb{Z}^+$ and $k_1 + \cdots + k_m = n$, let $Q_{i,j} = \mathrm{conv}(S_{i,j}), \widetilde{S}_i =$*

$\bigcup_{j=1}^{k_i} S_{i,j}$, *and* $\widetilde{Q}_i = \operatorname{conv}(\widetilde{S}_i)$. *If for each* i, *every positive dimensional face of* $\widetilde{Q}_i$ *intersecting* $S_{i,j}$, *for some* j, *on at least two points also intersects all* $S_{i,1}, \ldots, S_{i,k}$, *then*

$$\mathrm{MV}(Q_{1,1}, \ldots, Q_{m,k_m}) = \mathrm{MV}(\underbrace{\widetilde{Q}_1, \ldots, \widetilde{Q}_1}_{k_1}, \ldots, \underbrace{\widetilde{Q}_m, \ldots, \widetilde{Q}_m}_{k_m}).$$

In this collection of case studies, for each family of networks, we give the steady-state degree, the Bézout bound, and the mixed volume of the steady-state systems employing these results and other standard techniques.

3.3 Three families of networks

In what follows, we investigate three infinite families of reaction networks. The second two families result from successively joining, or gluing, smaller networks to form a larger network as defined in [46].

The first two families in this study showcase different methods that can be used to understand the steady-state degree, while the third family, mulitisite distributive sequential phosphorylation, requires more sophisticated methods. In particular, in the third case study, we describe the polytope Q_n obtained by taking the convex hull of the exponent vectors of the support of the system. We compute the normalized volume of Q_n, which bounds the number of non-boundary steady-states. This computation is done by first establishing the $\mathcal{H}$-representation of Q_n and then explicitly constructing a regular unimodular triangulation of Q_n.

3.3.1 Cluster-stabilization

The first case study is based on the ligand-independent cluster-stabilization reactions that appear in [52]. In [52], these clusters appear as part of a larger model of cell death. In particular, these reactions represent the self-stabilization of the transmembrane death receptor Fas in open form. Each network of the family has two species: Y and Z, the unstable and stable receptors, respectively. The nth reaction network in this family, denoted CS_n, has n complexes C_i of the form $C_i = (n-i)Y + iZ$, with $i = 1, \ldots, n$, and $n(n-1)/2$ reactions $C_i \xrightarrow{k_{i,j}} C_j$ such that $i < j$. The $m = 3$ case is the case that appears specifically as a subnetwork of the model proposed in [52].

The polynomial system associated to CS_n consists of one linear conservation equation in the variables x_Y and x_Z and their initial conditions $\mathbf{c} = (c_Y, c_Z)$ and two steady-state equations, one for each species. Specifically, the polynomial system of interest is

$$\begin{aligned} f_1 &= x_Y + x_Z - c_Y - c_Z = 0 \\ f_2 &= \dot{x}_Y = -\sum_{i,j,i\neq j}^{n} (j-i)k_{i,j}x_Y^j x_Z^{n-j} = 0 \\ f_3 &= \dot{x}_Z = \sum_{i,j,i\neq j}^{n} (j-i)k_{i,j}x_Y^j x_Z^{n-j} = 0. \end{aligned} \tag{3.3}$$

Since $\dot{x}_Z = -\dot{x}_Y$, there is only one unique steady-state equation of degree n. In this example, both the Bézout and BKK bounds are linear in n, with the BKK bound being slightly lower. In Proposition 3.3.4 we show that the steady-state degree, including boundary solutions, is given by the Bézout bound; see Remark 3.3.5.

Example 3.3.1. For $n = 4$, the cluster-stabilization model has two species, four complexes, and six reactions. Figure 3.3 shows the reaction graph for this model. The polynomial

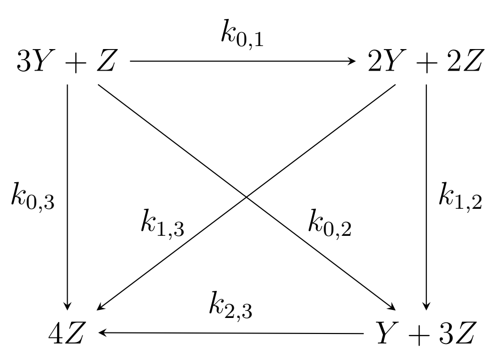

Figure 3.3: A chemical reaction network of type CS_4 with 4 complexes and 6 reactions.

system for CS_4 consists of one conservation equation and two steady-state equations, as

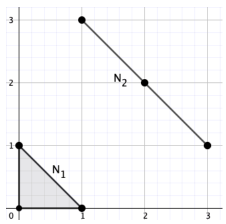

Figure 3.4: Newton polytopes for the polynomials corresponding to CS_4 in Example 3.3.1.

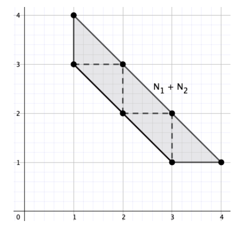

Figure 3.5: Minkowski sum of the Newton polytopes for the system in Example 3.3.1.

displayed below:

$$
\begin{aligned}
f_1 &= x_Y + x_Z - c_Y - c_Z = 0 \\
f_2 = \dot{x_Y} &= -k_{0,1}x_Y^3x_Z - 2k_{0,2}x_Y^3x_Z - 3k_{0,3}x_Y^3x_Z \\
&\qquad - k_{1,2}x_Y^2x_Z^2 - 2k_{1,3}x_Y^2x_Z^2 - k_{2,3}x_Yx_Z^3 = 0 \\
f_3 = \dot{x_Z} &= k_{0,1}x_Y^3x_Z + 2k_{0,2}x_Y^3x_Z + 3k_{0,3}x_Y^3x_Z \\
&\qquad + k_{1,2}x_Y^2x_Z^2 + 2k_{1,3}x_Y^2x_Z^2 + k_{2,3}x_Yx_Z^3 = 0.
\end{aligned}
\tag{3.4}
$$

Observe that $f_3 = -f_2$, hence we have a square system in two variables. △

Proposition 3.3.2. *The Bézout bound for the chemical reaction network CS_n is n.*

Proof. The Bézout bound can be seen from the system (3.3) — there are always three equations, one linear and two of degree n. However, the two degree n equations are identical, hence we have two equations and the Bézout bound is n. □

Proposition 3.3.3. *The polynomial system corresponding to the chemical reaction network CS_n has mixed volume $n - 2$.*

The proof of this result requires a direct computation of the mixed volume of the system. There are two Newton polytopes for any n, one of which is a line segment. Hence, the computation is straightforward. Recall that the mixed volume of m polytopes $Q_1, \ldots, Q_m \subset \mathbb{R}^n$ is $\mathrm{MV}(Q_1, \ldots, Q_m)$, which is the coefficient of $\lambda_1\lambda_2\cdots\lambda_m$ in the expansion of $\mathrm{vol}_n(\lambda_1 Q_1 + \lambda_2 Q_2 + \cdots + \lambda_m Q_m)$, with $\lambda_i \geq 0$.

Proof. Consider the system (3.3) for a network of type CS_n for some $n > 1$. As discussed earlier, we can consider only the first two polynomials f_1 and f_2, whose Newton polytopes in $\mathbb{R}^2$ are

$$\begin{aligned} N_1 &= \operatorname{conv}((1,0),(0,1),(0,0)) \\ N_2 &= \operatorname{conv}((1,n-1),(2,n-2),\ldots,(n-2,2),(n-1,1)) \end{aligned} \tag{3.5}$$

Note that N_1 is a triangle of area $\frac{1}{2}$ and N_2 is a line of length $\sqrt{2}(n-2)$. In this case, the mixed volume of (3.3) is the coefficient of $\lambda_1\lambda_2$ in the following expansion

$$\begin{aligned} \operatorname{vol}_2(\lambda_1 N_1 + \lambda_2 N_2) = \operatorname{vol}_2(N_1)\lambda_1^2 &+ 2\operatorname{vol}_2(N_1, N_2)\lambda_1\lambda_2 \\ &+ \operatorname{vol}_2(N_2)\lambda_2^2, \quad \lambda_1, \lambda_2 \geq 0, \end{aligned} \tag{3.6}$$

implying that

$$\operatorname{vol}_2(N_1, N_2) = \frac{1}{2}(\operatorname{vol}_2(N_1 + N_2) - (\operatorname{vol}_2(N_1) + \operatorname{vol}_2(N_2))). \tag{3.7}$$

Since N_1 is an equilateral right triangle of side length one, we have that $\operatorname{vol}_2(N_1) = \frac{1}{2}$, and because N_2 is a line, it follows that $\operatorname{vol}_2(N_2) = 0$. The polytope $N_1 + N_2$ is the Minkowski sum of the two Newton polytopes N_1 and N_2, that is $N_1 + N_2 = \operatorname{conv}(\{a + b \mid a \in N_1, b \in N_2\})$. The Minkowski sum of a line segment and an equilateral right triangle is a trapezoid, as shown in Figure 3.5 for $n = 4$. The two bases of the trapezoid have length $\sqrt{2}(n-2)$ and $\sqrt{2}(n-1)$, and the height of the trapezoid is $\frac{1}{\sqrt{2}}$. Hence, the area of $N_1 + N_2$ is

$$\operatorname{vol}_2(N_1 + N_2) = \frac{\sqrt{2}(2n-3)}{2} \cdot \frac{1}{\sqrt{2}} = \frac{2n-3}{2}, \tag{3.8}$$

and from (3.7) we have that $\operatorname{vol}_2(N_1, N_2) = \frac{n-2}{2}$. Thus, the coefficient of $\lambda_1\lambda_2$ in (3.6) is $n-2$, which is precisely $\operatorname{MV}(N_1, N_2)$. $\square$

Proposition 3.3.4. *For the chemical reaction network CS_n there are n steady states, in-*

cluding two boundary steady-states.

Proof. Based on the discussion following (3.3), we wish to solve a square polynomial system in two variables with one linear equation and one equation of degree n. This is easily done with elimination. Using the linear conservation equation, we can express one of the indeterminates, say x_Z, in terms of x_Y, that is $x_Z = c_Y - c_Z - x_Y$. Observe that we can factor out $x_Y x_Z$ in $\dot{x}_Y$, and substitute the expression for x_Z. This results in two boundary solutions of the form $(x_Z, y_Z) = (0, c_Y - c_Z), (c_Y - c_Z, 0)$, and $n-2$ complex solutions in $(\mathbb{C}^*)^2$. Hence, there are n steady-states, including the boundary steady-states. □

Remark 3.3.5. Based on Proposition 3.3.4, there are more steady-states than the mixed volume predicts. This is not contradictory, since the mixed volume gives a bound on the solutions in the torus $(\mathbb{C}^*)^n$, while the steady-state degree counts all solutions of the polynomial system. When there are boundary steady-states, i.e., solutions with some zero entries, the steady-state degree may be larger than the mixed volume. △

Remark 3.3.6. The proof of Proposition 3.3.4 finds the steady-state degree by finding a univariate polynomial. Such polynomials are helpful for understanding the number of real roots. The coefficients of the univariate polynomial in the proof are polynomial functions in the rate constants and initial conditions. By analyzing these coefficients it may be possible to determine semi-algebraic conditions for monostationarity and multistationarity using Descartes' rule of signs and generalizations. While this is not the main focus of this work, this would be an interesting direction to explore further. △

3.3.2 Edelstein model

The Edelstein model was proposed by B. Edelstein in 1970 [27]. It is known to exhibit multiple real, positive steady states [66] and thus is an example of a multistationary network. We study the behavior of the steady-state degree of the network after gluing n copies of the Edelstein model over shared complexes (see [46] for more details on gluing); we denote the new network E_n. The E_1 network models autocatalytic production of a species and posterior enzymatic degradation.

The model E_n is of particular interest in this study, because although the Bézout bound is exponential in the number of species, the mixed volume bound is constant and is achieved for all n. To construct E_n, we start with the Edelstein model E_1 itself: $\{A \rightleftarrows 2A, A + B \rightleftarrows B_1 \rightleftarrows B\}$. Then beginning at $i = 2$ and continuing until $i = n$, each step is defined by adding one new species B_i and four reactions gluing over the complexes $A + B$ and B. For instance, for $n = 2$, the network E_2 would have the form: $\{A \rightleftarrows 2A, A + B \rightleftarrows B_1 \rightleftarrows B, A + B \rightleftarrows B_2 \rightleftarrows B\}$. In general, the nth reaction network in this family has $n + 2$ species, $n + 4$ complexes, and $4n + 2$ reactions. The corresponding polynomial system consists of one conservation equation and $n + 2$ steady-state equations:

$$\begin{aligned}
f_1 &= x_B - c_B + \sum_{i=1}^{n}(x_{B_i} - c_{B_i}) = 0 \\
f_2 &= k_{23}x_Ax_B + k_{43}x_B - (k_{32} + k_{34})x_{B_1} = 0 \\
&\vdots \\
f_{n+1} &= k_{2,n+3}x_Ax_B + k_{4,n+3}x_B - (k_{n+3,2} + k_{n+3,4})x_{B_n} = 0 \\
f_{n+2} &= -k_{10}x_A^2 - (k_{23} + k_{25} + \cdots + k_{2,n+3})x_Ax_B + k_{01}x_A + k_{32}x_{B_1} = 0 \\
f_{n+3} &= -(k_{23} + k_{25} + \cdots + k_{2,n+3})x_Ax_B - (k_{43} + k_{45} + \cdots + k_{4,n+3})x_B = 0.
\end{aligned} \tag{3.9}$$

Observe that only $n + 1$ of the steady-state equations (the equations from (3.9) that don't include the conservation equation) are needed to define the steady-state system as there is a linear dependence between $f_2, \ldots, f_{n+1}$, and f_{n+3}, namely $f_{n+3} = -\sum_{i=2}^{n+1} f_i$. This means that a vector of species concentrations that satisfy $f_2 = 0, \ldots, f_{n+1} = 0$, will also satisfy $f_{n+3} = 0$. Despite the exponential Bézout bound shown in Proposition 3.3.7, we show that the mixed volume of the polynomial system (3.9) is constant and it is achieved as the steady-state degree.

Proposition 3.3.7. *The chemical reaction network E_n has a Bézout bound of 2^{n+1}.*

Proof. There are $n+3$ equations in the system, where one equation is linear and the rest $n+2$ are quadratic. Since $f_{n+3} = -\sum_{i=2}^{n+1} f_i$, we drop the polynomial f_{n+3} and are left with $n+1$ quadratic equations. This gives us a Bézout bound of 2^{n+1}. $\square$

Theorem 3.3.8. *The mixed volume of the polynomial system corresponding to E_n is 3.*

Example 3.3.9. Before we give a proof to Theorem 3.3.8 we give details for $n = 1$. The polynomial system for E_1 is

$$\begin{aligned} f_1 &= x_B + x_{B_1} - c_B - c_{B_1} = 0 \\ f_2 &= \dot{x}_{B_1} = k_{2,3}x_Ax_B - k_{3,2}x_{B_1} - k_{3,4}x_{B_1} + k_{4,3}x_B = 0 \\ f_3 &= \dot{x}_A = -k_{1,0}x_A^2 + k_{0,1}x_A - k_{2,3}x_Ax_B + k_{3,2}x_{B_1} = 0 \\ f_4 &= \dot{x}_B = -k_{2,3}x_Ax_B + k_{3,2}x_{B_1} + k_{3,4}x_{B_1} - k_{4,3}x_B = 0. \end{aligned} \tag{3.10}$$

Let S_i be the support of $f_i, i = 1, \ldots, 4$, and $Q_i = \operatorname{conv}(S_i)$, where $f_2 = -f_4$, so we consider only f_2. For ease of notation we write 101 for $(1, 0, 1)$. Then, the supports of the three polynomials are

$$\begin{aligned} S_1 &= \{000, 010, 001\} \\ S_2 &= \{110, 010, 001\} \\ S_3 &= \{200, 110, 100, 001\}. \end{aligned} \tag{3.11}$$

Let $S = S_1 \cup S_2 \cup S_3$, and $Q = \operatorname{conv}(S)$, see Figure 3.7. We will show that the collection of sets in (3.11) satisfies the hypothesis of Theorem 3.2.4. Let F be a facet of Q, which is a pyramid with a trapezoidal base. If F is one of the lateral facets, then F contains 001 which is a member of each set $S_i, i = 1, 2, 3$. If F is the base of the pyramid, then $F \cap S_i \neq \emptyset, i = 1, 2, 3$, since F contains at least two elements from each set S_i. If F is an edge containing 001, then $F \cap S_i \neq \emptyset, i = 1, 2, 3$. The edges containing 001 are the lateral edges. We now consider the four edges of the base of Q. In the case when $F = \operatorname{conv}(110, 010)$, we have that $F \cap S_i \neq \emptyset$ for all i. Otherwise, when F is one of the other three edges, condition (ii) of Theorem 3.2.4 is satisfied, since for at least one $i = 1, 2, 3, F \cap S_i$ is a singleton. Hence, each face of Q satisfies either condition (i) or (ii) of Theorem 3.2.4 and therefore the mixed volume of the system in (3.10) is the same as the normalized volume of the convex hull of the union of the Newton polytopes of the corresponding system. That is

$$\mathrm{MV}(Q_1, Q_2, Q_3) = 3!\,\mathrm{vol}_3(Q). \tag{3.12}$$

The Euclidean volume of Q is the number of simplices contained in a unimodular regular triangulation of Q, times the normalized volume of a unimodular three-dimensional simplex, which is $1/3!$. To see the triangulation, first we note that Q is a pyramid with a trapezoidal base. This base has a unimodular triangulation containing three simplices, see Figure 3.6. To construct Q we simply add the vertex 001 and cone over the existing simplices, see Figure 3.7. Hence, there are 3 simplices, each with volume $1/3!$. By (3.12) we have that

$$\mathrm{MV}(Q_1, Q_2, Q_3) = 3! \cdot 3 \cdot \frac{1}{3!} = 3. \tag{3.13}$$

$\triangle$

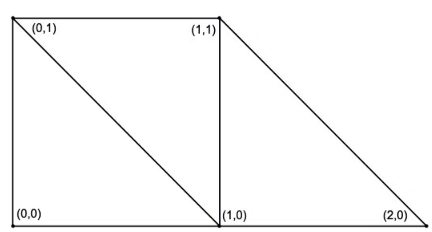

Figure 3.6: Unimodular triangulation of the trapezoidal base of Q in Example 3.3.9.

To prove Theorem 3.3.8, we use Theorem 3.2.4 and Corollary 3.2.5 to compute the mixed volume of the polynomial system in (3.9). Consider (3.9) and let $S_i = \mathrm{Newt}(f_i)$ for $i = 1, \ldots, n+2$. Observe that we omit the polynomial f_{n+3} as described above. Let $Q_i = \mathrm{conv}(S_i), i \in \{1, \ldots, n+2\}$, $\widetilde{S} = S_2 \cup \cdots \cup S_{n+1}$, $\widetilde{Q} = \mathrm{conv}(\widetilde{S})$, and $\mathcal{Q} = \mathrm{conv}(S_\cup)$, where $S_\cup = \bigcup_{i=1}^{n+2} S_i$.

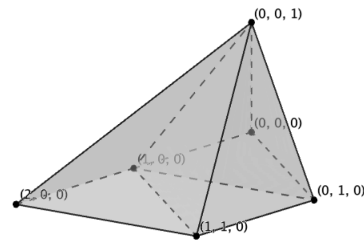

Figure 3.7: The polytope $Q = \mathrm{conv}(S)$ from Example 3.3.9 and its unimodular triangulation.

Lemma 3.3.10. *Let $n \geq 2$ and consider the chemical reaction network E_n and the corresponding polynomial system (3.9) (with $f_{n+3} = 0$ omitted). Then*

$$\mathrm{MV}(Q_1, \ldots, Q_{n+2}) = (n+2)!\,\mathrm{vol}_{n+2}(\mathcal{Q}). \tag{3.14}$$

Proof. The mixed volume computation in this case can be reduced to a *semi-mixed volume* computation, where some of the polytopes are identical. First, we want to show that

$$\mathrm{MV}(Q_1, \ldots, Q_{n+2}) = \mathrm{MV}(Q_1, \underbrace{\widetilde{Q}, \ldots, \widetilde{Q}}_{n}, Q_{n+2}).$$

Let the indeterminates of (3.9) be ordered lexicographically: $x_A, x_B, x_{B_1}, \ldots, x_{B_n}$, and let e_i be the corresponding exponent vetor for each monomial. We write e_0 for the zero vector in $\mathbb{R}^{n+2}$ and e_{ij} for $e_i + e_j$, where $i, j \in \{A, B, B_1, \ldots, B_n\}$. The supports of the f_is, $i \in \{1, \ldots, n+2\}$, in (3.9) are

$$\begin{aligned} S_1 &= \{e_0, e_B, e_{B_1}, \ldots, e_{B_n}\} \\ S_2 &= \{e_{AB}, e_B, e_{B_1}\} \\ &\vdots \\ S_{n+1} &= \{e_{AB}, e_B, e_{B_n}\}. \\ S_{n+2} &= \{2e_A, e_{AB}, e_A, e_{B_1} \ldots, e_{B_n}\} \end{aligned} \tag{3.15}$$

Observe that $S_2, \ldots, S_{n+1}$ differ by one element only, hence, they meet the criterion in Corollary 3.2.5 implying that

$$\mathrm{MV}(Q_1, \ldots, Q_{n+2}) = \mathrm{MV}(Q_1, \underbrace{\widetilde{Q}, \ldots, \widetilde{Q}}_{n}, Q_{n+2}). \tag{3.16}$$

Now, the mixed volume of the system with support (3.15) is the same as the mixed volume of the system below:

$$\begin{aligned} \widetilde{S}_1 &= \{e_0, e_B, e_{B_1}, \ldots, e_{B_n}\} \\ \widetilde{S}_j &= \{e_{AB}, e_B, e_{B_1}, \ldots, e_{B_n}\}, j = 2, \ldots, n+1 \\ \widetilde{S}_{n+2} &= \{2e_A, e_A, e_{AB}, e_{B_1}, \ldots, e_{B_n}\}. \end{aligned} \tag{3.17}$$

We want to show that the collection of $\widetilde{S}_i, i \in \{1, \ldots, n+2\}$, satisfies the hypothesis of Theorem 3.2.4. Let F be a positive dimensional face of $\mathcal{Q}$. If any of the vertices of F are in $S_\cap = \bigcap_{i=1}^{n+2} S_i$ then $F \cap \widetilde{S}_i \neq \emptyset$ for all $i \in \{1, \ldots, n+2\}$. In this case, F satisfies Theorem 3.2.4(i). Suppose that none of the vertices of F are in $S_\cap$. Then they must be in the set difference $D = S_\cup \backslash S_\cap = \{e_0, e_B, 2e_A, e_A, e_{AB}\}$. Note that $e_A \in D$ is in the interior of the edge $\{e_0, 2e_A\}$, so it is not a vertex. Suppose that the vertices of F are all of $D - \{e_A\}$. Then $F \cap \widetilde{S}_i \neq \emptyset$ for all i, and we are in case (i) of Theorem 3.2.4. If the vertices of F are a smaller subset of $D - \{e_A\}$, then F must be an edge. There are four such edges, and for each one of them, either $F \cap \widetilde{S}_i \neq \emptyset$ for all i, or for some j we have that $F \cap \widetilde{S}_j$ is a singleton. In this case we meet condition (ii) of the theorem. Hence, we have that

$$\mathrm{MV}(Q_1, \ldots, Q_{n+2}) = (n+2)!\,\mathrm{vol}_{n+2}(\mathcal{Q}). \tag{3.18}$$

$\square$

Proof of Theorem 3.3.8. To compute the volume of $\mathcal{Q}$ we construct a unimodular triangulation. Recall that the Euclidean volume of an n-dimensional unimodular simplex is $\frac{1}{n!}$. The vertices of $\mathcal{Q}$ are $\{e_0, 2e_A, e_{AB}, e_B, e_{B_i}\}$ where $i = 1, \ldots, n$. Note that all $e_j, j \in$

$\{A, B, B_i\}$ are the $\{0, 1\}$ unit vectors in $\mathbb{R}^{n+2}$, and that vectors e_{B_i} are linearly independent. This means that we can work with the polytope $P = \text{conv}(e_0, 2e_A, e_{AB}, e_B) \subset \mathbb{R}^2$. After constructing a unimodular triangulation of P we cone over it with each of the vertices $e_{B_i}, i \in \{1, \dots, n\}$. This process preserves unimodularity.

As shown in Figure 3.6, P is a trapezoid consisting of three unimodular simplices, each with area $\frac{1}{2!} = \frac{1}{2}$. In particular, we have

$$\begin{aligned} \sigma_1 &= \text{conv}(00, 10, 01) \\ \sigma_2 &= \text{conv}(10, 01, 11) \\ \sigma_3 &= \text{conv}(10, 20, 11). \end{aligned} \tag{3.19}$$

As we cone over the existing triangulation with each e_{B_i}, the number of simplices remains the same; see Figure 3.7 for example. Thus, $\mathcal{Q}$ has three $(n+2)$-dimensional simplices, each with volume $\frac{1}{(n+2)!}$. Hence, by Lemma 3.3.10 it follows that

$$\text{MV}(Q_1, \dots, Q_{n+2}) = (n+2)! \, \text{vol}_{n+2}(\mathcal{Q}) = (n+2)! \frac{3}{(n+2)!} = 3. \tag{3.20}$$

□

Theorem 3.3.11. *The steady-state degree of the chemical reaction network E_n is 3.*

Proof. We use elimination to reduce the system to a univariate cubic polynomial in x_A; the elimination algorithm is easy to see for E_1. The corresponding system (3.10) contains four polynomials in three variables with $f_2 = -f_4$, so we can reduce the system to three polynomials by forgetting f_4. Using f_1, we solve for x_{B_1} as a linear expression in x_B. Adding f_2 to f_3 and substituting for x_{B_1} in the sum, we can solve for x_B, and in turn for x_{B_1}, as a quadratic in x_A. Lastly, substituting for all variables in terms of x_A in f_3 results in a univariate cubic polynomial in x_A. Hence, there are exactly three complex solutions to (3.10).

The polynomial system for $n \geq 2$ has the general form of (3.9). Similar to the first case, using equations $f_2, \ldots, f_{n+1}$, for each $i = 1, \ldots, n$ we can express x_{B_i} as a bilinear expression in x_A and x_B. These expressions can then be substituted in f_1, from where we can solve for x_B (and respectively all x_{B_i}) as a rational expression in terms of x_A, with a quadratic numerator and a constant denominator in x_A. These operations are defined, since we assume that the collection of k_{ij}s is generic, and hence, no linear combination is zero, and also no k_{ij} is zero; moreover we assume that x_A is nonzero. Substituting the rational expressions for x_B and x_{B_i} into f_{n+2} and clearing the denominators results in a univariate cubic polynomial in x_A. Hence, there are three solutions to the system, i.e., the steady-state degree is 3. Using Descartes' rule of signs we can determine that there are either one or three real positive steady-state solutions. This result on the steady-state degree along with Lemma 3.3.10 shows that the BKK bound is tight for all n. □

3.3.3 Multi-site phosphorylation

The last family of networks we study is based on the one-site phosphorylation cycle, a mechanism that plays a role in the activation and deactivation of proteins. In particular, we look at the reaction network PC_n obtained by gluing n one-site distributive phosphorylation cycles over complexes. As an example, when two one-site distributive phosphorylation cycles are glued in this way, we obtain a two-site phosphorylation cycle [30].

The one-site distributive phosphorylation cycle consists of six species, six complexes, and six reactions: $\{S_0+E \rightleftarrows X_1 \rightarrow S_1+E, S_1+F \rightleftarrows Y_1 \rightarrow S_0+F\}$. The second copy of the one-site phosphorylation cycle will have the form $\{S_1+E \rightleftarrows X_2 \rightarrow S_2+E, S_2+F \rightleftarrows Y_2 \rightarrow S_1+F\}$ where all species with index i are replaced by the same type of species with index $i+1$, e.g., S_1 is replaced by S_2. We glue over the common complexes S_1+E and S_1+F. For n copies of the cycle, we have $3n+3$ species, $4n+2$ complexes, and $6n$ reactions. The reaction network PC_4 is shown in Figure 3.8. The corresponding polynomial system consists of three conservation equations and $3n+1$ distinct steady-state equations up to

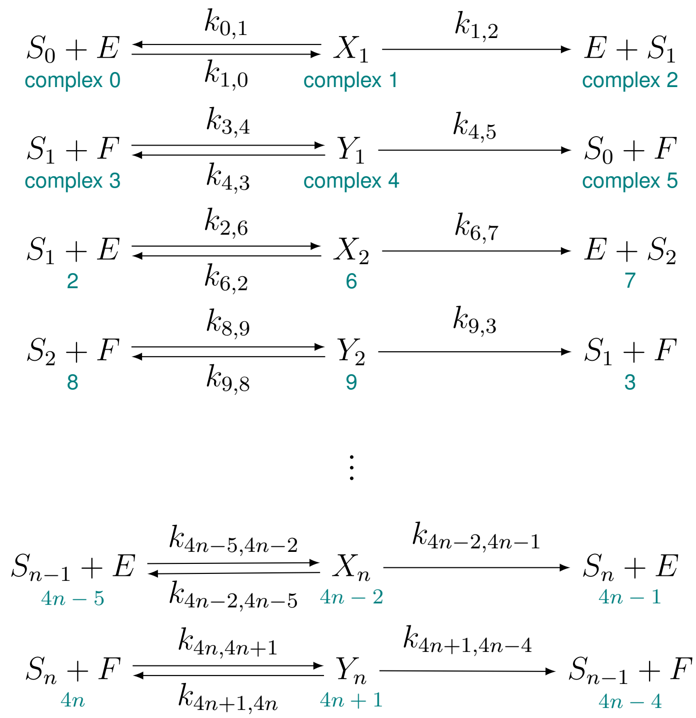

Figure 3.8: A chemical reaction network of type PC_n with labels for complexes and notation convention for reaction constants.

sign. The three conservation equations are

$$\begin{aligned}
f_1 &= x_E - c_E + \sum_{i=1}^{n}(x_{X_i} - c_{X_i}) = 0 \\
f_2 &= x_F - c_F + \sum_{i=1}^{n}(x_{Y_i} - c_{Y_i}) = 0 \\
f_3 &= \sum_{i=0}^{n}(x_{S_i} - c_{S_i}) - (x_E - c_E) - (x_F - c_F) = 0,
\end{aligned} \tag{3.21}$$

and the $3n+1$ distinct steady-state equations for $n \geq 2$ are

$$\begin{aligned}
f_4 = \dot{x}_{S_0} &= -k_{01}x_{S_0}x_E + k_{10}x_{X_1} + k_{45}x_{Y_1} = 0 \\
f_5 = \dot{x}_{S_1} &= -k_{26}x_{S_1}x_E - k_{34}x_{S_1}x_F + k_{12}x_{X_1} + k_{43}x_{Y_1} + k_{62}x_{X_2} + k_{93}x_{Y_2} = 0 \\
f_{j+4} = \dot{x}_{S_j} &= -k_{4j,4j+1}x_{S_j}x_F + k_{4j-2,4j-1}x_{X_j} + k_{4j+1,4j}x_{Y_j} - k_{4j-1,4j+2}x_{S_j}x_E = 0 \\
&\quad + k_{4j+2,4j-1}x_{X_{j+1}} + k_{4j+5,4j}x_{Y_{j+1}} = 0, \ j = 2, \ldots, n-1
\end{aligned}$$

$$
\begin{aligned}
f_{n+4} &= \dot{x}_{S_n} = -k_{4n,4n+1}x_{S_n}x_F + k_{4n-2,4n-1}x_{X_n} + k_{4n+1,4n}x_{Y_n} = 0 \\
f_{n+5} &= \dot{x}_{X_1} = k_{01}x_{S_0}x_E - (k_{10}+k_{12})x_{X_1} = 0 \\
f_{n+6} &= \dot{x}_{X_2} = k_{26}x_{S_1}x_E - (k_{62}+k_{67})x_{X_2} = 0 \\
f_{n+j+4} &= \dot{x}_{X_j} = k_{4j-5,4j-2}x_{S_{j-1}}x_E - (k_{4j-2,4j-5}+k_{4j-2,4j-1})x_{X_j} = 0,\ j = 3,\dots,n \\
f_{2n+5} &= \dot{x}_{Y_1} = k_{34}x_{S_1}x_F - (k_{43}+k_{45})x_{Y_1} = 0 \\
f_{2n+6} &= \dot{x}_{Y_2} = k_{89}x_{S_2}x_F - (k_{93}+k_{98})x_{Y_2} = 0 \\
f_{2n+j+4} &= \dot{x}_{Y_j} = k_{4j,4j+1}x_{S_j}x_F - (k_{4j+1,4(j-1)}+k_{4j+1,4j})x_{Y_j} = 0,\ j = 3,\dots,n.
\end{aligned}
\tag{3.22}
$$

The full list of steady-state equations includes $\dot{x}_E = -\sum_i \dot{x}_{X_i}$ and $\dot{x}_F = -\sum_i \dot{x}_{Y_i}$, which we disregard, since they are linear combinations of other polynomials from the system. Let $\widetilde{P}_n$ be the polynomial system for the reaction network PC_n consisting of the $3n+4$ equations from (3.21) and (3.22) set equal to zero. In what follows, we will focus on the setting where $n \geq 2$; in [30], the network PC_1 is studied and shown to be monostationary.

Proposition 3.3.12. *The Bézout bound for the reaction network PC_n is 2^{3n+1}.*

Proof. Note that each of the $3n+1$ steady-state equations in (3.22) is quadratic, and each of the three conservation equations in (3.21) is linear. Hence, the Bézout bound for the system $\widetilde{P}_n$ is 2^{3n+1}. $\square$

Since $\widetilde{P}_n$ is overdetermined, to compute the mixed volume and compare it with the Bézout bound, we consider the randomized system $P_n = M \cdot \widetilde{P}_n$, where $M \in \mathbb{C}^{(3n+3)\times(3n+4)}$ is a generic matrix. Note that every solution of $\widetilde{P}_n$ is a solution of P_n, so the mixed volume of P_n still provides an upper bound on the number solutions of $\widetilde{P_n}$ in $(\mathbb{C}^*)^n$. The system P_n is a square system with $3n+3$ equations where each polynomial is a linear combination of the polynomials f_i, $i = 1,\dots,3n+4$.

For the remainder of this section we work with the system P_n where each polynomial has support $S_n = \bigcup_{i=1}^{3n+4} S_i$ for $S_i = \mathrm{supp}(f_i),\ i = 1,\dots,3n+4$. Let $Q_n = \mathrm{conv}(S_n)$

be the Newton polytope of each polynomial of P_n. This leads to the main theorem of this section.

Theorem 3.3.13. *Let P_n be the randomized polynomial system for the reaction network PC_n. Then,*

$$\mathrm{MV}(\underbrace{Q_n, \ldots, Q_n}_{3n+3}) = (3n+3)!\,\mathrm{vol}_{3n+3}(Q_n) = \frac{(n+1)(n+4)}{2} - 1. \tag{3.23}$$

The first equality of (3.23) follows from the definition of mixed volume in the special case when all polytopes are identical. To prove the second equality we construct a triangulation T_n of the polytope Q_n. Provided T_n is *unimodular*, i.e., all simplices are unimodular, the normalized Euclidean volume of Q_n is the number of simplices in T_n. First we give a description of the vertices of Q_n, followed by a hyperplane representation of Q_n, which aids in the construction of the triangulation T_n with the desired number of simplices. We illustrate Theorem 3.3.13 with an example for $n = 1$.

Example 3.3.14. The reaction network for $n = 1$ is $\{S_0 + E \rightleftarrows X_1 \to S_1 + E, S_1 + F \rightleftarrows Y_1 \to S_0 + F\}$, and the corresponding polynomial system $\widetilde{P}_1$ is

$$\begin{aligned}
f_1 &= x_E + x_{X_1} - c_E - c_{X_1}\\
f_2 &= x_F + x_{Y_1} - c_F - c_{Y_1}\\
f_3 &= x_{S_0} + x_{S_1} - x_E - x_F - c_{S_0} - c_{S_1} + c_E + c_F\\
f_4 &= -k_{01}x_{S_0}x_E + k_{10}x_{X_1} + k_{45}x_{Y_1}\\
f_5 &= -k_{34}x_{S_1}x_F + k_{12}x_{X_1} + k_{43}x_{Y_1}\\
f_6 &= k_{01}x_{S_0}x_E - (k_{10} + k_{12})x_{X_1}\\
f_7 &= k_{34}x_{S_1}x_F - (k_{43} + k_{45})x_{Y_1}.
\end{aligned} \tag{3.24}$$

We take generic parameters k_{ij} and consider the randomized system P_1 with six equations in six variables with the following order: $x_{S_0}, x_E, x_{X_1}, x_{S_1}, x_F, x_{Y_1}$. Each polynomial in P_1

has the same support, namely

$$S_1 = \left\{ \begin{pmatrix} 0 \\ 0 \\ 0 \\ 0 \\ 0 \\ 0 \end{pmatrix}, \begin{pmatrix} 1 \\ 0 \\ 0 \\ 0 \\ 0 \\ 0 \end{pmatrix}, \cdots, \begin{pmatrix} 0 \\ 0 \\ 0 \\ 0 \\ 0 \\ 1 \end{pmatrix}, \begin{pmatrix} 1 \\ 1 \\ 0 \\ 0 \\ 0 \\ 0 \end{pmatrix}, \begin{pmatrix} 0 \\ 0 \\ 0 \\ 1 \\ 1 \\ 0 \end{pmatrix} \right\} = \{e_0, e_1, \ldots, e_6, e_{12}, e_{45}\}.$$

For $Q_1 = \operatorname{conv}(S_1) \subseteq \mathbb{R}^6$, the mixed volume for the system P_1 is

$$\operatorname{MV}(\underbrace{Q_1, \ldots, Q_1}_{6}) = 6! \operatorname{vol}_6(Q_1).$$

Observe that e_3 and e_6 are linearly independent from the rest of the vertices as vectors. In order to simplify computations, we will project away e_3 and e_6 and relabel the vertices. We will study the new polytope $K_1 = \operatorname{conv}(\mathcal{V}_1)$ in $\mathbb{R}^4$ where

$$\mathcal{V}_1 = \left\{ \begin{pmatrix} 0 \\ 0 \\ 0 \\ 0 \end{pmatrix}, \begin{pmatrix} 1 \\ 0 \\ 0 \\ 0 \end{pmatrix}, \cdots, \begin{pmatrix} 0 \\ 0 \\ 0 \\ 1 \end{pmatrix}, \begin{pmatrix} 1 \\ 1 \\ 0 \\ 0 \end{pmatrix}, \begin{pmatrix} 0 \\ 0 \\ 1 \\ 1 \end{pmatrix} \right\} = \{v_0, v_1, \ldots, v_4, v_{12}, v_{34}\}.$$

Then we will cone over the triangulation of K_1 with e_3 and then e_6 to recover Q_1. To compute the volume of K_1 we construct a placing triangulation $\mathcal{T}_1$, which is unimodular; see the proof of Lemma 3.3.17 and [18, 63] for more details.

We begin the triangulation by placing the first five vertices $v_0, \ldots, v_4$, which form a standard simplex in $\mathbb{R}^4$. Let $\sigma_1 = \operatorname{conv}(v_0, \ldots, v_4)$. Next we place the vertex v_{12}. Note that $v_{12} \notin \sigma_1$, but it is in the affine hull of σ_1. We consider the facets of σ_1 visible from v_{12}, where the only such facet is $F_1 = \operatorname{conv}(v_1, \ldots, v_4)$ since all other facets lie on the coordinate hyperplanes. We cone over F_1 with v_{12} and obtain the simplex $\sigma_2 = \operatorname{conv}(v_1, \ldots, v_4, v_{12})$. Lastly, we place v_{34} and observe that v_{34} is not in the convex hull of $\{v_0, v_1, \ldots, v_4, v_{12}\}$ but it is in their affine hull. None of the facets of σ_1 are visible from v_{34}, but two of the facets of σ_2 are visible: $F_{21} = \operatorname{conv}(v_1, v_3, v_4, v_{12})$ and $F_{22} = \operatorname{conv}(v_2, v_3, v_4, v_{12})$. We cone over each one with v_{34} constructing two more simplices: $\sigma_3 = \operatorname{conv}(F_{21} \cup \{v_{34}\})$ and $\sigma_4 = \operatorname{conv}(F_{22} \cup \{v_{34}\})$. The collection $\mathcal{T}_1 = \bigcup_{i=1}^{4} \sigma_i$ is a triangulation of K_1 by construction. Moreover, by a similar proof as the one for Lemma 3.3.17, $\mathcal{T}_1$ is a unimodular triangulation.

To construct a triangulation of Q_1, we embed K_1 in $\mathbb{R}^6$ and then we cone over each σ_i with e_3 and then e_6. This gives $T_1 = \bigcup_{i=1}^{4} s_i$, where

$$
\begin{aligned}
s_1 &= \operatorname{conv}(e_0, \ldots, e_6), \\
s_2 &= \operatorname{conv}(e_1, \ldots, e_6, e_{12}), \\
s_3 &= \operatorname{conv}(e_1, e_3, e_4, e_5, e_6, e_{12}, e_{45}), \\
s_4 &= \operatorname{conv}(e_2, e_3, e_4, e_5, e_6, e_{12}, e_{45}).
\end{aligned}
$$

The triangulation T_1 remains unimodular, hence the normalized Euclidean volume of each simplex is $1/6!$, and

$$
\operatorname{MV}(\underbrace{Q_1, \ldots, Q_1}_{6}) = 6! \operatorname{vol}_6(Q_1) = 6! \cdot \frac{4}{6!} = 4 = \frac{(n+1)(n+4)}{2} - 1.
$$

$\triangle$

Now lets consider the general case where the dimension of the ambient space of Q_n is $3n+3$. Let $e_i \in \mathbb{R}^{3n+3}$ represent the ith standard unit vector, e_0 be the zero vector, and $e_{ij} = e_i + e_j$. For $1 \le i \le d$, the vector e_i is the exponent vector of ith indeterminate in the following ordered list $(x_{S_0}, x_E, x_{X_1}, x_{S_1}, x_F, x_{Y_1}, x_{X_j}, x_{S_j}, x_{Y_j})_{j=2}^{n}$ of size $3n+3$. For $n = 1$ and $n = 2$ the vertices of Q_1 and Q_2 are given by the vector configurations

$e_0, e_1, \ldots, e_6, e_{12}, e_{45}$ and $e_0, e_1, \ldots, e_9, e_{12}, e_{24}, e_{45}, e_{58}$, respectively. Going from the $(j-1)$-site phosphorylation network to the j-site phosphorylation network ($j \geq 2$), we gain three new steady-state equations and five new monomials: $x_{X_j}, x_{S_j}, x_{Y_j}, x_{S_{j-1}}x_E, x_{S_j}x_F$. Hence, for $n \geq 3$ the vertices of Q_n are given by the $5n+4$ vectors of dimension $3n+3$ in the configuration

$$\begin{aligned} V_n = \{&e_0, e_1, \ldots, e_{3n+3}, e_{12}, e_{24}, e_{28}, \ldots, e_{2,3n-7}, e_{2,3n-4}, \\ &e_{45}, e_{58}, \ldots, e_{5,3n-1}, e_{5,3n+2}\}. \end{aligned} \tag{3.25}$$

Proposition 3.3.15. *Let Q_n be the Newton polytope of each polynomial in the system P_n for $n \geq 2$. The $\mathcal{H}$-representation of Q_n is given by*

$$\begin{aligned} 1 - x_1 - x_3 - x_4 - \sum_{i=6}^{3n+3} x_i &\geq 0 \\ 1 - x_1 - x_3 - x_5 - \sum_{i=2}^{n}(x_{3i} + x_{3i+1}) - x_{3n+3} &\geq 0 \\ 1 - x_2 - x_3 - x_5 - \sum_{i=2}^{n}(x_{3i} + x_{3i+1}) - x_{3n+3} &\geq 0 \\ 1 - x_2 - x_3 - \sum_{i=2}^{n}(x_{3i} + x_{3i+1}) - x_{3n+2} - x_{3n+3} &\geq 0 \\ x_i &\geq 0, \ i = 1, \ldots, 3n+3. \end{aligned} \tag{3.26}$$

Proof. Let $Q_n^{\mathcal{H}}$ be the polytope defined by (3.26). We aim to show that Q_n and $Q_n^{\mathcal{H}}$ coincide. Note that each coordinate $x_i, i \in \{1, \ldots, 3n+3\}$ is bounded in $Q_n^{\mathcal{H}}$; in particular, $0 \leq x_i \leq 1$. Otherwise, if $x_i > 1$ (or $x_i < 0$) at least one of the multivariate (resp. univariate) inequalities will be violated. It remains to show that the vertex sets of Q_n and $Q_n^{\mathcal{H}}$ coincide. Observe that none of the inequalities in (3.26) can be obtained by taking positive linear combinations of the remaining inequalities, implying that (3.26) is an *irredundant* description of $Q_n^{\mathcal{H}}$, hence each inequality defines a distinct facet [83].

A vertex of the polytope $Q_n^{\mathcal{H}}$ must be in the intersection of at least $3n+3$ hyperplanes described in (3.26). Hence, a vertex must satisfy a subsystem of (3.26) of size at least $(3n+3) \times (3n+3)$ at equality. We begin by considering subsets of $3n+3$ inequalities whose corresponding linear systems are consistent.

First, consider all $3n+3$ univariate equations and set $x_i = 0$ for all $i = 1, \cdots, 3n+3$; this yields the origin e_0 as a vertex of $Q_n^{\mathcal{H}}$. Next, select $3n+2$ variables x_i set equal to zero and one of the four multivariate equations. Note that some of these combinations will result in an inconsistent system. Those yielding a consistent system will have a solution with each coordinate zero except one of the x_is, which will be 1; there are $3n+3$ distinct choices for the nonzero x_i. These choices yield the vertices $e_1, \ldots, e_{3n+3}$. Thus far we have found $3n+4$ vertices of $Q_n^{\mathcal{H}}$ and each is also a vertex of Q_n.

Continuing in the same manner, we now choose $3n+1$ variables x_i set equal to zero and two of the four multivariate equations. Each of the nonzero variables must take the value 1. Otherwise we would have $0 < x_i, x_j < 1$, where $i \neq j$, implying that they appear together in both multivariate equations. In this case, each multivariate equation is reduced to $1 - x_i - x_j = 0$. However, this system yields a positive-dimensional face of $Q_n^{\mathcal{H}}$ and hence does not describe a vertex. Thus, both nonzero variables must be 1, and they cannot appear in the same multivariate equation. Independent of the choice of the two multivariate equations, the pair $\{x_i, x_j\}$ will be a subset of the variables in the symmetric difference of their supports. In particular, there are $2n$ distinct such choices: $\{x_1, x_2\}, \{x_2, x_4\}, \{x_4, x_5\}, \{x_2, x_{3j+2}\}, \{x_5, x_{3k+2}\}$, for $2 \leq j \leq n-1, 2 \leq k \leq n$. These combinations yield the $2n$ vertices $e_{12}, e_{24}, e_{28}, e_{2,11}, \ldots, e_{2,3n-1}, e_{45}, e_{58}, \ldots, e_{5,3n+2}$. Together with the previously found $3n+4$ vertices, we have a total of $5n+4$ vertices of $Q_n^{\mathcal{H}}$, which are exactly the vertices of Q_n shown in (3.25). It remains to show that $Q_n^{\mathcal{H}}$ does not have any more vertices.

Suppose that $Q_n^{\mathcal{H}}$ has a vertex $q \notin V_n$. Then, since we considered all vertices of $Q_n^{\mathcal{H}}$ with zero, one, or two nonzero entries, q must have more than two nonzero entries. Now suppose that for distinct i, j, and k, the entries q_i, q_j, and q_k are all nonzero, and the remaining $3n$

entries of q are zero. Note that q_i, q_j, and q_k must have value 1, otherwise q cannot satisfy a zero-dimensional system constructed from the inequalities in (3.26). Since $q_i = q_j = q_k$, the variables x_i, x_j, and x_k cannot appear in the same inequality. But there is no possible choice for three such variables, implying it is also not possible to have more than three nonzero variables. Therefore, we have found all vertices of $Q_n^{\mathcal{H}}$; in particular, they coincide with the vertex representation of Q_n, hence $Q_n^{\mathcal{H}} = Q_n$. □

Now we will compute the normalized Euclidean volume of Q_n by constructing a unimodular triangulation. Let $d_n = n + 3$. Similar to Example 3.3.14 we can reduce Q_n to a lower-dimensional polytope $K_n \subset \mathbb{R}^{d_n}$ by projecting down $2n$ dimensions corresponding to the vectors e_3, e_6, e_{3j+1}, and $e_{3j+3}, 2 \leq j \leq n$. These are the exponent vectors of the monomials x_{X_j} and x_{Y_j}. To avoid ambiguity of notation, we relabel the standard unit vectors and their sums after the projection (e.g. v_1 will be the 1st standard unit vector in $\mathbb{R}^{d_n}$ and $v_{12} = v_1 + v_2$), so $K_n = \mathrm{conv}(\mathcal{V}_n)$ where $|\mathcal{V}_n| = 3n + 4$ and

$$\mathcal{V}_n = \{v_0, v_1, \ldots, v_{d_n}, v_{12}, v_{23}, v_{25}, \ldots, v_{2,d_{n-1}}, v_{34}, v_{45}, \ldots, v_{4,d_n}\}. \tag{3.27}$$

Following the ideas of Example 3.3.14, we construct a *placing* triangulation $\mathcal{T}_n$ of K_n. Then we cone over $\mathcal{T}_n$ with the $2n$ remaining unit vectors from V_n to recover a unimodular triangulation of Q_n.

We will construct $\mathcal{T}_n$ by successively placing vertices. After placing each vertex, we will need information about the convex hull of the vertices already placed. The following lemma describes these intermediate polytopes and is used in the construction of $\mathcal{T}_n$. The proofs are omitted as they follow the same process and reasoning as the proof of Proposition 3.3.15.

Lemma 3.3.16. *Let $d_n = n + 3$. For each n, let K'_{n-1} be the embedding of K_{n-1} in $\mathbb{R}^{d_n}$. Let $K_n^* = \mathrm{conv}(K'_{n-1} \cup \{v_{d_n}\})$ and $\widetilde{K}_n = \mathrm{conv}(K_n^* \cup \{v_{2,d_{n-1}}\})$. Then:*

1. *The $\mathcal{H}$-representation of K_n^* is*

$$\begin{aligned}
1 - x_1 - x_3 - \sum_{j=2}^{n} x_{d_j} &\geq 0 \\
1 - x_1 - x_4 - x_{d_n} &\geq 0 \\
1 - x_2 - x_4 - x_{d_n} &\geq 0 \\
1 - x_2 - x_{d_{n-1}} - x_{d_n} &\geq 0 \\
x_i \geq 0, i = 1, \ldots, d_n = n+3.
\end{aligned} \tag{3.28}$$

2. *The $\mathcal{H}$-representation of $\widetilde{K}_n$ is*

$$1 - x_1 - x_3 - \sum_{j=2}^{n} x_{d_j} \geq 0 \tag{3.29}$$

$$1 - x_1 - x_4 - x_{d_n} \geq 0 \tag{3.30}$$

$$1 - x_2 - x_4 - x_{d_n} \geq 0 \tag{3.31}$$

$$x_i \geq 0, i = 1, \ldots, d_n. \tag{3.32}$$

Lemma 3.3.17. *Let $n \geq 2$ and $d_j = j+3, j \leq n$. Let $\mathcal{T}_1$ be the triangulation of K_1 as described in Example 3.3.14. Let $\mathcal{T}_n$ be the placing triangulation obtained from $\mathcal{T}_{n-1}$ by coning over the k_{n-1} simplices of $\mathcal{T}_{n-1}$ with apex v_{d_n} and placing $v_{2,d_{n-1}}$ and v_{4,d_n}, in that order. The simplices obtained by placing $v_{2,d_{n-1}}$ and v_{4,d_n} are*

$$\begin{aligned}
\sigma_{k_{n-1}+1} &= \operatorname{conv}\big(v_2, v_{d_{n-1}}, v_{d_n}, v_{12}, v_{23}, v_{25}, \ldots, v_{2,d_{n-1}}, v_{4,d_{n-1}}\big) \\
\sigma_{k_{n-1}+2} &= \operatorname{conv}\big(v_1, v_4, v_{d_n}, v_{12}, v_{34}, v_{45}, \ldots, v_{4,d_n}\big) \\
\sigma_{k_{n-1}+3} &= \operatorname{conv}\big(v_2, v_4, v_{d_n}, v_{12}, v_{23}, v_{25}, \ldots, v_{2,d_{n-1}}, v_{4,d_n}\big) \\
\sigma_{k_{n-1}+4} &= \operatorname{conv}\big(v_2, v_{d_n}, v_{12}, v_{23}, v_{34}, v_{45}, \ldots, v_{4,d_n}\big) \\
\sigma_{k_{n-1}+5} &= \sigma_{k_{n-1}+4} \backslash \{v_{34}\} \cup \{v_{25}\}
\end{aligned} \tag{3.33}$$

$$\vdots$$

$$\sigma_{k_{n-1}+d_{n-1}} = \sigma_{k_{n-1}+d_{n-1}-1} \backslash \{v_{4,d_{n-1}-1}\} \cup \{v_{2,d_{n-1}}\}.$$

Furthermore, $\mathcal{T}_n$ has $k_n = 4 + \sum_{j=2}^{n-1} d_j$ simplices and is unimodular.

Proof. The triangulation $\mathcal{T}_n$ is obtained inductively beginning with the explicit construction of $\mathcal{T}_1$ in Example 3.3.14 containing $k_1 = 4$ unimodular simplices. Suppose the triangulation $\mathcal{T}_{n-1}$ has been constructed by successively placing vertices as described in the statement of the lemma. Furthermore, assume $\mathcal{T}_{n-1}$ contains $k_{n-1} = 4 + \sum_{j=2}^{n-2} d_j$ unimodular simplices as described in (3.33). We embed K_{n-1} and its triangulation $\mathcal{T}_{n-1}$ into $\mathbb{R}^{d_n}$ and place the vertices (i) v_{d_n}, (ii) $v_{2,d_{n-1}}$, and (iii) v_{4,d_n} as follows.

(i) Placing v_{d_n} : Placing v_{d_n} increases the dimension of the polytope K_{n-1} by one from d_{n-1} to d_n. We cone over all simplices of $\mathcal{T}_{n-1}$ with v_{d_n} and obtain the first k_{n-1} simplices of $\mathcal{T}_n$. The resulting polytope is K_n^* and its facet defining inequalities are given in (3.28).

(ii) Placing $v_{2,d_{n-1}}$: Consider the facet defining inequalities of K_n^* in (3.28). Note that the hyperplane $1 - x_2 - x_{d_{n-1}} - x_{d_n} = 0$ is the only one separating $v_{2,d_{n-1}}$ and K_n^*. Facets of K_n^* contained in this hyperplane will be visible from $v_{2,d_{n-1}}$. There is only one such facet, namely

$$F_{2,d_{n-1},d_n} = \operatorname{conv}(v_2, v_{d_{n-1}}, v_{d_n}, v_{12}, v_{23}, v_{25}, \ldots, v_{2,d_{n-2}}, v_{4,d_{n-1}}),$$

containing d_n vertices and hence it is a simplex of dimension d_{n-1}. Coning over F_{2,d_{n-1},d_n} with $v_{2,d_{n-1}}$ yields the d_n-dimensional simplex $\sigma_{k_{n-1}+1}$. The resulting polytope after placing $v_{2,d_{n-1}}$ is $\widetilde{K}_n$ whose facet defining inequalities are given in (3.29) – (3.32).

(iii) Placing v_{4,d_n} : We aim to show that in this step we add $d_{n-1}-1$ new simplices. Investigating the facet defining inequalities of $\widetilde{K}_n$, we note that there are two hyperplanes separating v_{4,d_n} from $\widetilde{K}_n$, namely (3.30) and (3.31) containing the respective facets

$$
\begin{aligned}
F_{1,4,d_n} &= \operatorname{conv}(v_1, v_4, v_{d_n}, v_{12}, v_{34}, v_{45}, \ldots, v_{4,d_{n-1}}) \\
F_{2,4,d_n} &= \operatorname{conv}(v_2, v_4, v_{d_n}, v_{12}, v_{23}, v_{25}, \ldots, v_{2,d_{n-1}}, v_{34}, v_{45}, \ldots, v_{4,d_{n-1}}).
\end{aligned}
$$

Note that $F_{1,4,d_n}$ is a d_{n-1}-dimensional simplex, so coning over it with v_{4,d_n} results in the d_n-dimensional simplex $\sigma_{k_{n-1}+2}$.

The facet $F_{2,4,d_n}$ lies in the facet defining hyperplane $1 - x_2 - x_4 - x_{d_n} = 0$; it has $2d_{n-1} - 2$ vertices and a unimodular triangulation induced by the triangulation of $\widetilde{K}_n$. In particular, the simplices in the triangulation of $F_{2,4,d_n}$ are $\sigma_{k_{n-2}+3} \setminus \{v_{d_{n-1}}\} \cup \{v_{d_n}\}, \ldots, \sigma_{k_{n-2}+d_{n-2}} \setminus \{v_{d_{n-1}}\} \cup \{v_{d_n}\}$, $\sigma_{k_{n-1}+1} \setminus \{v_{d_{n-1}}\}$. These d_{n-1} dimensional simplices are obtained by considering the intersection of the simplices $\sigma_{k_{n-2}+1} \cup \{v_{d_n}\}, \ldots, \sigma_{k_{n-2}+d_{n-2}} \cup \{v_{d_n}\}$, $\sigma_{k_{n-1}+1}, \sigma_{k_{n-1}+2}$ of $\widetilde{K}_n$ with the hyperplane $1 - x_2 - x_4 - x_{d_n} = 0$; note that we do not need to consider the remaining simplices of $\widetilde{K}_n$, since each intersection with $F_{2,4,d_n}$ is necessarily of dimension less than d_{n-1}.

We cone over the triangulation of $F_{2,4,d_n}$ with v_{4,d_n} and obtain the $d_{n-2} - 1 = d_n - 3$ simplices $\sigma_{k_{n-1}+3}, \ldots, \sigma_{k_{n-1}+d_{n-1}}$. Hence, we have a total of

$$k_n = k_{n-1} + 2 + (d_n - 3) = k_{n-1} + d_{n-1} = 4 + \sum_{j=2}^{n-1} d_j$$

simplices in $\mathcal{T}_n$.

Finally, we show that the placing triangulation $\mathcal{T}_n$ is unimodular. The polytope K_n is a d_n-dimensional *compressed* polytope [18], implying that all of its *pulling* triangulations are unimodular. A placing triangulation is equivalent to a pushing triangulation. The latter is a regular triangulation with a lifting vector of heights $\omega : J \to \mathbb{R}$, where J is the set of labels on $\mathcal{V}_n$ with respect to some order. Reversing the order of the labels of $\mathcal{V}_n$ and the heights of the weight vector ω makes the pushing triangulation into a pulling triangulation [63, 18]. Hence, $\mathcal{T}_n$ as constructed is a regular unimodular triangulation. $\square$

Proof of Theorem 3.3.13. The first equality in (3.23) follows from the definition of mixed volume in the special case when all polytopes are identical. We aim to obtain a unimodular triangulation of Q_n. By Lemma 3.3.17 K_n has a triangulation $\mathcal{T}_n$ with

$$4 + \sum_{i=1}^{n-1} d_i = 4 + \sum_{i=1}^{n-1} i + 3 = \frac{(n+4)(n+1)}{2} - 1$$

simplices. To achieve a unimodular triangulation of Q_n, we cone over the triangulation $\mathcal{T}_n$ in the $2n$ originally-collapsed dimensions, which preserves the number of simplices. The polytope Q_n has dimension $3n+3$, hence the normalized Euclidean volume of each full dimensional unimodular simplex is $\frac{1}{(3n+3)!}$. The second equality of (3.23) now follows. $\square$

The mixed volume for the randomized system of PC_n is quadratic in n, which is a tighter bound than the exponential Bézout bound. Nonetheless, for it is still significantly higher than the steady-state degree of the ideal that we witness in computation. Indeed, based on numerical computations up to $n = 15$, we conjecture the following for the steady-state degree of PC_n, which is linear in n.

Conjecture 3.3.18. *The steady-state degree of the chemical reaction network PC_n is $2n+1$ for $n \geq 1$.*

Remark 3.3.19. We note the authors of [82] show that the number of real positive solutions is bounded above by $2n-1$ by using a positive reparameterization. Along the way they introduce a polynomial with degree $2n+1$. With careful treatment, we expect this polynomial could be used to establish steady-state degree of PC_n. $\triangle$

Our exploration of Q_n reveals that Newton polytopes of steady-state equations are interesting combinatorially on their own. Indeed, we finish our discussion of Q_n by showing that it is a matching polytope of a graph.

Let G_n be the multigraph on $n+3$ vertices with $d = 3n+3$ edges, such that G_n contains one four-cycle, $n-1$ edges incident with one node of the four-cycle, say s_1, and $2n$ parallel edges connecting s_1 diagonally with s_3. See Figure 3.9 for example. Each edge of G_n represents a species of PC_n.

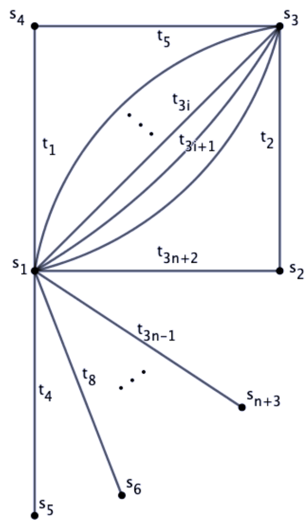

Figure 3.9: The graph $G_n; Q_n = P_{MA}(G_n)$.

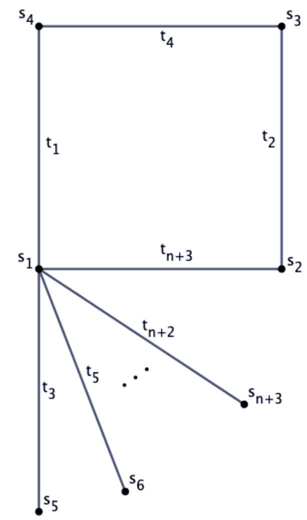

Figure 3.10: The graph $\widetilde{G}_n; K_n = P_{MA}(\widetilde{G}_n)$.

The *matching polytope* of the graph G_n is the convex hull of the incidence vectors of all matchings of G_n, i.e.,

$$P_{MA}(G_n) = \text{conv}\{\chi^M | M \text{ is a matching } of G_n\}.$$

A *matching* of G_n is a subset of edges $M \subseteq E(G_n)$ such that each vertex is incident with no more than one edge of M. The *incidence* vector $\chi^M \in \{0,1\}^{|E(G_n)|}$ of a matching M is

$$\chi_t^M = \begin{cases} 1, & t \in M, \\ 0, & \text{otherwise.} \end{cases}$$

Each matching of the graph G_n, equivalently each vertex of $P_{MA}(G_n)$, corresponds to the support of a monomial in the dynamical polynomial system P_n of Section 3.3.3, thus, we can think of G_n as encoding the species relationships between complexes.

Proposition 3.3.20. *The polytope Q_n is the matching polytope of the graph G_n described above, i.e., $Q_n = P_{MA}(G_n)$.*

Proof. The incidence vector of a matching of G_n containing only one edge t_i coincides with the standard vector e_i with entry 1 in the ith position. A matching of G_n can contain at most two edges, and each pair is either of the form $M_j = \{t_2, t_j\}, j = 1, 4, 8, 11, \ldots, 3n-1$ or of the form $M_\ell = \{t_5, t_\ell\}, \ell = 4, 8, 11, \ldots, 3n-1, 3n+2$. Note that the incidence vectors of the matchings of type M_j and M_ℓ can be represented as $e_{2,j}$ or $e_{5,\ell}$ for ℓ, j as specified above. Hence, the vertices of the matching polytope of G_n are the same as the vertices of Q_n as given in (3.25), implying the two polytopes coincide. □

Let $\widetilde{G}_n$ be the simple graph arising from G_n by deleting the $2n$ parallel edges $t_{3i}, t_{3i+1}, 1 \leq i \leq n$ and relabeling the remaining edges. Then $\widetilde{G}_n$ is the graph on $n+3$ vertices and $n+3$ edges.

Proposition 3.3.21. *The polytope K_n is the matching polytope for $\widetilde{G}_n$, i.e., $K_n = P_{MA}(\widetilde{G}_n)$.*

Proof. Similarly to the proof of Proposition 3.3.20, we will show that the vertices of K_n and $P_{MA}(\widetilde{G}_n)$ are the same. Note that the matching for $\widetilde{G}_n$ will be a subset of the matching of G_n. In particular, there will be $2n$ fewer singleton matchings resulting from the deletion of the $2n$ parallel edges. No two-edge matching will be lost in the construction of $\widetilde{G}_n$ from G_n. All single edge matchings correspond to the standard vectors e_i for $1 \leq i \leq n+3$, with e_0 representing the empty matching. As in the proof of Proposition 3.3.20, we have two-edge matchings of types $M_{j'}$ and $M_{\ell'}$ for $j' = 1, 3, 5, 6, \ldots, n-1$ and $\ell' = 3, 5, 6, \ldots, n$ corresponding to the vertices $v_{2,j'}$ and $v_{4,\ell'}$ from the vertex representation of K_n given in (3.27). Hence, $K_n = P_{MA}(\widetilde{G}_n)$. □

CHAPTER 4

SOLVING POLYNOMIAL SYSTEMS VIA HOMOTOPY CONTINUATION AND MONODROMY

The work in this chapter, with some modifications, is taken largely from the author's paper with Timothy Duff, Andres Jensen, Kisun Lee, Anton Leykin, and Jeff Sommars [26]. The paper has been published in the IMA Journal of Numerical Analysis.

4.1 Overview

Homotopy continuation has become a standard technique for finding approximations of solutions to polynomial systems. There is an early popular text on the subject and its applications by Morgan [67]. This technique is the backbone of numerical algebraic geometry, the area which classically addresses the questions of complex algebraic geometry through algorithms that employ numerical approximate computation. The chapter by Sommese, Verschelde, and Wampler [75, Chapter 8] is the earliest introduction and the book by Sommese and Wampler [76] is the primary reference in the area.

Families of polynomial systems with parametric coefficients play one of the central roles. Most homotopy continuation techniques could be viewed as going from a generic system in the family to a particular one. This process is commonly referred to as *degeneration*. Going in the reverse direction, it may be called *deformation*, *undegeneration*, or *regeneration*, depending on the literature. Knowing the solutions of a generic system, we can use *coefficient-parameter homotopy* [76, Chapter 7] to get to the solution of a particular one.

The main problem we address here is how to solve a generic system in a family of systems

$$F_p = (f_p^{(1)}, \dots, f_p^{(N)}) = 0, \quad f_p^{(i)} \in \mathbb{C}[p][x_1, \dots, x_n],\ i = 1, \dots, N,$$

with finitely many parameters p and variables $x_1, \cdots, x_n$. In the main body of the chapter we restrict our attention to *linear parametric* families of systems. These are systems with affine linear parametric coefficients, such that for a generic p we have a nonempty finite set of solutions $x = (x_1, \dots, x_n)$ to $F_p(x) = 0$. This implies there are at least as many equations as variables, i.e., $N \geq n$. The number of parameters is arbitrary, but we require that for a generic x there exists p with $F_p(x) = 0$. These restrictions are made for the sake of simplicity. Our approach can be applied in a more general setting following the modifications proposed in [26, Section 7].

Linear parametric systems form a large class that includes *sparse polynomial systems*. These are square systems, $n = N$, with a fixed monomial support for each equation, and a distinct parameter for the coefficient of each monomial. *Polyhedral homotopy* methods for solving sparse systems stem from the BKK (Bernstein, Khovanskii, Kouchnirenko) bound on the number of solutions [5]. The BKK bound is the number of solutions of a generic square system, which is the same as the mixed volume of the system. The early work on algorithm development was done in [54, 81]. Polyhedral homotopies provide an optimal solution to sparse systems in the sense that they are designed to follow exactly as many paths as the number of solutions of a generic system given by the BKK bound.

The method that we propose is not optimal in the above sense. The expected number of homotopy paths followed can be larger than the number of solutions, though not significantly larger. We use linear segment homotopies that are significantly simpler and less expensive to follow in practice. Our current implementation shows it is competitive with the state-of-the-art implementations of polyhedral homotopies in PHCpack [80] and HOM4PS2 [59] for solving sparse systems. In a setting more general than sparse, we demonstrate examples of linear parametric systems for which our implementation exceeds the capabilities of the existing sparse system solvers and blackbox solvers based on other ideas.

The idea of using the monodromy action induced by the fundamental group of the regular locus of the parameter space has been successfully employed throughout numerical algebraic geometry. One of the main tools in the area, *numerical irreducible decomposition*, can be efficiently implemented using the *monodromy breakup* algorithm, which first appeared in [79]. One parallel incarnation of the monodromy breakup algorithm is described in [62]. In fact, the main idea in that work is close in spirit to what we propose in this chapter. The idea to use monodromy to find solutions drives numerical implicitization [11] and appears in other works such as [9].

Our main contribution is a new framework to describe algorithms for solving polynomial systems using monodromy; we call it the *Monodromy Solver* (MS) framework. We analyze the complexity of our main algorithm experimentally on families of examples. For theoretical statistical analysis see [26, Section 4]. Our method and its implementation not only provide a new general tool for solving polynomial systems, but also can solve some problems out of reach for other existing software.

The structure of this chapter is as follows. We give a brief overview of the MS method along with some necessary preliminaries in Section 4.2. An algorithm following the MS framework depends on a choice of strategy, with several possibilities, outlined in Section 4.3. The implementation is discussed in Section 4.4. The results of our experiments on selected example families highlighting various practical computational aspects are in Section 4.5. The reader may also want look at examples of systems in Section 4.5.1 and Section 4.5.2 before reading some of the earlier sections.

4.2 Background and framework preliminaries

Let $m, n \in \mathbb{N}$ and $p \in \mathbb{C}^m$. We consider the complex linear space of square systems F_p, where the monomial support of $f_p^{(1)}, \dots, f_p^{(n)}$ in the variables $x = (x_1, \dots, x_n)$ is fixed and the coefficients vary. By a *base space* B we mean a parametrized linear variety of systems. We think of it as the image of an affine linear map $\psi : p \mapsto F_p$ from a parameter space $\mathbb{C}^m$ with coordinates $p = (p_1, \dots, p_m)$ to the space of systems.

We assume the structure of our family is such that the projection ϕ from the *solution variety*

$$V = \{(F_p, x) \in B \times \mathbb{C}^n \mid F_p(x) = 0\}$$

to B gives us a *branched covering*, i.e., the fiber $\phi^{-1}(F_p)$ is finite and of the same cardinality for a generic p. The *discriminant variety* D in this context is the subset of systems in the base space with nongeneric fibers; it is also known as the *branch locus* of the projection ϕ.

The *fundamental group* $\pi_1(B \setminus D)$ as a set consists of loops. These are paths in $B \setminus D$ starting and finishing at a fixed $p \in B \setminus D$, considered up to homotopy equivalence. The definition, found in Section 4.2.1, does not depend on the point p, since $B \setminus D$ is connected. Each loop induces a permutation of the fiber $\phi^{-1}(F_p)$, which is referred to as a *monodromy* action.

Our goal is to find the fiber of one generic system in our family. Our method is to find one pair (p_0, x_0) in the solution variety V and use the monodromy action on the fiber $\phi^{-1}(F_{p_0})$ to find its points. We assume that this action is transitive, which is the case if and only if the solution variety V is irreducible. If V happens to be reducible, we replace V with its unique dominant irreducible component as explained in Remark 4.2.2.

4.2.1 Monodromy

We briefly review the basic facts concerning monodromy groups of branched coverings. With notation as before, fix a system $F_p \in B \setminus D$ and consider a loop τ without branch points based at F_p; that is, a continuous path

$$\tau : [0,1] \to B \setminus D,$$

such that $\tau(0) = \tau(1) = F_p$. Suppose we are also given a point x_i in the fiber $\phi^{-1}(F_p)$ with d points $x_1, x_2, \ldots, x_d$. Since ϕ is a covering map, the pair (τ, x_i) corresponds to a unique *lifting* $\widetilde{\tau}_i$. This is a path

$$\widetilde{\tau}_i : [0,1] \to V,$$

such that $\widetilde{\tau}_i(0) = x_i$ and $\widetilde{\tau}_i(1) = x_j$ for some $1 \leq j \leq d$. Note that the reversal of τ and x_j lift to a reversal of $\widetilde{\tau}_i$. Thus, the loop τ induces a permutation of the set $\phi^{-1}(F_p)$. We have a group homomorphism

$$\varphi : \pi_1(B \setminus D, F_p) \to \mathrm{S}_d$$

whose domain is the usual fundamental group of $B \setminus D$ based at F_p, and S_d is the symmetric group on d elements. The image of φ is the *monodromy group* associated to $\phi^{-1}(F_p)$. The monodromy group acts on the fiber $\phi^{-1}(F_p)$ by permuting the solutions of F_p.

Remark 4.2.1. A reader familiar with the notion of a *monodromy loop* in the discussion of [76, Chapter 15.4] may think of this keyword referring to a representative of an element of the fundamental group, together with its liftings to the solution variety, and the induced action on the fiber. $\triangle$

We have not used any algebraic properties so far. The construction of the monodromy group above holds for an arbitrary covering with finitely many sheets. If the total space is connected, then the monodromy group is a transitive subgroup of S_d. In our setting, since we are working over $\mathbb{C}$, this occurs precisely when the solution variety is irreducible.

Remark 4.2.2. For a linear family, we can show that there is at most one irreducible component of the solution variety V for which the restriction of the projection $(F_p, x) \mapsto x$ is dominant; that is, its image is dense. We call such a component the *dominant component*.

Indeed, let U be the locus of points $(F_p, x) \in \phi^{-1}(B \setminus D)$ such that

- the restriction of the x-projection map is locally surjective, and
- the solution to the linear system of equations $F_p(x) = 0$ in p has the generic dimension.

Being locally surjective could be interpreted either in the sense of Zariski topology or as inducing surjection on the tangent spaces. Then either U is empty or $\overline{U}$ is the dominant component we need, since it is a vector bundle over an irreducible variety, and is hence irreducible. $\triangle$

In the remainder of this chapter, when we say *solution variety*, we mean the *dominant component of the solution variety*. In particular, for sparse systems, restricting our attention to the dominant component translates into looking for solutions only in the torus $(\mathbb{C}^*)^n$.

4.2.2 Homotopy continuation

Given two points F_{p_1} and F_{p_2} in the base space B, we may form the family of systems

$$H(t) = (1-t)F_{p_1} + tF_{p_2}\,, \quad t \in [0,1],$$

known as the *linear segment homotopy* between the two systems. If p_1 and p_2 are sufficiently generic, for each $t \in [0,1]$ we have that $H(t)$ is outside of the set D of real codimension two. Consequently, each system $H(t)$ has a finite and equal number of solutions. This homotopy is a path in B; a lifting of this path in the solution variety V is called a *homotopy path*. The homotopy paths of $H(t)$ establish a one-to-one correspondence between the fibers $\phi^{-1}(F_{p_1})$ and $\phi^{-1}(F_{p_2})$.

Remark 4.2.3. Note that for $\gamma \in \mathbb{C} \setminus \{0\}$, γF_p has the same solutions as F_p. Let us scale both ends of the homotopy by taking a homotopy between $\gamma_1 F_{p_1}$ and $\gamma_2 F_{p_2}$ for generic γ_1

and γ_2. If the coefficients of F_p are homogeneous in p then

$$H'(t) = (1-t)\gamma_1 F_{p_1} + t\gamma_2 F_{p_2} = F_{(1-t)\gamma_1 p_1 + t\gamma_2 p_2}\,, \quad t \in [0,1],$$

is a homotopy matching solutions $\phi^{-1}(F_{p_1})$ and $\phi^{-1}(F_{p_2})$, where the matching is potentially different from that given by $H(t)$. Similarly, for an affine linear family, $F_p = F'_p + C$ where F'_p is homogeneous in p and C is a constant system, we have

$$H'(t) = (1-t)\gamma_1 F_{p_1} + t\gamma_2 F_{p_2} = F'_{(1-t)\gamma_1 p_1 + t\gamma_2 p_2} + ((1-t)\gamma_1 + t\gamma_2)C.$$

We ignore the fact that $H'(t)$ may go outside B for $t \in (0,1)$, since its rescaling,

$$\begin{aligned} H''(t) &= \frac{1}{(1-t)\gamma_1 + t\gamma_2} H'(t) \\ &= F'_{\frac{(1-t)\gamma_1 p_1 + t\gamma_2 p_2}{(1-t)\gamma_1 + t\gamma_2}} + C = F_{\frac{(1-t)\gamma_1 p_1 + t\gamma_2 p_2}{(1-t)\gamma_1 + t\gamma_2}}\,, \quad t \in [0,1], \end{aligned}$$

does not leave B and has the same homotopy paths. Note that $H''(t)$ is well defined for generic γ_1 and γ_2 as $(1-t)\gamma_1 + t\gamma_2 \neq 0$ for all $t \in [0,1]$. △

One may use methods of *numerical homotopy continuation*, described, for instance, in [76, Section 2.3], to track the solutions as t changes from zero to one. In some situations the path in B may pass close to the branch locus D and numerical issues must be considered.

Remark 4.2.4. If the family F_p is nonlinear in the parameters p, one has to take the *parameter linear segment homotopy* in the parameter space, i.e., $H(t) = F_{(1-t)p_1 + tp_2}$, $t \in [0,1]$. This does not change the overall construction; however, the freedom to replace the systems F_{p_1} and F_{p_2} at the ends of the homotopy with their scalar multiples as in Remark 4.2.3 is lost. △

4.2.3 Graph of homotopies: main ideas

Some readers may find it helpful to use the examples of Section 4.2.4 for graphical intuition as we introduce notation and definitions below.

To organize the discovery of new solutions, we represent the set of homotopies by a finite undirected graph G. Let $E(G)$ and $V(G)$ denote the edge and vertex set of G, respectively. Any vertex v in $V(G)$ is associated to a point F_p in the base space. An edge e in $E(G)$, connecting v_1 and v_2 in $V(G)$, is decorated with two complex numbers, γ_1 and γ_2, and represents the linear homotopy connecting $\gamma_1 F_{p_1}$ and $\gamma_2 F_{p_2}$ along a line segment; see Remark 4.2.3. We assume that both p_i and γ_i are chosen so that the segments do not intersect the branch locus D. Choosing these at random (See Section 4.4.1 for a possible choice of distribution.) satisfies the assumption, since the exceptional set of choices where such intersections happen is contained in a real Zariski closed set; see [76, Lemma 7.1.3].

We allow multiple edges between two distinct vertices but no loops, since the latter induce trivial homotopies. For a graph G to be potentially useful in a monodromy computation, it must contain a cycle. Some of the general ideas behind the structure of a graph G are listed below.

(i) For each vertex v_i, we maintain a subset of *known* points $Q_i \subset \phi^{-1}(F_{p_i})$.

(ii) For each edge e between v_i and v_j, we record the two complex numbers γ_1 and γ_2 and store the known partial correspondences $C_e \subset \phi^{-1}(F_{p_i}) \times \phi^{-1}(F_{p_j})$ between known points Q_i and Q_j.

(iii) At each iteration, we choose an edge and a direction, track the corresponding homotopy starting with yet unmatched points, and update known points and correspondences between them.

(iv) We may obtain the initial "knowledge" as a *seed pair* (p_0, x_0) by picking $x_0 \in \mathbb{C}^n$ at random and choosing p_0 to be a generic solution of the linear system $F_p(x_0) = 0$.

We list basic operations that result in transition between one state of our algorithm, captured by G, Q_i for $v_i \in V(G)$, and C_e for $e \in E(G)$, to another.

1. For an edge $e = v_i \xleftrightarrow{(\gamma_1,\gamma_2)} v_j$, consider the homotopy

$$H^{(e)} = (1-t)\gamma_1 F_{p_i} + t\gamma_2 F_{p_j},$$

   where $(\gamma_1, \gamma_2) \in \mathbb{C}^2$ is the label of e.

   (i) Take a set of start points S_i to be a subset of the set of known points Q_i that does not have an established correspondence with points in Q_j.

   (ii) Track S_i along $H^{(e)}$ for $t \in [0,1]$ to get $S_j \subset \phi^{-1}(F_{p_j})$.

   (iii) Extend the known points for v_j. That is, let $Q_j := Q_j \cup S_j$ and record the newly established correspondences.

2. Add a new vertex corresponding to F_p for a generic $p \in B \setminus D$.

3. Add a new edge $e = v_i \xleftrightarrow{(\gamma_1,\gamma_2)} v_j$ between two existing vertices decorated with generic $\gamma_1, \gamma_2 \in \mathbb{C}$.

At this point a reader who is ready to see a more formal algorithm based on these ideas may skip to Algorithm 1.

4.2.4 Graph of homotopies: examples

We demonstrate the idea of graphs of homotopies, the core idea of the MS framework, by giving two examples.

Example 4.2.5. Figure 4.1 shows a graph G with two vertices and three edges. G is embedded in the base space B with paths partially lifted to the solution variety, which is a covering space with 3 sheets. The two fibers $\{x_1, x_2, x_3\}$ and $\{y_1, y_2, y_3\}$ are connected by three partial correspondences induced by the liftings of three egde-paths.

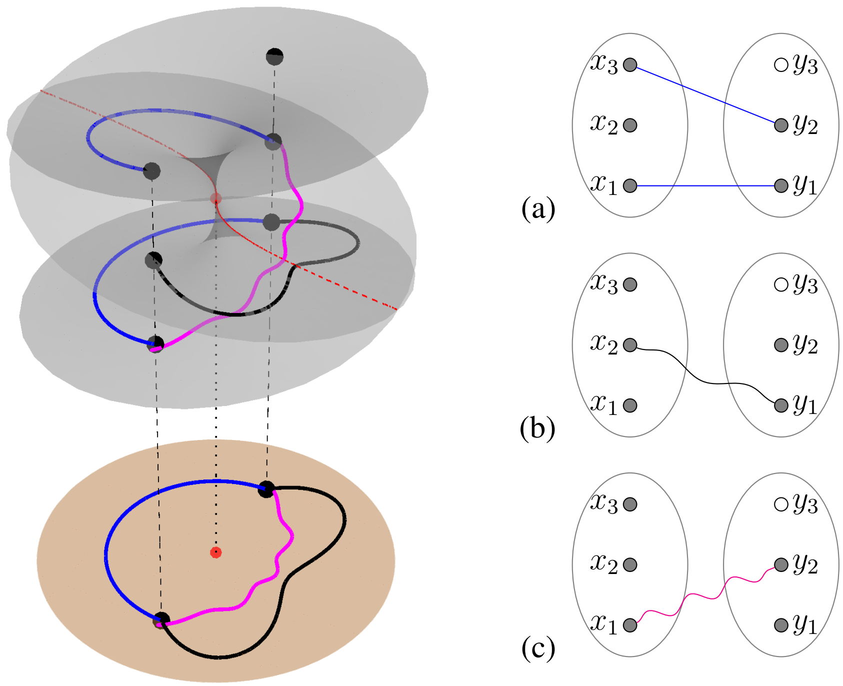

Figure 4.1: Selected liftings of three edges connecting the fibers of two vertices and induced correspondences.

Note that several aspects in this illustration are fictional. There is only one branch point in the actual complex base space B that we would like the reader to imagine. The visible self-intersections of the solution variety V are an artifact of drawing the picture in the real space. Also, in practice we use homotopy paths that are as simple as possible; however, here the paths are more involved for the purpose of distinguishing them in print.

An algorithm that we envision may hypothetically take the following steps:

(1) *Seed* the first fiber with x_1.

(2) Use a lifting of edge e_a to get y_1 from x_1.

(3) Use a lifting of edge e_b to get x_2 from y_1.

(4) Use a lifting of edge e_c to get y_2 from x_1.

(5) Use a lifting of edge e_a to get x_3 from y_2.

Note that it is *not* necessary to complete the correspondences (a), (b), and (c) in Figure 4.1. Doing so would require tracking nine continuation paths, while the hypothetical run above uses only four paths to find a fiber. $\triangle$

Example 4.2.6. Figure 4.2 illustrates two partial correspondences associated to two edges e_a and e_b, both connecting two vertices v_1 and v_2 in $V(G)$. Each vertex v_i stores the array of known points Q_i, which are depicted in solid. Both correspondences in the picture are subsets of a perfect matching, a one-to-one correspondence established by a homotopy associated to the edge.

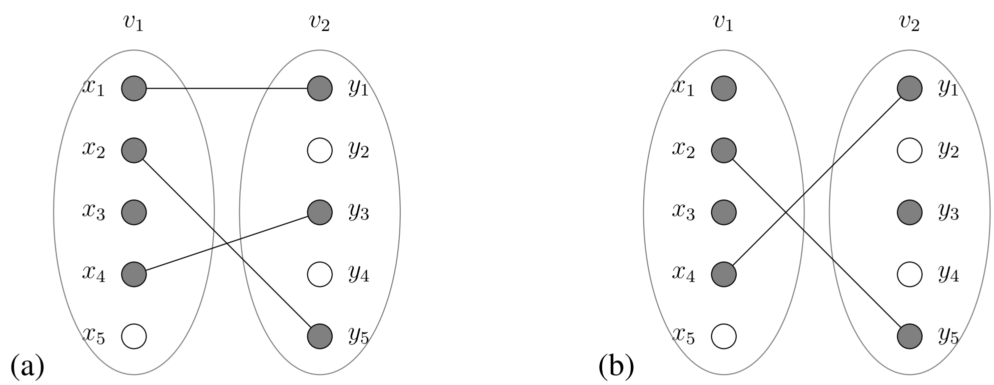

Figure 4.2: Two partial correspondences induced by edges e_a and e_b for the fibers of the covering map of degree $d = 5$ in Example 4.2.6.

Note that taking the set of start points $S_1 = \{x_3\}$ and following the homotopy $H^{(e_a)}$ from left to right is *guaranteed* to discover a new point in the second fiber. On the other hand, it is impossible to obtain new knowledge by tracking $H^{(e_a)}$ from right to left. Homotopy $H^{(e_b)}$ has a *potential* to discover new points if tracked in either direction. We can choose $S_1 = \{x_1, x_3\}$ as the start points for one direction and $S_2 = \{y_3\}$ for the other. In this scenario, following the homotopy from left to right is guaranteed to produce at least one new point, while going the other way may either deliver a new point or just augment the correspondences between the already known points. If the correspondences in (a) and (b) are completed to one-to-one correspondences of the fibers, taking the homotopy induced by the edge e_a from left to right followed by the homotopy induced by edge e_b from right to left would produce a permutation. However, the group generated by this permutation has to stabilize $\{x_2\}$, therefore, it would not act transitively on the fiber of v_1. One could also imagine a completion such that the given edges would not be sufficient to discover x_5 and y_4. $\triangle$

In our algorithm, we record and use correspondences; however, they are viewed as a secondary kind of knowledge. In particular, in Section 4.3.2.4 we develop heuristics driven by edge potential functions. These look to maximize the number of newly discovered solutions, or to extend the primary knowledge in some greedy way.

4.3 Algorithms and strategies

The operations listed in Section 4.2.3 give a great deal of freedom in the discovery of solutions. However, not all strategies for applying these operations are equally efficient. We distinguish between *static* strategies, where the graph is fixed throughout the discovery process, and *dynamic* strategies, where vertices and edges may be added. The former uses only the basic operation 1 of Section 4.2.3, while the latter uses basic operations 2 and 3.

4.3.1 A naive dynamic strategy

To visualize this strategy in our framework jump ahead and to the `flower` graph in Figure 4.3. Start with the seed solution at the vertex v_0 and proceed creating loops as petals in this graph. For example, use basic operations 2 and 3 to create v_1 and two edges between v_0 and v_1, track the known solutions at v_0 along the new petal to potentially find new solutions at v_0, then "forget" the petal and create an entirely new one in the next iteration.

This strategy populates the fiber $\phi^{-1}(F_{p_0})$, but how fast? Assume the permutation induced by a petal permutation on $\phi^{-1}(F_{p_1})$ is uniformly distributed. Then for the first petal the probability of finding a new solution is $(d-1)/d$ where d is the cardinality of the fiber $\phi^{-1}(F_{p_1})$, i.e., $d = |\phi^{-1}(F_{p_1})|$. This probability is close to one when d is large. However, for the other petals the probability of arriving at anything new at the end of one tracked path decreases as the known solution set grows.

Finding the expected number of iterations (petals) to discover the entire fiber is equivalent to solving the *coupon collector's problem.* The number of iterations is $d\,\ell(d)$ where $\ell(d) := \frac{1}{1} + \frac{1}{2} + \cdots + \frac{1}{d}$. The values of $\ell(d)$ can be regarded as lower and upper sums for two integrals of the function $x \mapsto x^{-1}$, leading to the bounds $\ln(d+1) \leq \ell(d) \leq \ln(d)+1$. Simultaneously tracking all known points along a petal gives a better complexity, since different paths cannot lead to the same solution.

We remark that the existing implementations of numerical irreducible decomposition in Bertini [4], PHCpack [80], and `NumericalAlgebraicGeometry` for Macaulay2 [60] that use monodromy are driven by a version of the naive dynamic strategy.

4.3.2 Static graph strategies

Reusing edges of the graph is an advantage. In a static strategy the graph is fixed and we discover solutions according to Algorithm 1.

The algorithm can be specialized in several ways. We may:

- Choose the graph G.
- Specify a stopping criterion `stop`.
- Choose a strategy for picking the edge $e = (j, k)$.

We address the first choice in Section 4.3.2.1 by listing several graph layouts that can be used. Stopping criteria are discussed in Section 4.3.2.2 and Section 4.3.2.3, while strategies for selecting an edge are discussed in Section 4.3.2.4.

Remark 4.3.1. We notice that if the stopping criterion is never satisfied, the number of paths being tracked by Algorithm 1 is at most $d|E(G)|$, where d is the number of solutions of a generic system. $\triangle$

Algorithm 1: Static graph strategy

Let the base space be given by a map $\psi : p \mapsto F_p$.
$(j, Q_j) = \texttt{monodromySolve}(G, Q', \texttt{stop})$
Input:

- A graph G with vertices decorated with p_i's and edges decorated with pairs $(\gamma_1, \gamma_2) \in \mathbb{C}^2$.
- Subsets $Q'_i \subset \phi^{-1}(\psi(p_i))$ for $i \in 1, \ldots, |V(G)|$, not all empty.
- A stopping criterion `stop`.

Output: A vertex j in G and a subset Q_j of the fiber $\phi^{-1}(F_{p_j})$ with the property that Q_j cannot be extended by tracking homotopy paths represented by G.

$Q_i := Q'_i$ for $i \in 1, \ldots, |V(G)|$.
while there exists an edge $e = (j, k)$ in G such that Q_j has points not yet tracked with $H^{(e)}$ **do**
  Choose such an edge $e = (j, k)$.
  Let $S \subset Q_j$ be a nonempty subset of the set of points not yet tracked with $H^{(e)}$.
  Track the points S with $H^{(e)}$ to obtain elements $T \subset \phi^{-1}(\varphi(p_k)) \setminus Q_k$.
  Let $Q_k := Q_k \cup T$.
  if the criterion `stop` is satisfied (e.g., $|Q_k|$ equals a known solution count) **then**
    return (k, Q_k)
  end if
end while
Choose some vertex j and return (j, Q_j).

4.3.2.1 Two static graph layouts

We present two graph layouts to be used for the static strategy in Figure 4.3.

`flower(s,t)`: The graph consists of a *central node* v_0 and s additional vertices (number of petals), each connected to v_0 by t edges.

`completeGraph(s,t)`: The graph has s vertices. Every pair of vertices is connected by t edges.

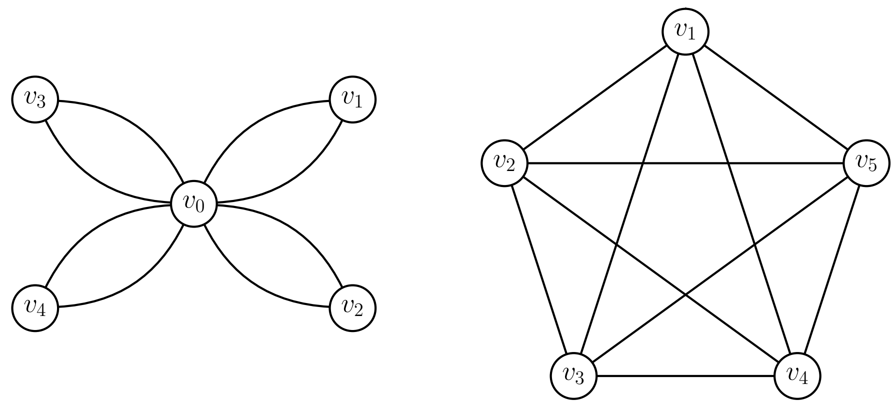

Figure 4.3: Graphs for the `flower(4,2)` strategy and `completeGraph(5,1)`.

4.3.2.2 *Stopping criterion if a solution count is known*

Suppose the cardinality of the fiber $\phi^{-1}(F_p)$, for a generic value of p, is known. Then, a natural stopping criterion for our algorithm is to terminate when the set of known solutions Q_i at any node i reaches that cardinality. In particular, for a generic sparse system with fixed monomial support we can rely on this stopping criterion due to the BKK bound [5], which can be obtained by a *mixed volume* computation.

4.3.2.3 *Stopping criterion if no solution count is known*

For a static strategy one natural stopping criterion is *saturation* of the known solution correspondences along all edges. In this case, the algorithm simply cannot derive any additional information. It also makes sense to consider a heuristic stopping criterion based on *stabilization*. The algorithm terminates when no new points are discovered in a fixed number of iterations. This avoids saturating correspondences unnecessarily. In particular, this could be useful if a static strategy algorithm is a part of the dynamic strategy of Section 4.3.3.

Remark 4.3.2. In certain cases it is possible to provide a stopping criterion using the *trace test* [74, 61]. This is particularly useful when there is an equation in the family $F_p(x) = 0$ that describes a generic hypersurface in the parameter space, e.g., an affine linear equation with indeterminate coefficients. In full generality, one could restrict the parameter space to a generic line and, hence, restrict the solution variety to a curve. Now, thinking of $F_p(x) = 0$ as a system of bihomogeneous equations in p and x, one can use the multihomogeneous trace test [61, 50].

We note that the multihomogeneous trace test complexity depends on the degree of the solution variety, which may be significantly higher than the degree d of the covering map, where the latter is the measure of complexity for the main problem here. For instance, the system (4.5) corresponding to the reaction network in Figure 4.4 has four solutions, but an additional set of eleven points is necessary to execute the trace test. See `example-traceCRN.m2` at [25]. $\triangle$

4.3.2.4 Edge-selection strategy

We propose two methods for selecting the edge e in Algorithm 1. The default is to select an edge and a direction at random. A more sophisticated method is to select an edge and a direction based on the potential of that selection to deliver new information; see the discussion in Example 4.2.6. Let $e = v_i \xleftrightarrow{(\gamma_1,\gamma_2)} v_j$ be an edge in the direction from v_i to v_j.

`potentialLowerBound`: This equals the minimal number of new points guaranteed to be discovered by following a chosen homotopy using the maximal batch of starting points S_i. That is, it equals the difference between the numbers of known unmatched points $(|Q_i| - |C_e|) - (|Q_j| - |C_e|) = |Q_i| - |Q_j|$ if this difference is positive, and zero otherwise.

`potentialE`: This equals the expected number of new points obtained by tracking one unmatched point along e. This is the ratio $\frac{d-|Q_j|}{d-|C_e|}$ of undiscovered points among all unmatched points if $|Q_i| - |C_e| > 0$ and zero otherwise.

Note that `potentialE` assumes we know the cardinality of the fiber, while the edge-selection strategy `potentialLowerBound` does not depend on that piece of information.

There is a lot of freedom in choosing potentials in our algorithmic framework. The two above potentials are natural "greedy" choices that are easy to describe and implement. It is evident from our experiments summarized in Tables 4.1 and 4.2 that they may order edges differently resulting in varying performance.

4.3.3 An incremental dynamic graph strategy

Consider a dynamic strategy that augments the graph when one of the above "static" criteria terminates Algorithm 1 for the current graph. One simple way to design a dynamic stopping criterion, we call it *dynamic stabilization*, is to decide how augmentation is done and fix the number of augmentation steps the algorithm is allowed to make without increasing the solution count. A dynamic strategy, which is simple to implement, is one that starts with a small graph G and augments it if necessary.

Algorithm 2: Dynamic graph strategy

Let us make the same assumptions as in Algorithm 1.
$(j, Q_j) = \texttt{dynamicMonodromySolve}(G, x_1, \texttt{stop}, \texttt{augment})$

Input:

- A graph G as in Algorithm 1.
- One seed solution $x_1 \in \phi^{-1}(\psi(p_1))$.
- A stopping criterion `stop`.
- An augmenting procedure `augment`.

Output: A vertex j in G and a subset Q_j of the fiber $\phi^{-1}(F_{p_j})$.

```
Q_1 := {x_1} and Q_i = ∅ for i ∈ 2, ..., |V(G)|.
loop
  (j, Q_j) = monodromySolve(G, Q, stop) {here Q_i are modified in-place and
  passed to the next iteration}
  if stop| (i.e., stopping criterion is satisfied) then
    return (j, Q_j)
  end if
  G := augment(G)
end loop
```

We emphasize that the criteria described in this subsection and parts of Section 4.3.2.3

are *heuristic* and there is a lot of freedom in designing such. In Section 4.5.2 we successfully experiment using a static stabilization criterion with some examples, for which the solution count is generally not known.

4.4 Implementation

We implement the package `MonodromySolver` in Macaulay2 [43] using the functionality of the package `NumericalAlgebraicGeometry` [60]. The source code and examples used in the experiments in the next section are available at [25].

The main function `monodromySolve` realizes Algorithms 1 and 2; see the documentation for details and many options. The tracking of homotopy paths in our experiments is performed with the native routines implemented in the kernel of Macaulay2, however, `NumericalAlgebraicGeometry` provides an ability to outsource this core task to an alternative tracker (PHCpack or Bertini). Main auxiliary functions—`createSeedPair`, `sparseSystemFamily`, `sparseMonodromySolve`, and `solveSystemFamily`—are there to streamline the user's experience. The last two are blackbox routines that don't assume any knowledge of the framework described in this paper.

The overhead of managing the data structures is supposed to be negligible compared to the cost of tracking paths. However, since our implementation uses the interpreted language of Macaulay2 for other tasks, this overhead could be sizable (up to 10% for large examples in Section 4.5). Nevertheless, most of our experiments are focused on measuring the *number of tracked paths* as a proxy for computational complexity.

Remark 4.4.1. This chapter's discussion focuses on linear parametric systems with a nonempty dominant component. However, the implementation works for other cases where our framework can be applied.

For instance, if the system is linear in parameters but has no dominant component, there may still be a unique "component of interest" with a straightforward way to produce a seed pair. This is so, for instance, in the problem of finding the degree of the variety $SO(n)$, which we use in Table 4.3. The point x is restricted to $SO(n)$, the special orthogonal group, which is irreducible as a variety. This results in a unique "component of interest" in the solution variety, the one that projects onto $SO(n)$; see [8] for details. △

4.4.1 Randomization

Throughout the paper we refer to *random* choices we make, that, we assume, avoid various nongeneric loci. For implementation purposes, we make simple choices. For instance, the vertices of the graph get distributed uniformly in a cube in the base space, with the exception of the seeded vertex `createSeedPair`, which picks $(p_0, x_0) \in B \times \mathbb{C}^n$ by choosing x uniformly in a cube, then choosing p_0 uniformly in a box in the subspace $\{p \mid F_p(x) = 0\}$.

A choice of probability distribution on B translates to some (discrete) distribution on the symmetric group S_d. However, it is simply too hard to analyze – there are virtually no studies in this direction. We make the simplest possible assumption of uniform distribution on S_d. There is an interesting, more involved, alternative to this assumption in [36, 35], which relies on the intuition in the case $n = 1$.

4.4.2 Solution count

The BKK bound, computed via mixed volume, is used as a solution count in the examples of sparse systems in Section 4.5.1.1 and Section 4.5.1.2. In the latter we compute mixed volume via a closed formula that involves permanents, while the former relies on general algorithms implemented in several software packages. Our current implementation uses PHCpack [80], which incorporates the routines of MixedVol further developed in Hom4PS-2 [59]. The computation of the mixed volume is not a bottleneck in our algorithm. The time spent in that preprocessing stage is negligible compared to the rest of the computation.

4.5 Experiments

In this section we report on experiments with our implementation and various examples in Section 4.5.1 and Section 4.5.2. We compare our results against other software in Section 4.5.3.

4.5.1 Sparse polynomial systems

The example families in this subsection have the property that the support of the equations is fixed, while the coefficients can vary freely, as long as they are generic. We run the static graph strategy Algorithm 1 on these examples.

4.5.1.1 Cyclic roots

The cyclic n-roots polynomial system is

$$\begin{cases} i = 1, 2, 3, 4, \ldots, n-1 : \displaystyle\sum_{j=0}^{n-1} \prod_{k=j}^{j+i-1} x_{k \bmod n} = 0 \\ x_0 x_1 x_2 \cdots x_{n-1} - 1 = 0. \end{cases} \tag{4.1}$$

This system is commonly used to benchmark polynomial system solvers. We will study the modified system with randomized coefficients and seek solutions in $(\mathbb{C} \setminus \{0\})^n$. Therefore, the solution count can be computed as the mixed volume of the Newton polytopes of the the polynomials in the left-hand side, providing a natural stopping criterion discussed in Section 4.3.2.2. This bound is 924 for cyclic-7.

Tables 4.1 and 4.2 contain averages of experimental data from running twenty trials of Algorithm 1 on cyclic-7. The main measurement reported is the average number of paths tracked, as the unit of work for our algorithm is tracking a single homotopy path. The experiments were performed with ten different graph layouts and three edge-selection strategies.

Table 4.1: Cyclic-7 experimental results for the `flower` strategy.

(#vertices-1, edge multiplicity)	(3,2)	(4,2)	(5,2)	(3,3)	(4,3)
$\|E(G)\|$	6	8	10	9	12
$\|E(G)\| \cdot 924$	5544	7392	9240	8316	11088
completion rate	100%	100%	100%	100%	100%
Random Edge	5119	6341	7544	6100	7067
`potentialLowerBound`	5252	6738	8086	6242	7886
`potentialE`	4551	5626	6355	4698	5674

Table 4.2: Cyclic-7 experimental results for the `completeGraph` strategy.

(#vertices, edge multiplicity)	(2,3)	(2,4)	(2,5)	(3,2)	(4,1)
$\|E(G)\|$	3	4	5	6	6
$\|E(G)\| \cdot 924$	2772	3698	4620	5544	5544
completion rate	65%	80%	90%	100%	100%
Random Edge	2728	3296	3947	4805	5165
`potentialLowerBound`	2727	3394	3821	4688	5140
`potentialE`	2692	2964	2957	3886	4380

4.5.1.2 Nash equilibria

Semi-mixed multihomogeneous systems arise when one is looking for all totally mixed Nash equilibria (TMNE) in game theory. A specialization of mixed volume using matrix permanents gives a concise formula for a root count for systems arising from TMNE problems [29]. We provide an overview of how such systems are constructed based on [29]. Suppose there are N players with m options each. For player $i \in \{1, \ldots, N\}$ using option $j \in \{1, \ldots, m\}$ we have the equation $P_j^{(i)} = 0$, where

$$P_j^{(i)} = \sum_{\substack{k_1,\ldots,k_{i-1},\\ k_{i+1},\ldots,k_N}} a^{(i)}_{k_1,\ldots,k_{i-1},j,k_{i+1},\ldots,k_N} p^{(1)}_{k_1} p^{(2)}_{k_2} \cdots p^{(i-1)}_{k_{i-1}} p^{(i+1)}_{k_{i+1}} \cdots p^{(N)}_{k_N}. \tag{4.2}$$

The parameters $a^{(i)}_{k_1,k_2,\ldots,k_N}$ are the payoff rates for player i when players $1, \ldots, i-1, i+1, \ldots, N$ are using options $k_1, \ldots, k_{i-1}, k_{i+1}, \ldots, k_N$, respectively. Here, the unknowns are $p^{(i)}_{k_j}$, representing the probability that player i will use option $k_j \in \{1, \ldots, m\}$. There is one constraint on the probabilities for each player $i \in \{1, \ldots, N\}$; namely, the condition that

$$p_1^{(i)} + p_2^{(i)} + \cdots + p_m^{(i)} = 1. \tag{4.3}$$

The system (4.2) consists of $N \cdot m$ equations in $N \cdot m$ unknowns. Using condition (4.3) reduces the number of unknowns to $N(m-1)$. Lastly, we eliminate the $P_j^{(i)}$ by constructing

$$P_1^{(i)} = P_2^{(i)},\ P_1^{(i)} = P_3^{(i)},\ \ldots\ , P_1^{(i)} = P_m^{(i)}, \qquad \text{for each } i \in \{1, \ldots, N\}. \tag{4.4}$$

The final system is a square system of $N(m-1)$ equations in $N(m-1)$ unknowns.

For one of our examples (`paper-examples/example-Nash.m2` at [25]), we choose the generic system of this form for $N = 3$ players with $m = 3$ options for each. The result is a system of six equations in six unknowns and 81 parameters with ten solutions.

Remark 4.5.1. It can be *certified* numerically that these solutions are correct; see [26, Section 5.3] for more details. $\triangle$

4.5.2 Chemical reaction networks

A family of interesting examples arises from chemical reaction network theory. A chemical reaction network gives rise to a system of polynomial ordinary differential equations describing the network dynamics under the assumption of mass-action kinetics; see Chapter 3 for more extensive details. The solutions of the polynomial system represent the equilibria for the given reaction network [44, 65]. These polynomial systems are not generically sparse and we cannot easily compute their root count. In our experiments, we used the stabilization stopping criterion, terminating the algorithm after a fixed number of iterations that do not deliver new points; the default is ten fruitless iterations.

Figure 4.4 gives an example of a small chemical reaction network. Applying the laws of mass-action kinetics to the reaction network in Figure 4.4, we obtain the polynomial system (4.5) consisting of the corresponding steady-state and conservation equations. Here, the k_is

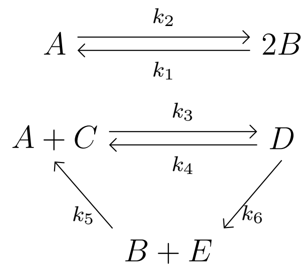

Figure 4.4: Chemical reaction network example.

represent the reaction rates, the x_is represent species' concentrations with respect to time, and the c_is are initial concentrations of each species. The reader may wish to view Chapter Section 3.2 of Chapter 3 for further details on chemical reaction networks.

$$\begin{aligned}
\dot{x_A} &= k_1 x_B^2 - k_2 x_A - k_3 x_A x_C + k_4 x_D + k_5 x_B x_E \\
\dot{x_B} &= 2k_1 x_A - 2k_2 x_B^2 + k_4 x_D - k_5 x_B x_E \\
\dot{x_C} &= -k_3 x_A x_C + k_4 x_D + k_5 x_B x_E \\
\dot{x_D} &= k_3 x_A x_C - (k_4 + k_6) x_D \\
\dot{x_E} &= -k_5 x_B x_E + k_6 x_D \\
0 &= 2x_A + x_B - x_C + x_D - c_1 \\
0 &= -2x_A - x_B + 2x_C + x_E - c_2
\end{aligned} \tag{4.5}$$

Typically, systems resulting from chemical reaction networks are overdetermined. With the current implementation one needs to either square the system, or use a homotopy tracker that supports following a homotopy in a space of overdetermined systems.

Although we may obtain large systems, they typically have very low root counts compared to the sparse case. For example, the polynomial system (4.5) has four solutions. A larger example is the *WNT signaling pathway* from systems biology [44] consisting of 19 polynomial equations with nine solutions. All nine solutions are obtained in less than a second with Algorithm 1.

4.5.3 Timings and comparison with other solvers

All timings appearing in this section are done on one thread and on the same machine. Remark 4.3.1 shows that we should expect the number of tracked paths in Algorithms 1 and 2 to be linear (with a small constant!) in the number of solutions of the system. In this section we highlight one aspect of the practicality of our approach.

Notably, the monodromy method dramatically extends our computational ability for systems where the solution count is significantly smaller than the count corresponding to a more general family, for example, the BKK count for sparse systems. This means that the existing blackbox methods, whose complexity relies on a larger count, are likely to spend significantly more time in computation compared to our approach. In Table 4.3, we collect timings on several challenging examples mentioned in recent literature where smaller solution counts are known, thus providing us with rigorous test cases for our heuristic stopping criterion. The first system in the table is that of the WNT signaling pathway reaction network mentioned in Section 4.5.2. The others come from the problem of computing the degree of $SO(n)$, the special orthogonal group, as a variety [8].

Table 4.3: Examples with solution count smaller than BKK bound (timings in seconds).

problem	WNT	$SO(4)$	$SO(5)$	$SO(6)$	$SO(7)$
count	9	40	384	4768	111616
MonodromySolver	0.52	4	23	528	42791
Bertini	42	81	10605	out of memory	
PHCpack	862	103	$>$ one day		

Remark 4.5.2. In comparison with the naive dynamic strategy discussed in Section 4.3.1, our framework loses slightly only in one aspect: memory consumption. For a problem with d solutions the naive approach stores up to (and typically close to) $2d$ points. The number of points our approach stores is up to (and typically considerably fewer than) d times the number of vertices.

The number of tracked paths is significantly lower in our framework: for example, the naive strategy tracks about 7500 paths on average for cyclic-7. Even before looking at

Table 4.1 it is clear that running the `flower` strategy in combination with the incremental dynamic strategy of Section 4.3.3 guarantees to dominate the naive strategy. $\triangle$

REFERENCES

[1] M. Akian, S. Gaubert, and A. Guterman, "Tropical polyhedra are equivalent to mean payoff games", *International Journal of Algebra and Computation*, vol. 22, no. 01, p. 1 250 001, 2012.

[2] X. Allamigeon, S. Gaubert, and E. Goubault, "The tropical double description method", *arXiv preprint arXiv:1001.4119*, 2010.

[3] F. Baccelli, G. Cohen, G. J. Olsder, and J.-P. Quadrat, "Synchronization and linearity: An algebra for discrete event systems", 1992.

[4] D. J. Bates, J. D. Hauenstein, A. J. Sommese, and C. W. Wampler, *Numerically solving polynomial systems with Bertini*. SIAM, 2013, vol. 25.

[5] D. N. Bernstein, "The number of roots of a system of equations", *Funkcional. Anal. i Priložen*, vol. 9, no. 3, pp. 1–4, 1975, ISSN: 0374-1990.

[6] F. Bihan, A. Dickenstein, and M. Giaroli, "Lower bounds for positive roots and regions of multistationarity in chemical reaction networks", *arXiv preprint arXiv:1807.05157*, 2018.

[7] A. L. Birkmeyer, A. Gathmann, and K. Schmitz, "The realizability of curves in a tropical plane", *Discrete & Computational Geometry*, vol. 57, no. 1, pp. 12–55, 2017.

[8] M. Brandt, J. Bruce, T. Brysiewicz, R. Krone, and E. Robeva, "The degree of SO$(n,\mathbb{C})$", in *Combinatorial Algebraic Geometry*, G. Smith and B. Sturmfels, Eds., ser. Fields Institute Communications, vol. 80, Stockholm: Springer, 2017, pp. 229–246.

[9] A. M. del Campo and J. I. Rodriguez, "Critical points via monodromy and local methods", *Journal of Symbolic Computation*, vol. 79, pp. 559–574, 2017, ISSN: 0747-7171.

[10] F. Catanese, S. Hoşten, A. Khetan, and B. Sturmfels, "The maximum likelihood degree", *American Journal of Mathematics*, vol. 128, no. 3, pp. 671–697, 2006.

[11] J. Chen and J. Kileel, "Numerical Implicitization for Macaulay2", *arXiv preprint arXiv:1610.03034*, 2016.

[12] T. Chen, "Unmixing the mixed volume computation", *Discrete Comput. Geom.*, vol. 62, no. 1, pp. 55–86, 2019, ISSN: 0179-5376. DOI: 10.1007/s00454-019-00078-x. [Online]. Available: https://doi.org/10.1007/s00454-019-00078-x.

[13] G. Cohen, S. Gaubert, and J.-P. Quadrat, “Duality and separation theorems in idempotent semimodules”, *Linear Algebra and its Applications*, vol. 379, pp. 395–422, 2004.

[14] G. Cohen, S. Gaubert, J.-P. Quadrat, and I. Singer, “Max-plus convex sets and functions”, *Contemporary Mathematics*, vol. 377, pp. 105–130, 2005.

[15] C. Conradi, E. Feliu, M. Mincheva, and C. Wiuf, “Identifying parameter regions for multistationarity”, *PLoS computational biology*, vol. 13, no. 10, e1005751, 2017.

[16] C. Conradi, A. Iosif, and T. Kahle, “Multistationarity in the space of total concentrations for systems that admit a monomial parametrization”, *arXiv preprint arXiv:1810.08152*, 2018.

[17] R. A. Crowell and N. M. Tran, “Tropical geometry and mechanism design”, *arXiv preprint arXiv:1606.04880*, 2016.

[18] J. A. De Loera, *Triangulations structures for algorithms and applications*, eng, ser. Algorithms and computation in mathematics ; v. 25. Heidelberg ; New York: Springer-Verlag, 2010, ISBN: 9783642129711.

[19] M. Develin, “Tropical secant varieties of linear spaces”, *Discrete & Computational Geometry*, vol. 35, no. 1, pp. 117–129, 2006.

[20] M. Develin, F. Santos, and B. Sturmfels, “On the rank of a tropical matrix”, in *Combinatorial and computational geometry*, ser. Math. Sci. Res. Inst. Publ. Vol. 52, Cambridge Univ. Press, Cambridge, 2005, pp. 213–242.

[21] M. Develin and B. Sturmfels, “Tropical convexity”, *Doc. Math*, vol. 9, no. 1-27, pp. 7–8, 2004.

[22] M. Develin and J. Yu, “Tropical polytopes and cellular resolutions”, *Experimental Mathematics*, vol. 16, no. 3, pp. 277–291, 2007.

[23] A. Dickenstein, “Biochemical reaction networks: An invitation for algebraic geometers”, in *Mathematical Congress of the Americas*, American Mathematical Soc., vol. 656, 2016, pp. 65–83.

[24] J. Draisma, E. Horobeţ, G. Ottaviani, B. Sturmfels, and R. R. Thomas, “The euclidean distance degree of an algebraic variety”, *Foundations of computational mathematics*, vol. 16, no. 1, pp. 99–149, 2016.

[25] T. Duff, C. Hill, A. Jensen, K. Lee, A. Leykin, and J. Sommars, *MonodromySolver: a Macaulay2 package for solving polynomial systems via homotopy continuation and monodromy*, Available at http://people.math.gatech.edu/∼aleykin3/MonodromySolver.

[26] T. Duff, C. Hill, A. Jensen, K. Lee, A. Leykin, and J. Sommars, "Solving polynomial systems via homotopy continuation and monodromy", *IMA Journal of Numerical Analysis*, vol. 39, no. 3, pp. 1421–1446, 2018.

[27] B. B. Edelstein, "Biochemical model with multiple steady states and hysteresis", *Journal of Theoretical Biology*, vol. 29, no. 1, pp. 57–62, 1970, ISSN: 0022-5193. DOI: http://dx.doi.org/10.1016/0022-5193(70)90118-9. [Online]. Available: http://www.sciencedirect.com/science/article/pii/0022519370901189.

[28] D. Eisenbud and J. Harris, "On varieties of minimal degree", in *Proc. Sympos. Pure Math*, vol. 46, 1987, pp. 3–13.

[29] I. Z. Emiris and R. Vidunas, "Root counts of semi-mixed systems, and an application to counting nash equilibria", in *Proceedings of the 39th International Symposium on Symbolic and Algebraic Computation*, ser. ISSAC '14, Kobe, Japan: ACM, 2014, pp. 154–161, ISBN: 978-1-4503-2501-1. DOI: 10.1145/2608628.2608679. [Online]. Available: http://doi.acm.org/10.1145/2608628.2608679.

[30] E. Feliu and C. Wiuf, "Enzyme sharing as a cause of multistationarity in signaling systems", *Journal of the Royal Society, Interface*, vol. 9, no. 71, pp. 1224–1232, Jun. 2012. DOI: 10.1098/rsif.2011.0664.

[31] E. Feliu and M. Helmer, "Multistationarity and bistability for Fewnomial chemical reaction networks", *Bull. Math. Biol.*, vol. 81, no. 4, pp. 1089–1121, 2019, ISSN: 0092-8240. DOI: 10.1007/s11538-018-00555-z. [Online]. Available: https://doi.org/10.1007/s11538-018-00555-z.

[32] S. Felsner and K. Knauer, "Distributive lattices, polyhedra, and generalized flows", *European J. Combin.*, vol. 32, no. 1, pp. 45–59, 2011, ISSN: 0195-6698. DOI: 10.1016/j.ejc.2010.07.011. [Online]. Available: https://doi-org.proxy.ub.uni-frankfurt.de/10.1016/j.ejc.2010.07.011.

[33] A. Fink and F. Rincón, "Stiefel tropical linear spaces", *J. Combin. Theory Ser. A*, vol. 135, pp. 291–331, 2015, ISSN: 0097-3165. DOI: 10.1016/j.jcta.2015.06.001. [Online]. Available: https://doi-org.proxy.ub.uni-frankfurt.de/10.1016/j.jcta.2015.06.001.

[34] D. Flockerzi, K. Holstein, and C. Conradi, "N-site phosphorylation systems with 2n-1 steady states", *Bulletin of mathematical biology*, vol. 76, no. 8, pp. 1892–1916, 2014.

[35] A. Galligo and L. Miclo, "On the cut-off phenomenon for the transitivity of randomly generated subgroups", *Random Structures & Algorithms*, vol. 40, no. 2, pp. 182–219, 2012.

[36] A. Galligo and A. Poteaux, “Computing monodromy via continuation methods on random Riemann surfaces”, *Theoretical Computer Science*, vol. 412, no. 16, pp. 1492–1507, 2011.

[37] S. Gaubert and R. D. Katz, “Minimal half-spaces and external representation of tropical polyhedra”, *Journal of Algebraic Combinatorics*, vol. 33, no. 3, pp. 325–348, 2011.

[38] S. Gaubert and F. Meunier, “Carathéodory, helly and the others in the max-plus world”, *Discrete & Computational Geometry*, vol. 43, no. 3, pp. 648–662, 2010.

[39] M. Giaroli, R. Rischter, M. Millán, and A. Dickenstein, “Parameter regions that give rise to 2 [n/2]+ 1 positive steady states in the n-site phosphorylation system.”, *Mathematical biosciences and engineering: MBE*, vol. 16, no. 6, p. 7589, 2019.

[40] M. Giaroli, F. Bihan, and A. Dickenstein, “Regions of multistationarity in cascades of goldbeter–koshland loops”, *Journal of mathematical biology*, pp. 1–31, 2018.

[41] S. Gober and S. N. Sergeev, “Cyclic projections and separability theorems in idempotent semi-modules”, *Fundam. Prikl. Mat.*, vol. 13, no. 4, pp. 31–52, 2007, ISSN: 1560-5159. DOI: 10.1007/s10958-008-9243-8. [Online]. Available: https://doi.org/10.1007/s10958-008-9243-8.

[42] D. R. Grayson and M. E. Stillman, *Macaulay2, a software system for research in algebraic geometry*, 2002. [Online]. Available: http://www.math.uiuc.edu/Macaulay2/.

[43] D. R. Grayson and M. E. Stillman, *Macaulay2, a software system for research in algebraic geometry*, Available at http://www.math.uiuc.edu/Macaulay2/.

[44] E. Gross, H. A. Harrington, Z. Rosen, and B. Sturmfels, “Algebraic systems biology: A case study for the Wnt pathway”, *Bulletin of Mathematical Biology*, vol. 78, no. 1, pp. 21–51, 2016.

[45] E. Gross, H. A. Harrington, Z. Rosen, and B. Sturmfels, “Algebraic systems biology: A case study for the wnt pathway”, *Bulletin of mathematical biology*, vol. 78, no. 1, pp. 21–51, 2016.

[46] E. Gross, H. Harrington, N. Meshkat, and A. Shiu, “Joining and decomposing reaction networks”, *J. Math. Biol.*, vol. 80, no. 6, pp. 1683–1731, 2020, ISSN: 0303-6812. DOI: 10.1007/s00285-020-01477-y. [Online]. Available: https://doi.org/10.1007/s00285-020-01477-y.

[47] E. Gross and C. Hill, *The steady-state degree and mixed volume of a chemical reaction network*, 2020. arXiv: 1909.06652 `[math.CO]`.

[48] C. Haase, G. Musiker, and J. Yu, "Linear systems on tropical curves", *Mathematische Zeitschrift*, vol. 270, no. 3-4, pp. 1111–1140, 2012.

[49] S. Hampe, "Tropical linear spaces and tropical convexity", *Electron. J. Combin.*, vol. 22, no. 4, Paper 4.43, 20, 2015.

[50] J. D. Hauenstein and J. I. Rodriguez, "Multiprojective witness sets and a trace test", *arXiv preprint arXiv:1507.07069*, 2015.

[51] C. Hill, S. Lamboglia, and F. P. Simon, *Tropical convex hulls of polyhedral sets*, 2020. arXiv: 1912.01253 [math.CO].

[52] K. L. Ho and H. A. Harrington, "Bistability in apoptosis by receptor clustering (bistability in apoptosis by receptor clustering)", eng, *PLoS Computational Biology*, vol. 6, no. 10, 2010, ISSN: 1553-734X.

[53] K. Holstein, D. Flockerzi, and C. Conradi, "Multistationarity in sequential distributed multisite phosphorylation networks", *Bulletin of mathematical biology*, vol. 75, no. 11, pp. 2028–2058, 2013.

[54] B. Huber and B. Sturmfels, "A polyhedral method for solving sparse polynomial systems", *Math. Comp.*, vol. 64, no. 212, pp. 1541–1555, 1995, ISSN: 0025-5718.

[55] B. Joshi and A. Shiu, "A survey of methods for deciding whether a reaction network is multistationary", *Mathematical Modelling of Natural Phenomena*, vol. 10, no. 5, pp. 47–67, 2015.

[56] M. Joswig, "Tropical convex hull computations", *Contemporary Mathematics*, vol. 495, p. 193, 2009.

[57] M. Joswig and K. Kulas, "Tropical and ordinary convexity combined", *Advances in geometry*, vol. 10, no. 2, pp. 333–352, 2010.

[58] M. Joswig and G. Loho, "Weighted digraphs and tropical cones", *Linear Algebra and its Applications*, vol. 501, pp. 304–343, 2016.

[59] T.-L. Lee, T.-Y. Li, and C.-H. Tsai, "HOM4PS-2.0: A software package for solving polynomial systems by the polyhedral homotopy continuation method", *Computing*, vol. 83, no. 2-3, pp. 109–133, 2008.

[60] A. Leykin, "Numerical algebraic geometry", *The Journal of Software for Algebra and Geometry*, vol. 3, pp. 5–10, 2011.

[61] A. Leykin, J. I. Rodriguez, and F. Sottile, "Trace test", *arXiv preprint arXiv:1608.00540*, 2016.

[62] A. Leykin and J. Verschelde, "Decomposing solution sets of polynomial systems: A new parallel monodromy breakup algorithm", *International Journal of Computational Science and Engineering*, vol. 4, no. 2, pp. 94–101, 2009.

[63] G. Loho and B. Smith, "Face posets of tropical polyhedra and monomial ideals", *arXiv preprint arXiv:1909.01236*, 2019.

[64] D. Maclagan and B. Sturmfels, *Introduction to tropical geometry*. American Mathematical Soc., 2015, vol. 161.

[65] A. L. MacLean, Z. Rosen, H. M. Byrne, and H. A. Harrington, "Parameter-free methods distinguish Wnt pathway models and guide design of experiment", *Proceedings of the National Academy of Science*, vol. 112, pp. 2652–2657, Mar. 2015. DOI: 10.1073/pnas.1416655112. arXiv: 1409.0269 [q-bio.QM].

[66] I. Martífffdfffdnez-Forero, A. Peláez-López, and P. Villoslada, "Steady state detection of chemical reaction networks using a simplified analytical method", *PLOS ONE*, vol. 5, no. 6, pp. 1–6, Jun. 2010. DOI: 10.1371/journal.pone.0010823. [Online]. Available: https://doi.org/10.1371/journal.pone.0010823.

[67] A. Morgan, *Solving polynomial systems using continuation for engineering and scientific problems*. Englewood Cliffs, NJ: Prentice Hall Inc., 1987, pp. xiv+546, ISBN: 0-13-822313-0.

[68] S. Müller, E. Feliu, G. Regensburger, C. Conradi, A. Shiu, and A. Dickenstein, "Sign conditions for injectivity of generalized polynomial maps with applications to chemical reaction networks and real algebraic geometry", *Foundations of Computational Mathematics*, vol. 16, no. 1, pp. 69–97, 2016.

[69] K.-M. Nam, B. M. Gyori, S. V. Amethyst, D. J. Bates, and J. Gunawardena, "Robustness and parameter geography in post-translational modification systems", *PLoS computational biology*, vol. 16, no. 5, e1007573, 2020.

[70] *Numerically solving polynomial systems with Bertini*. SIAM, 2013, vol. 25.

[71] N. Obatake, A. Shiu, X. Tang, and A. Torres, "Oscillations and bistability in a model of ERK regulation", *J. Math. Biol.*, vol. 79, no. 4, pp. 1515–1549, 2019, ISSN: 0303-6812. DOI: 10.1007/s00285-019-01402-y. [Online]. Available: https://doi.org/10.1007/s00285-019-01402-y.

[72] J. Richter-Gebert, B. Sturmfels, and T. Theobald, "First steps in tropical geometry", in *Idempotent mathematics and mathematical physics*, ser. Contemp. Math. Vol. 377, Amer. Math. Soc., Providence, RI, 2005, pp. 289–317. DOI: 10.1090/conm/377/06998. [Online]. Available: https://doi.org/10.1090/conm/377/06998.

[73] E. Robeva, B. Sturmfels, N. Tran, and C. Uhler, "Maximum likelihood estimation for totally positive log-concave densities", *arXiv preprint arXiv:1806.10120*, 2018.

[74] A. J. Sommese, J. Verschelde, and C. W. Wampler, "Symmetric functions applied to decomposing solution sets of polynomial systems", *SIAM J. Numer. Anal.*, vol. 40, no. 6, pp. 2026–2046, 2002.

[75] A. J. Sommese, J. Verschelde, and C. W. Wampler, "Introduction to numerical algebraic geometry", in *Solving Polynomial Equations: Foundations, Algorithms, and Applications*, A. Dickenstein and I. Z. Emiris, Eds., Berlin, Heidelberg: Springer Berlin Heidelberg, 2005, pp. 301–337, ISBN: 978-3-540-27357-8. DOI: 10.1007/3-540-27357-3_8. [Online]. Available: https://doi.org/10.1007/3-540-27357-3_8.

[76] A. J. Sommese and C. W. Wampler II, *The numerical solution of systems of polynomials*. World Scientific Publishing Co. Pte. Ltd., Hackensack, NJ, 2005, pp. xxii+401, ISBN: 981-256-184-6.

[77] "The minkowski theorem for max-plus convex sets", *Linear Algebra and its Applications*, vol. 421, no. 2-3, pp. 356–369, 2007.

[78] "Tropical halfspaces", *Combinatorial and computational geometry*, vol. 52, pp. 409–431, 2005.

[79] "Using monodromy to decompose solution sets of polynomial systems into irreducible components", in *Applications of Algebraic Geometry to Coding Theory, Physics and Computation*. Dordrecht: Springer Netherlands, 2001, pp. 297–315, ISBN: 978-94-010-1011-5. DOI: 10.1007/978-94-010-1011-5_16. [Online]. Available: http://dx.doi.org/10.1007/978-94-010-1011-5_16.

[80] J. Verschelde, "Algorithm 795: PHCpack: A general-purpose solver for polynomial systems by homotopy continuation", *ACM Trans. Math. Softw.*, vol. 25, no. 2, pp. 251–276, 1999.

[81] J. Verschelde, P. Verlinden, and R. Cools, "Homotopies exploiting Newton polytopes for solving sparse polynomial systems", *SIAM J. Numer. Anal.*, vol. 31, no. 3, pp. 915–930, Jun. 1994, ISSN: 0036-1429. DOI: 10.1137/0731049. [Online]. Available: http://dx.doi.org/10.1137/0731049.

[82] L. Wang and E. D. Sontag, "On the number of steady states in a multiple futile cycle", *Journal of mathematical biology*, vol. 57, no. 1, pp. 29–52, 2008.

[83] G. M. Ziegler, *Lectures on polytopes*. Springer Science & Business Media, 2012, vol. 152.